A FUNDAMENTAL STUDY OF THE OXIDATION BEHAVIOR OF SI PRIMARY REFERENCE FUELS WITH PROPIONALDEHYDE AND DTBP AS AN ADDITIVE

A Thesis

Submitted to the Faculty

of

Drexel University

by

Rodney Johnson

in partial fulfillment of the

requirements for the degree

of

Doctor of Philosophy

June 2008

DEDICATION

To my family

for their support, love and patience

ACKNOWLEDGMENTS

I would like to thank all of the people that have contributed and supported me during the completion of my Masters Thesis. Specifically I would like to thank my advisors Dr. Nicholas P. Cernansky and Dr. David L. Miller for their support and guidance. I would especially like to thank them for the willingness to allow me to perform independent research in areas that were of particular interest to me.

I would also like to acknowledge my family and friends for continuing to push me to finish what I started no matter how discouraged I became. Special thanks goes to past researchers in the Combustion Chemistry Group for answering all the questions I had when I first came to Drexel, as well as teaching me valuable techniques that I have used in obtaining my PhD. These include Dr. David B. Lenhert, Dr. Jincai Zheng, and DR. Xiahoui Gong.

I also appreciate all the friends I have made along the way. The include Ashutosh Gupta, Robert Natelson, Matthew Kurman, Jamie Lane, Charles Avila, Yi Ma, Mike Foster and Temi Sodunke. You have all been a source of entertainment and fun.

My deepest appreciation goes to my future wife, Afton. Without her support, love and patience, it would have been impossible to finish this work. I greatly thank my parents and my extended family for their continual support.

Finally, I would like to give special thanks to the various funding sources that allowed me to complete this research. This research was funded by the U.S. Army Research Office (Grant No. DAAD19-03-1-0070) and the National Science Foundation (Grant No. CTS-9910563). Also for supporting my education, I would like to

acknowledge the Frederic O. Hess and the Albert and Harriet Soffa Fellowship, and last but not least the NSF GK-12 program. Their funding was greatly appreciated.

TABLE OF CONTENTS

LIST OF TABLES

LIST OF FIGURES

Abstract

A Fundamental Study of the Oxidation Behavior of SI Primary Reference Fuels with Propionaldehyde and DTBP as an Additive.

Rodney Johnson

David L. Miller Ph.D. and Nicholas P. Cernansky Ph.D.

In an effort to combine the benefits of SI and CI engines, Homogeneous Charge Compression Ignition (HCCI) engines are being developed. HCCI combustion is achieved by controlling the temperature, pressure, and composition of the fuel and air mixture so that autoignition occurs in proper phasing with the piston motion. This control system is fundamentally more challenging than using a spark plug or fuel injector to determine ignition timing as in SI and CI engines, respectively. As a result, this is a technical barrier that must be overcome to make HCCI engines applicable to a wide range of vehicles and viable for high volume production.

One way to tailor the autoignition timing is to use small amounts of ignition enhancing additives. In this study, the effect of the addition of DTBP and propionaldehyde on the autoignition behavior of SI primary reference fuels was investigated.

The present work was conducted in a new research facility built around a single cylinder Cooperative Fuels Research (CFR) octane rating engine but modified to run in HCCI mode. It focused on the effect of select oxygenated hydrocarbons on hydrocarbon fuel oxidation, specifically, the primary reference fuels n-heptane and iso-octane. This work was conducted under HCCI operating conditions.

Previously, the operating parameters for this engine were validated for stable combustion under a wide range of operating parameters such as engine speeds,

equivalence ratios, compression ratios and inlet manifold temperature. The stable operating range under these conditions was recorded and used for the present study.

The major focus of this study was to examine the effect of the addition of DTBP or propionaldehyde on the oxidation behavior of SI primary reference fuels. Under every test condition the addition of the additives DTBP and propionaldehyde caused a change in fuel oxidation. DTBP always promoted fuel oxidation while propionaldehyde promoted oxidation for lower octane number fuels and delayed autoignition for higher octane number (>50) fuels.

The results discussed in this work show that the addition of propionaldehyde or DTBP effects negative temperature coefficient (NTC) during HCCI combustion. This effect on NTC behavior subsequently affects ignition delay. For DTBP the effect is to always reduce NTC behavior across the entire octane number of PRF blends examined. It is important to note that as octane number increased the effect on NTC becomes less pronounced. For propionaldehyde, the effect on NTC behavior changed with changing PRF octane number. For the same engine operating conditions, as the amount of iso-octane content in the fuel increased, the effect of propionaldehyde addition goes from advancing autoignition for a mixture with 0 % iso-octane content to delaying autoignition for mixtures with over 50 % iso-octane.

Gas samples as a function of crank-angle degree (CAD) before the onset of autoignition were collected and analyzed by gas chromatography for PRF's at selected engine operating conditions with and without the addition of propionaldehyde or DTBP. The results were used to elucidate the effects of these additives on the chemical kinetics controlling HCCI operation. Closer examination of the species evolution profiles

suggest that the mechanism behind the ignition promoting effect of DTBP is due to an increase in the local gas temperature and subsequently a reduction in NTC behavior. The effects caused by propionaldehyde is due to both propionaldehyde acting as a radical scavenger as well as propionaldehyde reacting with itself producing OH•. It is also suggested that the mode of action of DTBP in promoting oxidation is thermal rather than chemical for the fuels tested.

CHAPTER 1. INTRODUCTION

In the last century, the development of Internal Combustion (IC) engines has achieved a high level of success. These engines have been gradually optimized for best performance and emissions. In the early years, increasing engine power and engine reliability were the most important goals for engine manufacturers. Within the past five decades, however, the regulation of exhaust emissions and the decline of petroleum resources have brought increased attention to development of clean and efficient engine designs.

1.1 Motivation

The primary fossil fuel energy conversion technique, combustion, is a major source of air pollutants including particulates, oxides of nitrogen (NOx), UHC, CO and greenhouse gases (particularly CO_2). More than 50 % of NOx emissions come from transportation sources, mainly diesel and spark ignition engines. This realization has caused governments around the world to require a reduction in emissions and a significant improvement in efficiency. By the year 2010 U.S federal regulations mandate a 90 % reduction in NOx and an 80 % reduction in particulates compared to 2004 levels for heavy-duty diesel engines.

Spark ignition (SI) engines use a premixed charge of fuel and air and have very good power density. Emission reduction has also been achieved with the advent of catalyst concepts, however SI engines leave much to be desired in terms of efficiency. Most SI engines operate at a compression ratio of 9 to 10.5. Efficiency increases with an increase in compression ratio up to ~15:1 when mechanical losses overwhelm thermal efficiency gains, however in SI engines the compression ratio cannot be increased to those values. Compression ratio is limited by the occurrence of engine knock, where the fuel-air mixture autoignites prematurely causing a knocking sound and a loss in power. If this behavior continues, engine damage can occur. Thus, SI engines are limited in their efficiency by the inability of the fuel to burn smoothly at high compression ratios.

Compression ignition engines (CI) are not subject to this limitation and run at high compression ratios. This contributes to their high efficiency. They also run lean and since they run unthrottled the pumping work is low, further increasing their efficiency over the SI engine. Unfortunately, while CI engines have higher efficiency than SI engines, they are a major source of NOx and particulate emissions.

In an effort to combine the benefits of both engine types, a class of engines employing Homogeneous Charge Compression Ignition (HCCI) is currently being developed. HCCI is an advanced mode of engine operation, which is attractive because its efficiency is as high as a CI engine, and it has very low NOx and particulate matter (PM) emissions (Bhave et al., 2005).

The start of ignition in HCCI engines is not directly initiated by an external event such as the firing of a spark plug in SI engines or the beginning of fuel injection in

standard CI engines; instead HCCI relies solely on the fuel chemistry leading to autoignition to control the combustion phasing. HCCI engines control load by varying equivalence ratio. Therefore, since equivalence ratio in turn strongly affects the autoignition process, ignition timing must be modulated with engine load. One approach to tailor the ignition properties to the desired load condition is to use small amounts of ignition-altering additives. Di-tertiary-butyl-peroxide (DTBP, $C_8H_{18}O_2$), and propionaldehyde (C_2H_5CHO) are possible candidates for these additives.

Previous work in our research group has investigated these additives in a pressurized flow reactor. The results showed that their addition to hydrocarbon fuels alters the low temperature reactivity, as well as the negative temperature coefficient (NTC) behavior (Gong et al., 2005a, Gong et al., 2005c, Zheng et al., 2005). Past work which examined the interaction of these additives with hydrocarbon fuels of various octane numbers, in a single cylinder research engine, showed that the HCCI operating range was very narrow. The HCCI operating ranges shift to leaner equivalence ratio region as both 1.5 % propionaldehyde and 1.5 % DTBP by volume are added to PRF's. It was also suggested that engine operating condition has an impact on the effectiveness of DTBP addition, but under the conditions tested does not cause any reversal of effect as was seen with propionaldehyde addition. Specifically, DTBP addition has a relatively large effect at lower compression ratios and engine speeds, but it has almost a negligible effect at the highest compression ratio (Johnson, 2007).

This work explored the effects of propionaldehyde and DTBP on oxidation in an engine operating in HCCI mode using neat SI primary reference fuels (PRF's), which contain n-heptane and iso-octane, blends as a baseline. Our goal was to better

understand how the selected oxygenated hydrocarbon addition affects fuel oxidation, and subsequently autoignition.

In this work I examined the effect of both additives on NTC behavior in a single cylinder engine modified to run in HCCI mode. I then ran similar fuels collecting gas samples at selected crank angle degree (CAD) with and without the additives present to examine the additive affects on intermediate compositions during PRF oxidation. All data collected is constrained by two stability criteria. The lean limit was constrained by the coefficient of variation (COV) of the indicated mean effective pressure (IMEP), which must be about 5.0 % for data to be considered usable. For the rich limit, the data was constrained by a maximum rate of pressure rise (MRPR) of 10 bar/CAD in order to avoid engine damage. The additives were used in volume percentages of either 1.5 or 3.0 %.

1.2 Overview of the Study

The overall goal of this research program was two-fold. First, using a single cylinder engine I wanted:

1) To investigate the effects of both propionaldehyde and DTBP on NTC behavior and ignition delay using blends of PRFs
2) To collect species evolution profiles to aid in investigating the effect of the selected additives on PRF fuel oxidation as a result of the each additive's chemical and thermal effects. I also wanted to provide clarification of the mode of action of DTBP.

The experiments were conducted in a single cylinder engine research engine operated in HCCI mode. The fuels studied were PRF 0, PRF 20, PRF 50, and PRF 87. The fuels were all tested neat and with an addition of either 1.5 % or 3.0 % by volume of propionaldehyde or DTBP. The approach used was to examine the effect of these additives on NTC behavior by observing the CO concentration in the engine exhaust during motored operation of the engine. Species evolution profiles prior to autoignition were then collected using in cylinder sampling and gas chromatographic analysis. Following a detailed literature review in the next chapter, the experimental facilities and procedures are described in Chapter 3.

CHAPTER 2. BACKGROUND AND LITERATURE REVIEW

Instead of reviewing all aspects of hydrocarbon combustion, this chapter mainly provides a background description and reviews the past research work related to the scope of this research program. First, a comparison between the CI, SI and HCCI combustion process and emissions is made. Second, the history and development of HCCI engines are reviewed. Then, previous research on hydrocarbon oxidation and autoignition and mechanism development are discussed, followed by a brief description of Propionaldehyde and DTBP chemistry. Finally, related research work on fuel additives and an introduction to their effects on hydrocarbon oxidation are presented.

2.1 Comparison of CI, SI and HCCI Engine Combustion and Emissions

HCCI combines the best characteristics of conventional SI gasoline engines with those of CI diesel engines. Many major automobile and engine manufacturers are exploring HCCI technology, which could boost fuel economy in cars by about 20 percent and generate fewer polluting emissions such as NOx and soot. Research projects are also under way at national labs and universities with goals of overcoming the challenge of controlling the start of combustion (SOC) on each engine cycle for HCCI engines. This will enable implementation of the HCCI technology for a wide range of engine loads and the consequent reduction in pollutant emission for oil derived fuel propulsion and power.

Conventional SI engines use one or more spark plugs to ignite a fuel-air mixture in a cylinder's combustion chamber. In a CI engine, air is compressed to a high

temperature, and then fuel is injected directly into the combustion chamber. The high temperature of the compressed air triggers the autoignition of the vaporizing fuel.

An SI engine typically has a high power output at high speeds. The current emissions technologies enable exhaust emissions to be exceptionally low. The downside is relatively low efficiency, particularly in light-load operation, and consequently high fuel consumption.

A CI engine, by comparison, has high torque output at low and moderate speeds. It's inherently more efficient than an SI engine, particularly at light-load operation. The downside of a CI engine is greater emissions, particularly NOx and carbon particulates (soot) when operating on diesel fuel.

HCCI engines are a hybrid of SI and CI engines. They use a premixed charge of fuel and air, as in SI engines, but the charge is forced to autoignite by compression, as in CI engines. The advantages of HCCI engines are very low NOx, no PM, and improved efficiency.

2.2 Homogenous Charge Compression Ignition (HCCI) Engines

As mentioned earlier, HCCI engines have the potential to provide dramatic increases in fuel efficiency over standard stoichiometric SI engines as measured by brake specific fuel consumption. HCCI engines can run with diesel-like efficiency, but produce no soot and up to a 98 % reduction in NOx. However, they pose a number of difficult performance and control issues, which must be overcome before they can be serious competitors with conventional internal combustion engines.

For HCCI engines there is no external initiator of combustion timing, and combustion staging is determined by the autoignition characteristics of the in-cylinder

fuel-air mixture, typically called the charge. Therefore, understanding the chemical kinetics of autoignition and heat release is key to addressing the control problems.

HCCI relies on a very lean, premixed fuel and air mixture that is introduced into the engine cylinder. The mixture is compressed until it autoignites and then the mixture expands doing work on the piston. The autoignition occurs at multiple locations in the combustion chamber causing the rest of the charge to burn uniformly. This can be accomplished with most hydrocarbon fuels by the appropriate selection of the conditions. This progression is shown in Figure 2.1.

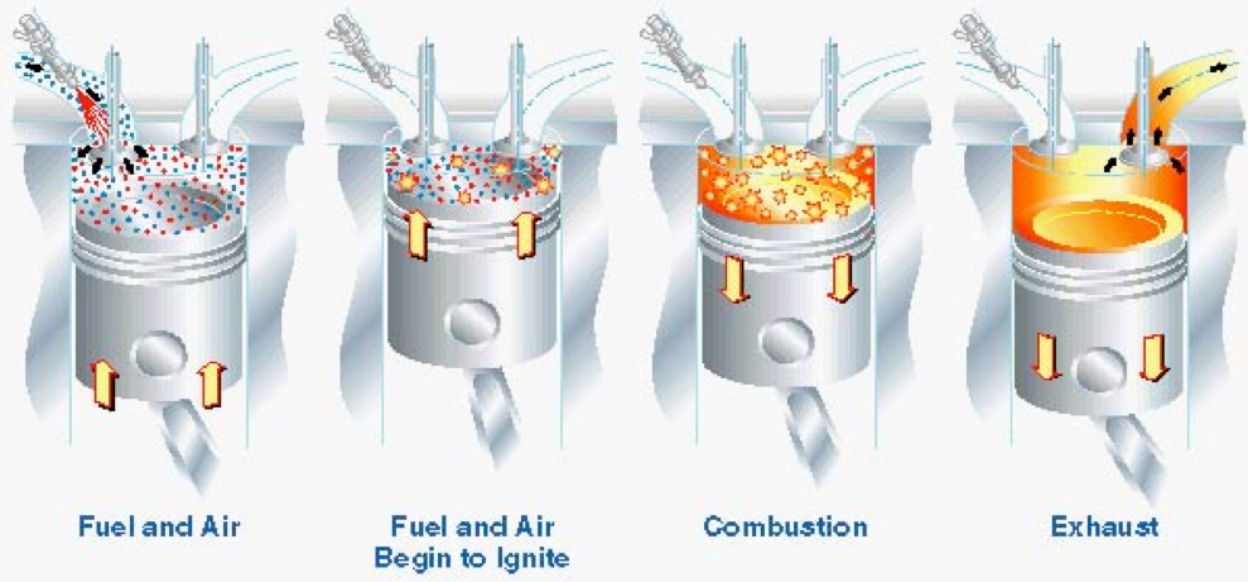

Figure 2.1: Typical HCCI engine cycle (Ryan and Matheaus, 2003)

2.2.1 Introduction to HCCI

HCCI combustion studies began almost three decades ago with the work of Onishi et al. (1979) and Noguchi et al. (1979) that showed the basic characteristics of

HCCI. These characteristics were very little cycle-to-cycle variation and no flame propagation. Onishi reported this unique combustion behavior, which was called “Active Thermo-Atmosphere Combustion (ATAC)” from studies on a two-stroke gasoline engine under relatively lean conditions. The ATAC process achieved lower fuel consumption and low emissions in the region of light and medium loads, with less noise and vibration. High-speed Schlieren photographs showed that ATAC was initiated by a multipoint autoignition without discernable flame propagation.

Noguchi et al. (1979) conducted a spectroscopic study of ATAC combustion in a two-stroke engine and observed many radical species. These radicals included high levels of CHO, HO_2, and O radicals, which were present in the cylinder prior to the time of autoignition. This demonstrated that preignition chemical reactions had occurred and certainly contributed to the autoignition. In a traditional SI engine, these preignition radical species are primarily associated with end-gas autoignition, also known as knock. After autoignition took place, H, CH, and OH radicals were detected, which were indicative of high-temperature chemical reactions. Also, the combustion process seemed to start at lower temperatures and pressure than those for conventional modes of combustion.

These initial research efforts were done using two-stroke engines with low compression ratios and very high residual gas fractions in the cylinder. Najt and Foster 1983) first ran HCCI on a four-stroke engine. They conducted fundamental studies in pursuit of understanding this combustion phenomenon. They successfully carried out experiments with blends of paraffinic and aromatic fuels over a range of engine speeds and dilution levels in a four-stroke CFR test engine with a variable compression ratio.

They utilized heated intake air to achieve HCCI operation and mimic the benefit of high levels of internal residuals present in two-stroke engines. Ignition and smooth energy release was obtained by varying the engine operating parameters, such as equivalence ratio, inlet temperature, and EGR rate. They analyzed the experimental results with global autoignition chemistry and kinetics. It was concluded that HCCI ignition is controlled by low temperature (below 950 K) hydrocarbon oxidation. They also concluded that the energy release process is controlled by the high temperature (above 1000 K) hydrocarbon oxidation kinetics as characterized by Dryer and Glassman (1978). An empirical equation was also developed based on Dryer and Glassman's global kinetics that successfully predicted the average rate of energy release.

2.2.2 Advantages of HCCI

The main motivation for studying HCCI combustion behavior is the potential for a significant reduction in NOx and particulates emissions when compared to conventional SI and other CI engines, such as traditional diesel engines. Overviews of combustion efficiency issues and exhaust emissions concerns for conventional SI and CI engines are provided in this section.

Nitrogen Oxide Emissions

Among the most appreciated properties of the HCCI engine are the low NOx emissions. From a fundamental combustion point of view, the biggest difference between a HCCI engine and established engine types, SI and CI engines, is the absence of flame zones (Amneus et al., 2005).

Flame propagation is one of the major factors that are different between the SI and CI engine. It is important to note that the combustion process in CI diesel engines is very complex and is still not well understood. In CI engines, fuel is injected in the compressed air filled combustion chamber, partially vaporizes, and then combustion begins. This initial combustion after ignition is called the pre-mixed combustion phase; it consumes only about 5 % to 10 % of the fuel used by the engine at typical full-load operation. At the end of the pre-mixed combustion phase, most of the fuel has yet to be injected or is still in a region that is too rich to burn. But injection continues and fuel continues to vaporize and mix with air, aided by the heat release and turbulence generated by the initial combustion. The thermal and chemical variation in this spray is the cause of very complex oxidation behavior and is the source of both high levels of NOx and particulates. Surrounding the atomized droplets, a thin diffusion flame exists. This region reaches very high temperatures accounting for large levels of NOx. The diffusion flame consumes all the local oxygen; therefore inside the diffusion flame an area where exists rich combustion. The products of rich combustion are then oxidized at the diffusion flame surface. An oxygen deficient condition is available inside the diffusion flame sheath and the constituents and temperatures existing inside the sheath are ideal for the formation of diesel particulate (Flynn et al., 1999b).

In the SI engine, a charge of premixed fuel-air mixture is drawn into the combustion chamber through intake valves where the charge is then compressed by the motion of the piston. The compressed fuel-air mixture is then ignited by one or more spark plugs. The combustion occurs as a premixed flame, which traverses the combustion chamber. As a result of flame combustion, a high local temperature occurs. At these temperatures which approach adiabatic flame temperature, the oxides of nitrogen (NOx) form from paths which involve reactions of molecular and atomic nitrogen and oxygen, a reaction set called Zeldovich. (Heywood, 1988) Operating at lean equivalence ratios, HCCI engines produce much lower maximum temperatures than comparable SI and CI engines and reduce the NOx production from the Zeldovich mechanism.

Christensen and Johansson (2000) investigated the emission of NOx in HCCI engines. They found that NOx emissions were nearly zero. They explained that most of the NOx formed is formed at high temperatures and is governed by the Zeldovich mechanism. Heywood (1988) presented an equation for NO formation rate based on the Zeldovich Mechanism, Equation 2-1.

$$\frac{d[NO]}{dt} = \frac{6\times10^{16}}{T^{\frac{1}{2}}} e^{\left(\frac{-69{,}090}{T}\right)} [O_2]_e^{\frac{1}{2}} [N_2]_e \qquad \text{Eqn. (2-1)}$$

In this equation $[\ ]_e$ denotes an equilibrium concentration and T is the temperature. The calculations were conducted assuming equilibrium O_2 and N_2 concentrations. This equation is valid at an NO concentration close to zero, where [NO]/

$[NO]_e$ << 1. Here the strong dependence of NO formation rate on temperature can be seen in the exponential term. The rate of [NO] change with respect to temperature is plotted in Figure 2.2. We can see that NO formation is predicted to start at elevated temperatures around 1800 K, and it then increases rapidly.

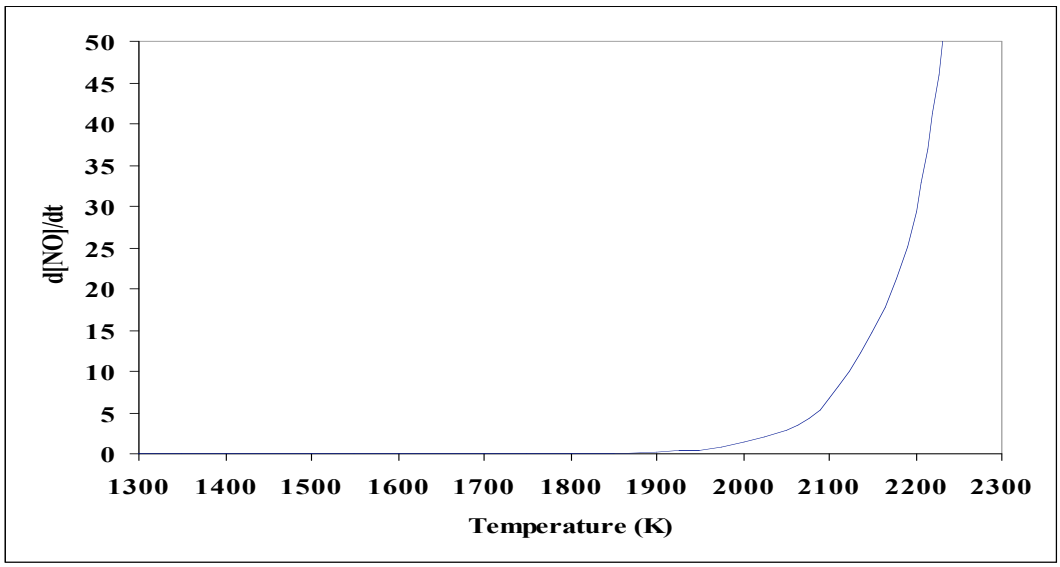

Figure 2.2: NOx formation rate based on Zeldovich Mechanism (Heywood, 1988)

Particulate Matter

Another advantage of HCCI combustion is the low levels of smoke and particulate matter (PM) emissions produced compared to CI engines (Stanglmaier and Roberts, 1999). While detailed mechanisms for smoke and PM formation aren't well understood, the reason for low PM in HCCI is. One proposal is that HCCI eliminates

diffusion-limited combustion and localized fuel rich regions, which limit the formation of soot.

Hydrocarbons

While the temperatures in an HCCI engine are an excellent means to reduce NOx, the low temperatures may result in incomplete combustion with increased emissions of HC (Christensen et al., 1997, Christensen and Johansson, 1998, and, Christensen and Johansson, 2000). In practical uses, HCCI engines utilize a lean highly diluted mixture. This lean highly diluted mixture is another factor that promotes lower combustion temperature.

Another study in HCCI showed that using small amounts of exhaust gas recirculation (EGR) into the intake charge improved combustion efficiency (Oakley et al., 2001). The introduction of exhaust gas increases the heat capacity of the mixture lowering the peak combustion temperature. Lowered peak combustion temperature reduces the loss of thermal energy to combustion chamber surfaces, leaving more available for conversion to mechanical work during the expansion stroke. Along with an improvement in combustion efficiency, a significant reduction in HC emissions. The authors concluded that this was proof that temperature and species compositions of the charge mixture play an important role in HCCI combustion.

Carbon Monoxide

Much like hydrocarbon emissions, carbon monoxide emissions are generally high in HCCI combustion. The reason is almost the same as with hydrocarbon emissions. CO emissions are said to be caused by incomplete combustion of the intermediate species. Flowers et al. (2000) speculated that the specific caused of increased CO is the diminished OH radical concentration in these systems. As a result, less CO is converted to CO_2.

2.2.3 The Importance of HCCI Research

Although stable HCCI operation and its substantial benefits have been demonstrated at selected steady-state conditions, several technical barriers must be overcome before HCCI can be widely applied to production automobile and heavy-truck engines. The main disadvantages of HCCI are listed below:

- Control of ignition timing and combustion rate;
- Excess CO and UHC emissions, particularly at lower load conditions;
- Narrow operating range;
- Difficult cold start and light operation at light load;
- High NOx at high load.

2.2.3.1 HCCI Fuels

One major advantage of HCCI combustion is its intrinsic fuel flexibility. HCCI combustion has little sensitivity to fuel characteristics such as lubricity and laminar flame speed. Fuels with any octane or cetane number can be burned, although the operating conditions must be adjusted to accommodate different fuels, which ultimately impacts efficiency. Najt and Foster (1983) performed engine experiments in a CFR engine using three different fuels. The fuels used were primary reference fuel (PRF) blends containing 70 % iso-octane and 30 % n-heptane (PRF 70), and 60 % iso-octane and 40 % n-heptane (PRF 60), along with blend of 60 % iso-propylbenzene and 40 % n-heptane. The two PRF blends were chosen to explore the effect of octane number on HCCI combustion, while the third blend was chosen to explore the effect of chemical structure on HCCI combustion. The study found that using different fuels altered the HCCI combustion process by changing the low temperature oxidation kinetics. The nature of these elementary reactions differ from fuel to fuel, thus the conditions necessary for successful HCCI combustion differ from fuel to fuel. The high temperature oxidation reactions were largely unaffected by changes in fuel type. The reason is the same radicals, O, OH, and H, control the same basic high temperature reactions for hydrocarbons. Finally the study showed that fuels with a lower motor octane number (MON) were more readily ignited in an HCCI engine, which means that these fuels required lower initial charge temperature.

Christensen et al. (1999) also demonstrated the multi-fuel capability of HCCI engines. Fuels used in this study were primary reference fuels (iso-octane and n-heptane) and commercial fuels (gasoline and diesel fuels). The combustion chamber

was modified such that compression ratio could be altered by adjusting a secondary piston in the cylinder head. An electrical heater was installed on the inlet manifold to control the inlet air temperature to selected values over the range of 30-120º C, in steps of 20º C. The use of dual port injection systems made it possible to alter the ratio of the two different fuels. The lambda for these test ranged from 2.8 to 3.1. Lambda is the air to fuel ratio (A/F) present during combustion, stoichiometric ration has value 1.0, numbers >1 are fuel lean.

The test results showed that almost all liquid fuels could be used in an HCCI engine using variable compression ratios. Without the use of preheated air, operation with pure n-heptane required a compression ratio of about 11:1. Under the same condition iso-octane (RON = MON = 100) required a compression ratio of 21.5:1 and a high-octane gasoline (98 RON) required 22.5:1. NOx was generally low, and did not increase with increasing compression ratio. Smoke was found in some cases with diesel fuels, and emissions of unburned hydrocarbons increased with decreased compression ratio.

Gasoline has multiple advantages as an HCCI fuel. Gasoline has a high octane number (87 to 92 in the U.S. and up to 98 in Europe), which allows the use of reasonably high compression ratios in HCCI engines. Actual compression ratios for gasoline-fueled HCCI engine data vary from 12:1 to 21:1 depending on the fuel octane number, intake air temperature, and the engine design (which may affect the amount of hot residual gases naturally retained). This compression ratio range allows gasoline-fueled HCCI engines to achieve relatively high thermal efficiencies (in the range of CI engine efficiencies). A potential drawback to higher compression ratios is that the

engine design must accommodate the relatively high cylinder pressures that can result, particularly at high engine loads. Ishibashi and Asai (1996) used gasoline to fuel a two-stroke, single-cylinder engine that was capable of operating in HCCI mode at low to moderate loads and switched to conventional SI operation at high loads. This combination demonstrated considerable advantages in fuel economy and was 27 percent better than a regular two-stroke cycle engine under "real-life" driving conditions. Hydrocarbon emissions were also reduced by 50 percent with respect to a regular two-stroke cycle engine. However, without emission controls, hydrocarbon emissions were still very high compared to the current automotive emissions standards.

Ryan and Callahan (1996) and Gray and Ryan (1997) investigated HCCI operation using diesel fuel. For the first time, Knock Intensity (KI) was used to trace knock and determine the acceptable HCCI operating range. According to the definition, knock that is just marginally audible is used to define a KI of 5 on a scale from zero to ten. The rate of pressure rise is collected and processed to yield a KI. A KI of 4 was used to identify permissible HCCI operations. The HCCI operating envelop was mapped by varying EGR rate, compression ratio, and inlet temperature. They found that management of EGR rate and equivalence ratio was critical to achieving HCCI. Under 50 percent EGR rate and stoichiometric fresh charge condition, the engine would produce acceptable power output with near total elimination of smoke. A simple empirical model was also proposed to predict HCCI ignition delay time:

$$t_d = 0.021*(O_2)^{-0.53}*(Fuel)^{0.05}*(\rho)^{0.13}*\exp(5914/T)$$

Where t_d is the ignition delay time (ms), O_2 is the oxygen molecular fuel concentration (moles/m^3), Fuel is the fuel molecular fuel concentration (moles/m^3), ρ is the density (kg/m^3), and T is the air temperature (K). However, compression ratio had to be lowered from 16:1 to 8:1 to achieve HCCI operation, and the unburned hydrocarbons were very high. Also, they found that it makes little difference whether the dilute mixture was achieved by going very lean (e.g., below the equivalence ratio in which a flame can propagate, $\phi \sim 0.6$ or 0.7) or by adding exhaust gas recirculation.

2.2.3.2 Operating Range

To make HCCI a reality one of the challenges that needs to be overcome is the rapid energy release rate. This rapid energy release rate leads to a maximum rate of pressure rise limitation and low specific power output which is the maximum output per unit weigh. This is as a result of the charge not igniting at the optimum position, which is at top dead center (TDC). HCCI engines also run with very lean mixtures further decreasing the specific power output. In addition, many of the suggested control strategies for HCCI require thermal preheating of the charge which reduces the density and hence the mass of the air/fuel charge in the combustion chamber, also reducing power. These factors make increasing the power in HCCI inherently challenging. Many researchers have investigated methods for extending the operating range for HCCI engines, as well as increasing power density.

Thring (1989) investigated the HCCI operation range of a four-stroke engine with different fuels. He used both unleaded gasoline and diesel fuels (DF-2). In this study, it

was found that HCCI required high EGR rates or high intake temperatures or sometimes both. He concluded that EGR rates and the charge temperature could regulate the timing for combustion initiation. Thring also investigated different compression ratios. In his study satisfactory operation was not achieved with a CR of 15:1, even after gradually increasing the internal EGR to eliminate knocking. Thring found that using a CR of 8:1 gave him satisfactory operation with virtually no knock.

From his study, Thring concluded that there were three regions of unsatisfactory HCCI operation. There is a “misfire region”, a “power-limited region”, and a “knock region”. In the misfire region, either the mixture was too rich, or the EGR rates were too high to sustain consistent combustion. In the power-limited region, the mixture was too lean, or the EGR rates were too excessive for the combustion to produce enough power to overcome friction. Under the power-limited region, combustion was steady and smooth, the pressure rates were not excessive, and the engine seemed to operate smoothly. As a result it was concluded that this region was an acceptable region for light load and idle conditions. In the knock regions, pressure rise rates were extremely high and could result in damage to the engine.

Christensen et al. (1998) investigated the use of three different fuels, supercharging, and CR on HCCI to improve power output, and to find the effects on operating range. The fuels investigated were iso-octane, ethanol, and natural gas. The results showed that natural gas required a richer mixture for satisfactory operation than did ethanol or iso-octane. When one bar of boost pressure was applied, the inlet temperature must be higher for natural gas. He concluded that this might be due to the higher octane number of natural gas. When a boost of two bars was used, natural gas

required less preheating than ethanol. Also, at the compression ratio of 19:1, iso-octane could not be used due to overly advanced combustion timing. In general, with ethanol and natural gas the attainable IMEP was higher for the lower compression ratio tested (17:1). The study concluded that supercharging slightly advances the combustion timing; also, it was shown that supercharging causes iso-octane to exhibit more knocking like behavior than ethanol or natural gas.

These studies show that the HCCI operating range can be influenced by many variables. The equivalence ratio normally ranges between 0.1 and 0.4, which is much lower than that of combustion in conventional engines. The equivalence ratio needed to achieve HCCI operation depends on the operating conditions and the fuel distribution. The fuel distribution can vary depending on the fuel introduction technique. The lower limit of equivalence ratio is determined by the minimum combustion stability. The upper limit is defined by the maximum rate of energy release, which leads to the maximum rate of pressure rise. The combustion duration has a strong dependence on the equivalence ratio. When operating close to an equivalence ratio of 0.4, the combustion process is very rapid. Using a leaner mixture, the combustion process can be slowed down; however it is still fast when compared to normal SI engines. This suggests that the combustion duration is highly dependent on equivalence ratio (Christensen and Johansson, 1998). This study also showed that supercharging could increase the operating range of an HCCI engine as a result of advanced ignition timing leading to high IMEP.

2.2.3.3 Methods in Controlling HCCI Operation

As a result of the way HCCI engines operate, controlling the ignition timing has proven very difficult. Over the past two decades, technologies have been developed to control ignition for HCCI engines in both two-stroke and four-stroke engines with various fuels. The remaining challenges involve the control of ignition timing over the entire range of engine speeds and loads. The problem of controlling HCCI combustion is directly linked to ignition timing management as described by Milovanovic and Chen (2001). They explained that two requirements for practical HCCI combustion are that the start of autoignition should occur at top dead center (TDC), and the energy release rate should be controllable. At the present time, there are no direct control methods. Some indirect methods for controlling the timing of autoignition and the energy release rate of HCCI combustion are described in the following sections.

Modifying Fuel-air Mixture Properties

There are numerous ways to control HCCI combustion through adjusting in-cylinder mixture properties: increasing intake temperature, adjusting fuel-air ratio, and using EGR. Each will be discussed individually.

Intake Temperature

Milovanovic and Chen (2001) showed that adjusting the intake air temperature is one method to achieve HCCI combustion and control ignition timing. They concluded that a high intake air temperature causes a higher rate of energy release. Ultimately, a high intake air temperature advances the start of the first stage ignition, thus reducing the ignition delay between first and second stage ignition. The reason is that the high intake air temperature enhances the reactivity of the charge.

While intake air temperature can be used to modify HCCI combustion phasing, the controllable range has severe limits. Outside this range the engine volumetric and thermal efficiency are largely reduced due to over advanced autoignition timing. Also varying intake temperature is generally a slow process, so this method is not really practical, especially under transient conditions (Sjöberg et al., 2005).

Lü et al. (2005) concluded that since HCCI combustion is dominated by chemical reaction, then the intake charge temperature becomes the most important factor that effects the HCCI ignition. They also showed that in general, the start of cool flames in the low temperate region and the hot flame in the high temperature regions advance linearly with the rising inlet temperature. They also noted that the ignition timing of RON 75 advances more rapidly than other fuels. They explained this by the following rationale. During the compression stroke, the gas temperature rise rate is largely dependent on the heat capacity of gas mixture and low-temperature heat release.

Equivalence Ratio

Varying equivalence ratio is another method of controlling HCCI combustion and ignition. In general, increasing the equivalence ratio causes an increase in the rate of combustion due to the higher charge energy density. Consequently, decreasing the equivalence ratio causes a delay in ignition timing (Milovanovic and Chen, 2001).

Aceves et al. (1999) showed that the efficiency increases as the equivalence ratio is decreased. For high equivalence ratios, combustion occurs before TDC, resulting in significant negative work on the piston. Reducing the equivalence ratio delays combustion and reduces the negative work, increasing the efficiency.

Soylu (2005) concluded that one of the potential advantages of HCCI combustion is that the lean limit of the mixture can be extended significantly. The lean limit of numerous fuels can be extended to an equivalence ratio of 0.45 for the given operating conditions, which results in low peak pressure and temperature with high efficiency. The low heat content of the lean mixture reduces the peak temperature of combustion and, thus, reduces NOx emissions. They showed that as the equivalence ratio is increased, both the peak pressure and temperature increase significantly, which can eventually lead to higher NOx emissions and engine knock. Also, the IMEP increases with equivalence ratio; however, the efficiency did not show the same behavior.

Exhaust Gas Recirculation

The effect of EGR gases on HCCI combustion was investigated recently by several groups. Law et al. (2001) concluded that internal EGR could have two effects on combustion. They showed that EGR has both a thermal effect (due to its high temperature) and a chemical effect (due to its chemical contents, where the active species promoted and initiated combustion, while the nitrogen and other inert gases slowed down the reaction). Specifically, the larger heat capacity of EGR gases tends to retard the start of autoignition. The dilution of oxygen by EGR has little effect on onset of autoignition but it has a similar effect on extends the combustion duration just like dilution. The dilution effect of EGR on lowering the heat release rate is only noticeable at high concentrations. Finally, they showed that the chemical effect of CO_2 and H_2O was negligible. When hot EGR is used in HCCI combustion, the charge heating effect of

EGR has much greater effect on ignition timing and a less significant effect on the combustion duration and heat release rate than the other effects.

Oakley et al. (2001) also studied the effect on charge temperature, dilution, and heat capacity when using internal EGR. They proposed that EGR advanced autoignition timing due to raising the charge temperature. They also showed that dilution did not change autoignition timing, but it extended combustion duration. The dilution slowed the heat release rate only for large levels of EGR (> 30 %). The heat capacity effect was mainly responsible for the reduction in the heat release rate, and it had a similar effect in extending the combustion duration as dilution.

Zheng et al. (2003) examined the effects of high levels of internal gas recirculation on the pre-ignition chemistry and reactivity behavior of two and four-stoke HCCI engines. Zheng showed that by increasing internal EGR in an unloaded spark ignited two-stroke engine, UHC was reduced from 7800 ppm to 3000 ppm, CO decreased from 3 % to 0.2 %, and cyclic variability was diminished. These results demonstrated that stable engine operation could be obtained with additional internal EGR. Improvements were obtained at stoichiometric and lean conditions. Zheng showed that preignition reactions are enhanced by internal EGR, but are unaffected by the addition of an equivalent amount of air, where no reduction of UHC or CO is observed. Further, in both two and four stroke cycle experiments spark ignition was possible with high levels of internal EGR but was not possible with an equivalent amount of air or N_2.

Lü and Qian (2006) investigated the effect internal EGR and other operation parameters including engine speed, equivalence ratio, coolant-out temperature, and

intake charge temperature on the basic characteristics of a single-cylinder homogeneous charge compression ignition (HCCI) engine powered with reformulated iso-octane fuels. They showed that the effects of EGR on the combustion and emissions are remarkable when the EGR rate is higher than 25 %. Specifically they showed that with the high EGR the autoignition is significantly delayed and the UHC and CO emissions greatly diminished.

Modifying Engine Operation

Modifying engine operating and design parameters are ways to alter the combustion process to deal with the control issues facing HCCI. For example, using a variable compression ratio (VCR) mechanism can alter the TDC temperatures. Also, variable valve timing (VVT) changes the effective compression ratio and/or the amount of hot residual retained in the cylinder. VCR and VVT are particularly attractive because their time response could be made sufficiently fast to handle rapid transients. Although these techniques have shown strong potential, they are not yet fully proven, and cost and reliability issues must be addressed.

Variable Compression Ratio (VCR)

A VCR engine has the potential to achieve satisfactory operation in HCCI mode over a wide range of conditions because the compression ratio can be adjusted as the operating conditions change. Conditions change quickly in vehicular applications; consequently, a fast control system that modifies the compression ratio in fractions of a second is necessary. Several options have been studied to obtain VCR engines. One option is to mount a plunger in the cylinder head whose position can be varied to change the compression ratio (Christensen et al., 1999). The compression ratio could

also be varied by using an opposed-piston engine design having variable phase shifting between the two crankshafts (Flynn et al., 1999a). SAAB has developed another method that is based on a hinged, tilting cylinder arrangement (Sharke, 2000).

The U.S. DOE has sponsored a unique VCR engine design, which is being developed by Envera and tested at Argonne National Laboratory. Similar to the SAAB approach (Sharke, 2000), the Envera approach varies the distance between the cylinder head and the crankshaft. However, unlike the SAAB approach, the VCR mechanism fits inside the crankcase and is expected to provide a faster response and require less energy. This concept was validated in July 2001. The engine ran for about twenty hours, with no bearing or engine wear detected. The engine ran at full-throttle for several hours, with noise and vibration characteristics well within acceptable limits. The compression ratio was varied from 8.5 to 17.5 without degradation of engine characteristics and with the lowest hydraulic pressure level available.

While any of these systems or some other mechanism might succeed, only the variable-position plunger system has been demonstrated in an HCCI engine (Christensen et al., 1999). For these tests, the plunger was controlled by a hydraulic system allowing its position to be varied during engine operation. The data show that the VCR system is capable of controlling HCCI ignition timing to maintain optimal combustion phasing across a very wide range of intake temperatures and fuel types of varying octane number. Although transient operation and variations in speed and load were not reported, the results suggest that a VCR system with sufficiently fast response time is a strong candidate for HCCI engine speed and load control. VCR would add cost and complexity to the engine.

Variable Valve Timing (VVT)

Variable valve timing has the ability to optimize HCCI engine performance by continuously adjusting intake and exhaust valve timing in relation to the crankshaft. This adjustment can change the amount of compression after the gases are trapped by intake-valve closure. As a result, VVT can achieve a similar effect on HCCI combustion as varying the geometric compression ratio of the engine.

More important, engines with VVT have the added benefit of allowing changes in the temperature and composition of the incoming charge by retaining hot residual gases from the previous cycle in the cylinder. Increasing the temperature of the charge in this manner can be used to induce HCCI combustion even with relatively low geometric compression ratios or under cold-engine conditions once the first firing has been achieved.

Kaahaaina et al. (2001) demonstrated the use of an electro-hydraulic VVT system. They showed that the VVT system could be used to control combustion timing and to switch between SI and HCCI operation from one cycle to the next. While more recently, Sellnau (2006) demonstrated two-step variable valve actuation using early-intake valve closing as a strategy for high fuel economy on spark-ignited gasoline engines. In this work two discrete valve-lift profiles were used with continuously variable cam phasing. Two-step VVA systems are attractive because of their low cost to benefit, relative simplicity, and ease-of-packaging on new engines such as HCCI.

Dynamometer tests on a multi-cylinder engine equipped two-step variable valve actuation indicated a 6.9 percent fuel economy benefit on the EPA city cycle relative to the production engine with exhaust cam phasing alone. Combustion enhancement

significantly contributed to the overall fuel economy benefit. Vehicle tests showed less fuel economy improvement than steady state dynamometer tests due, in part, to cam phaser control limitations. For warmed-up Phase 3 EPA tests (cycles 19-23), a 5.5 % improvement was measured with 46 % reduction in NOx. For the whole EPA city test including cold start, a 4.8 % improvement was measured. Further improvements in vehicle fuel economy are expected with refinement in transient control and calibration.

Ignition-Enhancing Additives

HCCI engine control can potentially be achieved by using two fuels with different octane ratings. The system can be designed to have a main fuel with a high octane number, while the secondary fuel, with a low octane number, is injected as needed to advance combustion. The potential of this procedure has been studied for a combination of methane and dimethyl ether (DME) (Flowers et al., 2000). A similar approach using iso-octane and n-heptane was demonstrated on a six-cylinder HCCI research engine (Olsson et al., 2001). This study showed that the dual-fuel method could be used to maintain good combustion timing in all cylinders over a relatively wide range of speeds and loads. However, this method would require carrying and refilling two fuel tanks. Ideally, the amount of the secondary fuel being consumed would be minimal and the tank could be refueled only at the maintenance intervals, which may pose problems with fuel stability. The intention of this work was to demonstrate a functioning control system for a dual fuel HCCI engine rather than propose a concept for a commercial engine. Alternatively, the addition of ozone to the intake has been shown to be an excellent HCCI ignition improver (Flynn et al., 1999a), substantially advancing HCCI combustion even at very low concentrations. The system for producing the ozone

is inexpensive and has a fast response, but does require electrical power.

2.3 Hydrocarbon Oxidation and Autoignition Chemistry Studies

The autoignition process of hydrocarbon fuels is very complex involving a large number of chemical species and reactions. Due to the nature of the chemistry, phenomena such as cool flames, negative temperature coefficient (NTC) behavior, single and two-stage ignition, occur during preignition reactions. As autoignition controls combustion phasing in HCCI engines, understanding the chemical processes of preignition is critical for developing HCCI engines. A detailed review of the HCCI related hydrocarbon oxidation and autoignition chemistry is necessary to identify the major focus of the present work. A review of DTBP and propionaldehyde will also be discussed.

2.3.1 Review of Engine Autoignition and Hydrocarbon Oxidation Studies

Studies of autoignition and hydrocarbon oxidation in engines began in the early 1900's when knock was identified as a limitation on engine output and fuel efficiency. Over the years, sampling, measurement and analysis techniques have improved and so has our understanding of the fundamentals of autoignition and hydrocarbon oxidation.

Historically, some of the interesting low and intermediate temperature hydrocarbon oxidation phenomena were encountered accidentally. As early as 1920, researchers noticed the differences in the autoignition characteristics of different pure hydrocarbons. A negative temperature coefficient behavior was found when Pease was studying oxidation of propane in a flow reactor in 1929 (Pease and Munro, 1929,

Dechaux, 1973). The first evidence of preflame reactions was presented by Rassweiler and Withrow (1933). In 1948, Lovell published an extensive review and tabulation of the autoignition characteristics of over 325 hydrocarbons (Lovell, 1948). Notably, Lovell related the chemical structure of hydrocarbons to the tendency for fuel autoignition. However, Lovell did not forward a kinetic or mechanistic explanation for the observed phenomena. It was not until Walsh (1963) proposed a mechanistic link between autoignition tendency and fuel structure that there was a reasonable explanation for the wide differences in knock behavior. Walsh suggested that the isomerization of the RO_2 radical (where R is the original fuel molecule, minus one hydrogen atom) plays a critical role in the oxidation of hydrocarbons, since the isomerized radical can lead to a series of chain branching reactions. Thus, began an effort to understand the autoignition behavior of a fuel by investigating the mechanism of the fuel decomposition and oxidation prior to the point of autoignition.

Since Walsh, extensive studies have been conducted on the oxidation of hydrocarbons, greatly increasing the understanding of the combustion process. In general, the combustion process may be described as a series of complex chain branching, carrying, and terminating reactions involving stable and radical species. It is commonly accepted that the hydrocarbon oxidation process may be separated into three distinct temperature regimes.

i) Low temperature, < 650 K

ii) Intermediate temperature, 650-1000 K

iii) High temperature, > 1000 K

Corresponding to each of these temperature regimes is a dominant branching agent (Wilk, 1986; Koert, 1990; Dryer, 1991), namely alkylperoxy radicals in the low temperature region, hydroperoxy radical in the intermediate temperature region, and hydroxyl and atomic oxygen and hydrogen radicals in the high temperature region. Generally, the combustion environment, such as temperature, pressure, and equivalence ratio effects the location of the boundaries between each regime.

The performance of internal combustion engines is controlled by the chemical kinetics of the fuel oxidation, specifically hydrocarbon oxidation. The reactions in the low and intermediate temperature range relate to the phenomena of autoignition and engine knock

Since many of the reactions in each regime are pressure dependent, the temperature of each regime will shift as the pressure of the combustion process increases. The temperature regime where the autoignition process occurs has been experimentally measured by several researchers, e.g. Gluckstein and Walcutt (1964); Smith et al. (1985); Griffiths et al. (1997), it is generally accepted that the fuel autoignites in the intermediate temperature regime, Figure 2.3. Figure 2.3, shows the temperatures and pressures which envelop the three combustion regimes. Since the fuel spends considerable time in the low temperature regime, it becomes critical to understand the oxidation process in both the low and intermediate temperature regimes at elevated pressures in order to understand the autoignition phenomena.

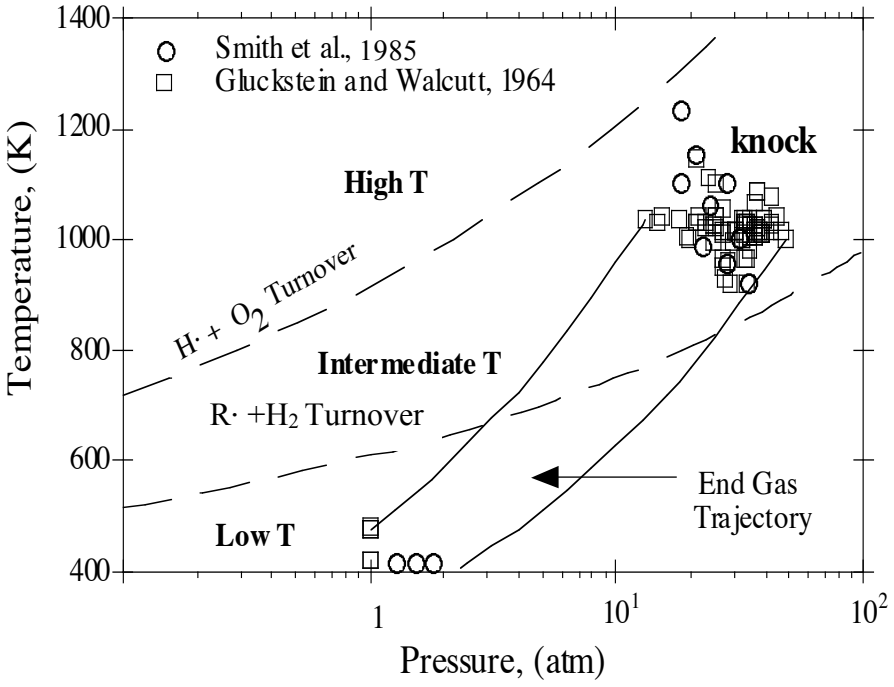

Figure 2.3: Typical SI engine envelope of end gas temperature and pressure histories leading up to the point of knock (Wang, 1999)

Fuel chemical structure has a very large influence on the reactions between 650 and 1000 K. Milovanovic and Chen (2001) explained that low temperature processes are strongly dependent on the size and structure of molecules. For example, at low temperature, the rate of chain branching for n-heptane is much higher than that of iso-octane due to the different structure of the C_7H_{15} radical compared to i-C_8H_{17}. This leads to higher rates of alkylperoxide radical isomerization. It was shown that the low

temperature region is characterized by the reactions of alkylperoxy radicals for smaller hydrocarbon fuels and the reactions of hydroperoxyalkyl radicals for larger hydrocarbon fuels by the formation of stable oxygenated hydrocarbons. The work of Koert (1990) helped to confirm these pathways.

The combustion chemistry that occurs below 1000 K exhibits interesting phenomena such as cool flames, negative temperature coefficient behavior and two-stage ignition. Semenov (1958) introduced the concept of degenerate branched chain reactions to explain the negative temperature coefficient behavior. The general process is that fuel and oxygen first form a pool of relatively unreactive intermediate species. The intermediates subsequently react along one of two paths to form either stable molecules, which lead to non-chain branching, or highly reactive free radicals, which lead to chain branching. The relative importance of either path is influenced strongly by the reaction conditions. Essentially, the oxidation process can be modeled by a sequence of elementary chemical reactions in which radicals are created, propagated, or destroyed. For hydrocarbon with two-stage ignition behavior, the first stage ignition is the result of “cool flame” combustion and NTC behavior, which can be explained in detail by the low temperature chemical analysis. These reactions can be grouped into several fundamental classifications Pilling (1997):

a. Primary Initiation: formation of radicals from parent fuel molecule;

b. Secondary Initiation: radicals formed from other “stable” intermediates;

c. Chain Propagation: reaction where the number of radicals remain unchanged;

d. Chain Branching: reaction where the number of radicals increases;

e. Termination: removal of radicals from the reactive pool.

Benson introduced a general oxidation mechanism for low molecular weight alkanes in the low temperature regime Benson (1981). According to Dryer (1991), this mechanism can be written as follows:

$RH + O_2 + M = R\bullet + HO_2\bullet + M$ (2-1)

$R\bullet + O_2\bullet = RO_2\bullet$ (2-2)

$RO_2\bullet (+M) = \text{olefin} + HO_2\bullet (+M)$ (2-3)

$RH + RO_2\bullet = ROOH + R\bullet$ (2-4)

$RO_2\bullet = R'CHO + R''O$ (2-5)

$RH + HO_2\bullet = HOOH + R\bullet$ (2-6)

$ROOH = RO\bullet + OH\bullet$ (2-7)

$OH\bullet + RH = H_2O + R\bullet$ (2-8)

$R'CHO + O_2 = R'CO\bullet + HO_2\bullet$ (2-9)

$RO_2\bullet \rightarrow$ destruction (2-10)

$HO_2\bullet \rightarrow$ destruction (2-11)

and extended to higher temperature with

$HOOH + M = OH\bullet + OH\bullet$ (2-12)

and for larger alkanes

$RO_2\bullet$ = QOOH• (2-13)

Olefin + $HO_2\bullet$ = epoxide + OH• (2-14)

QOOH• + O_2 = R'CHO + ketone + 2OH• (2-15)

Where RH and R'CHO represent the fuel and aldehydes, respectively, and reactions (2-1) to (2-11) describe the low temperature oxidation mechanism for C_2's and C_3's alkanes, along with other reactions having to be added as temperature increases (e.g., reaction 2-12) and as the initial fuel hydrocarbon molecule becomes larger than 3 carbon atoms (e.g., reactions 2-13 to 2-15). Some of these reactions are not elementary processes (e.g., reaction 2-15) but represent the resultant of several elementary reactions.

A brief description of this mechanism is as follows. In general, alkanes are essentially unreactive below 400 K unless either chemical or photochemical initiators are active. Above 420 K, reaction is initiated by the abstraction of hydrogen from a fuel molecule (RH) by O_2 to form an alkyl radical R• and $HO_2\bullet$ (2-1). This is an initiation step and is called an abstraction reaction. This reaction is highly endothermic, roughly 45-55 kcal/mol depending on the bond energy of the abstracted H atom, and is relatively slow. Due to the variations in the bond energies, the abstraction process is very selective as to which hydrogen is removed and, depending on the abstraction site, a different alkyl radical R• will be formed (Westbrook et al., 1991; Leppard, 1992). At high temperatures (T > 1000 K) beta scission of the alkyl radical is favored, however in the low temperature regime, the next step is that molecular oxygen reacts with the alkyl

radical R• forming alkylperoxide radicals, RO_2• (2-2). Reaction (2-4) and (2-7) represent small molecule chain branching. The chain branching agent, ROOH, is produced by RO_2• reacting with the parent fuel (2-4). ROOH can then decompose to form two radicals OH• and RO• (2-7).

It is important to note that ROOH is the primary branching agent for smaller hydrocarbon fuels. However for larger hydrocarbon molecules (>C3) an important internal isomerization reaction (2-13) will occur and chain branching follows. Reaction (2-15) represents the overall result of this branching. The consumption of the parent fuel molecule is accomplished by reactions (2-4), (2-6) and (2-8). Due to the high reactivity of the hydroxyl radical OH•, the fuel is consumed primarily by the attack of radicals such as OH• via (2-8).

For many hydrocarbons, there is a NTC temperature range, which is usually between 600 to 800 K. This is a complicated phenomenon and is described briefly in terms of the mechanism (2-1) to (2-15). As temperature increases, reaction (2-2) becomes effectively reversible. The alkylperoxide can further decompose (2-3) to produce alkenes, HO_2•, and relatively stable species. Since (2-3) produces alkenes and HO_2•, relatively stable species at these temperatures, it has an inhibiting effect on the overall reaction rate. The mechanism shift explains the decrease of overall reaction rate with the increase of temperature (due to effectively reversible reaction (2-2) and non-chain branching reaction (2-3)), known as negative temperature coefficient (NTC) behavior. As the temperature is further increased into the intermediate temperature regime, the decomposition of hydrogen peroxide becomes the dominant chain branching path (2-12) and the reaction again accelerates.

Based on this work, subsequent research clarified the oxidation processes and resulted in a general oxidation mechanism for hydrocarbons. A schematic diagram for the branching pathways of low and intermediate temperature regions is shown in Figure 2.4.

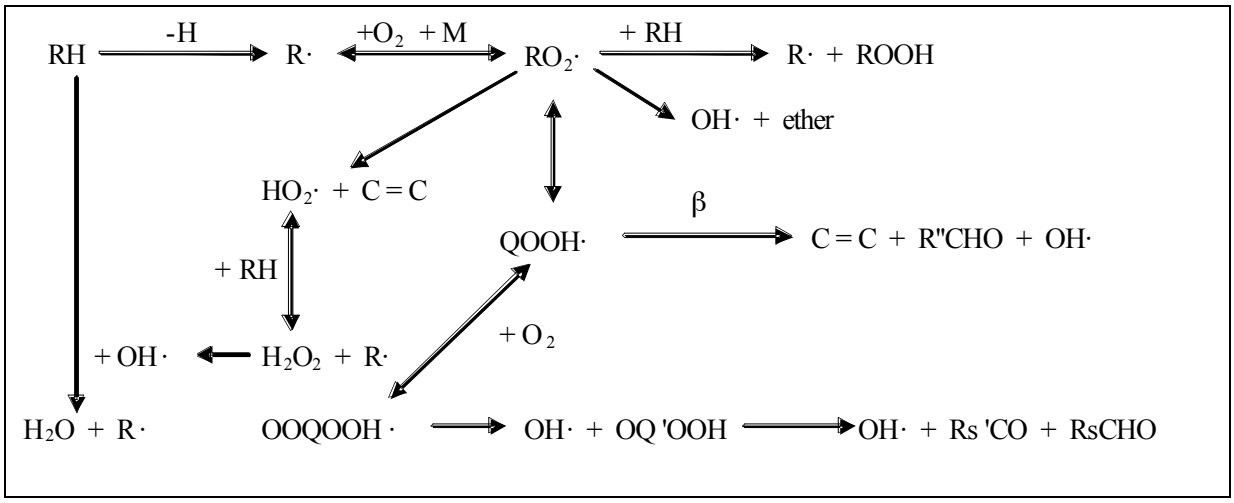

Figure 2.4: Branching pathways for hydrocarbon oxidation at low and intermediate temperature (Westbrook et al., 1991)

The intermediate temperature region is dominated by the reactions of HO_2• radicals and the characteristic stable products are alkenes, stable oxygenated hydrocarbons, and methane. When the process reaches the high temperature region, the reactions are dominated by OH•, O•, and H• radicals, and unimolecular decomposition of alkyl radicals, via beta-scission, becomes important.

2.3.2 DTBP Chemistry

Figure 2.5 shows the proposed mechanism for the decomposition of DTBP (Griffiths et al., 1990). According to this description DTBP thermally decomposes into two t-butoxy radicals, in the 600 to 650 K temperature range, ($C_3H_{18}O_2 \rightarrow CH_9CO\bullet + CH_9CO\bullet$). These radicals internally rearrange very quickly, primarily forming acetone (C_3H_6CO) and a methyl radical ($CH_3\bullet$). The acetone is stable and lingers in the cycle until the main ignition promoting reactions commencing at temperatures of approximately 1000 K. Unlike acetone, the methyl radicals undergo oxidation on a microsecond timescale to yield molecular products (e.g., formaldehyde, methanol and hydrogen peroxide) and to generate heat. There is no direct evidence that chain propagation is initiated from this secondary oxidation of methyl radicals and no chain branching occurs (Griffiths et al., 1990). The subsequent oxidation of formaldehyde and the decomposition of hydrogen peroxide occur readily at temperatures in excess of 850 K, and these reactions may promote further chain initiation.

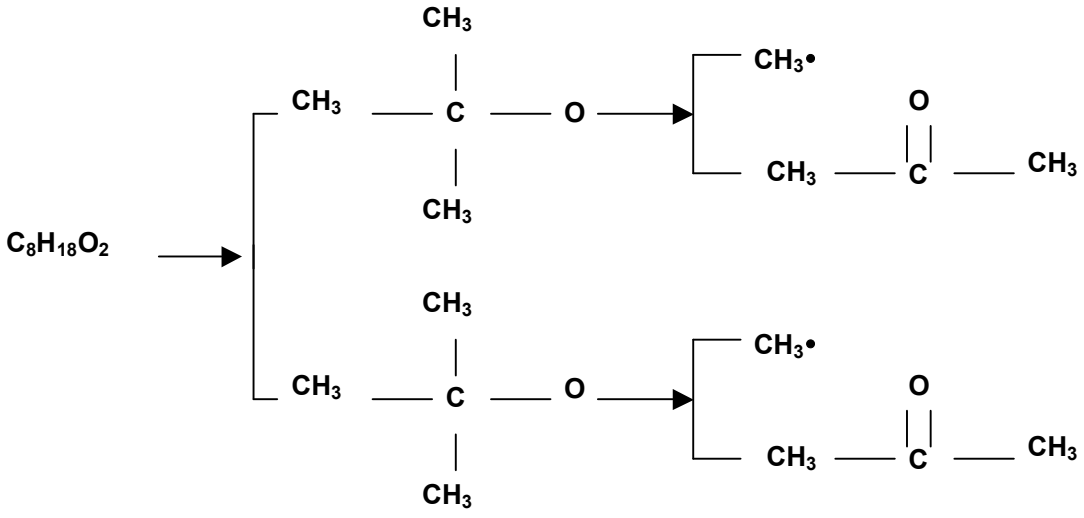

Figure 2.5: Decomposition of DTBP at low temperatures (Griffiths et al., 1990)

2.3.3 Propionaldehyde Chemistry

Litzinger (1990) reviewed the effect of aldehyde addition on the knock chemistry in engines, and found propionaldehyde promotes reactivity, triggering more knock behavior. Figure 2.6 shows the major pathways of propionaldehyde oxidation at T>550 K (Kaiser, 1987). Propionaldehyde is consumed primarily by OH, HO_2, or alkoxy radicals to form the propionyl radical (C_2H_5CO). The ratio of CO and CO_2 is controlled by competition between the addition of O_2 to the propionyl radical and its unimolecular decomposition. Subsequent reactions of $C_2H_5CO_3$ generate $C_2H_5CO_2$, which can decompose to form carbon dioxide. This pathway forms an ethyl radical (C_2H_5). The ethyl radical can react with O_2 to produce $C_2H_5O_2$ in a reversible reaction or C_2H_4. Reactions of $C_2H_5CO_2$, form ethylhydroperoxide ($C_2H_5O_2H$) or ethoxy radicals (C_2H_5O). The ethoxy radical can react with propionaldehyde or decompose unimolecularly to promote the remaining oxygenated species, CH_3O_2H, CH_3OH, and CH_2O.

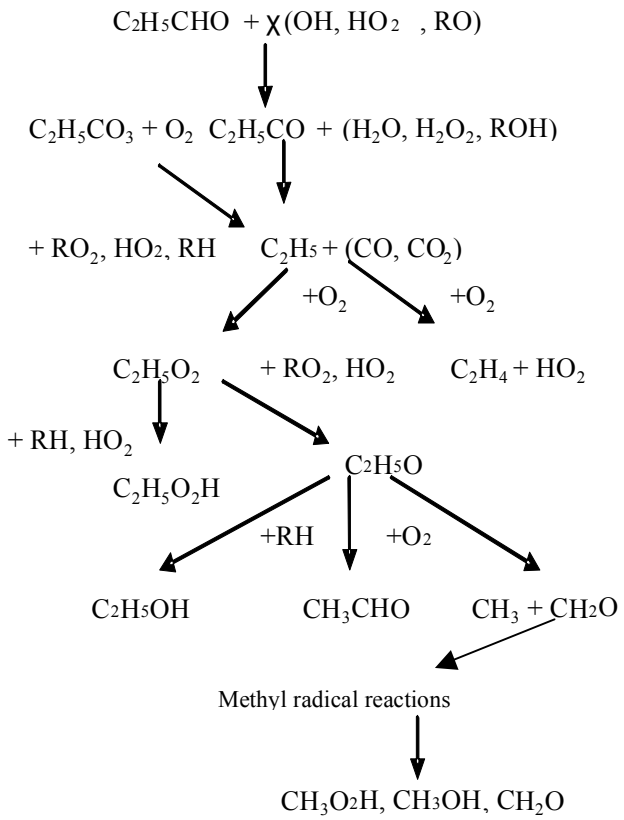

Figure 2.6: Flow diagram of the major reaction paths of propionaldehyde oxidation for temperatures greater than 550 K (Kaiser, 1987)

2.4 Closure

This chapter summarized some of the key work that has been done in the area of HCCI research. Some of the advantages of HCCI operation were highlighted such as low levels of NOx and PM emissions, as well as fuel flexibility, albeit with a slight increase in CO and THC emissions. The limited operation range with HCCI was discussed as well, along with various methods that can be used to extend the limits of stable operation.

The various methods of HCCI control that have been investigated were discussed as well. Some methods included using EGR and other operation parameters such as equivalence ratio and intake charge temperature. Using fuel additives is another way that researchers are studying to alter the combustion process.

Modifying engine operating and design parameters using VVT and VCR are also ways to alter the combustion process to deal with the control issues facing HCCI. VCR and VVT are particularly attractive because their time response could be made sufficiently fast to handle rapid transients.

Also chemical kinetics was highlighted since HCCI engines with no direct initiation of combustion by spark plugs or fuel injection timing control combustion phasing by chemical kinetics.

This review has shown the value of fuel composition as a technique for controlling HCCI operation. It has also highlighted the need to determine the mode of action of DTBP and propionaldehyde in controlling autoignition. The next few chapters will present the work performed to satisfy this need.

CHAPTER 3. EXPERIMENTAL FACILITIES AND GENERAL TEST METHODOLOGY

The experimental portion of this work was carried out in a four-stroke engine system modified to run under HCCI conditions. It aimed at elucidating the interaction of both DTBP and propionaldehyde with hydrocarbon fuels under HCCI conditions. The facility and the experimental methodology employed are described in the following sections.

3.1 The Engine Facility

The HCCI engine experiments in this study were conducted in a newly developed Cooperative Fuel Research (CFR) engine test facility at Drexel University. A schematic of the complete engine test facility used in this study is shown in Figure 3.1. The diagram illustrates the main components of the facility: the engine, the dynamometer, intake system, the exhaust system, fuel injector, data acquisition system, and gas analyzers.

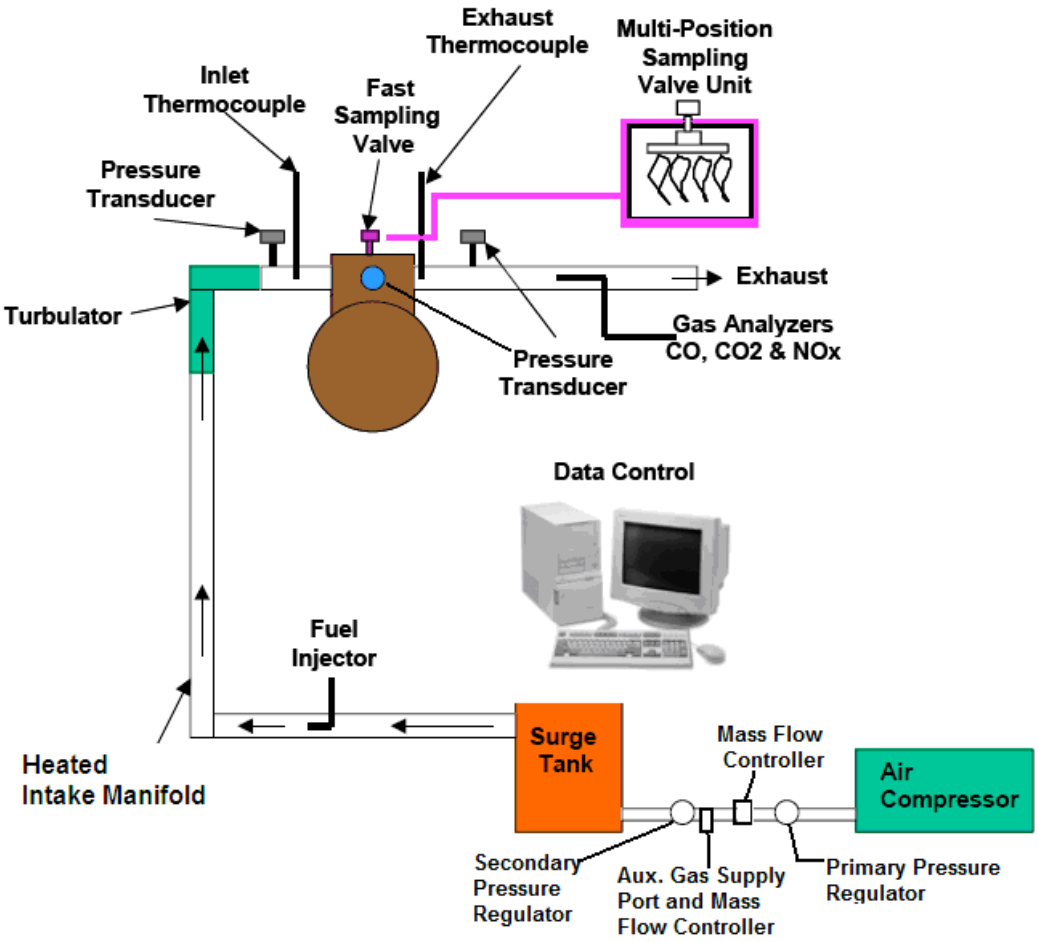

Figure 3.1: Single cylinder engine schematic

3.1.1 Research Engine

The engine is a 611.6 cm^3 displacement, single cylinder, four-stroke, water cooled Waukesha Motor Corporation Model 48D CFR engine direct coupled to a GE CD258AT DC motor/ generator dynamometer. The engine has an 8.255 cm cylinder bore and an 11.43 cm piston stroke, with a movable cylinder head, which allows variation of the compression ratio from 4:1 to 18:1. Detailed engine specifications are listed in Table 3.1.

Table 3.1: Engine geometry

Stroke	114.3 mm
Displacement	611.6 cm^3
Compression Ratio	4:1-18:1
Intake Valve Opens	10 deg bTDC
Intake Valve Closes	34 deg aBDC
Exhaust Valve Opens	40 deg bBDC
Exhaust Valve Closes	15 deg aTDC

3.1.2 Cylinder Cooling

The engine cylinder is cooled using a liquid water-cooling system. This system consists of a heat exchanger (Mayer Autotherm) that is capable of varying liquid coolant temperature. External piping is connected to the Autotherm and mounted to the cooling jacket that surrounds the cylinder head. The Autotherm is capable of varying the coolant temperature from room temperature to up to 150° Celsius. The Autotherm circulates stored water through the system and has an integrated temperature controller which draws in fresh cooler water when it needs to decrease the coolant temperature, thus allowing the coolant temperature to remain constant. Figure 3.2 shows a diagram of the cylinder head, and cooling jacket.

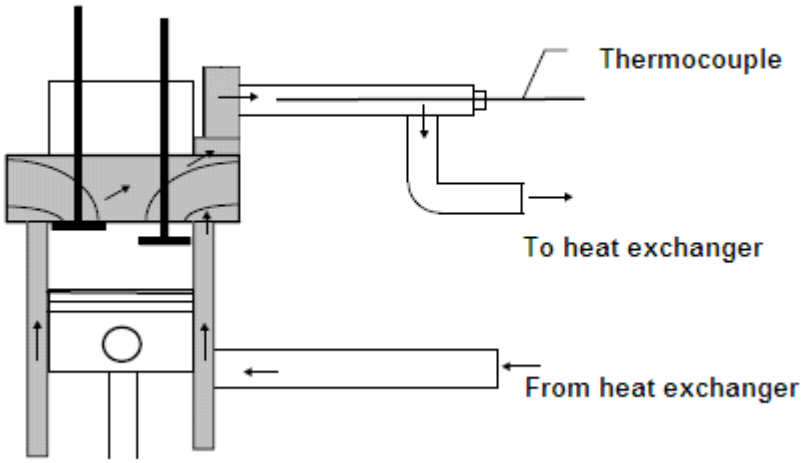

Figure 3.2: Diagram of cooling jacket and external piping

3.1.3 Engine Dynamometer

The engine is controlled by a General Electric DV-500 electric controller, with a DV-300 control module. The controller operates on 480 VAC, three phase power, and the control module converts the AC electrical supply to 300 VDC power. The control module is wired to a General Electric, 20 horsepower, 33 ampere, and direct current motor/generator dynamometer with a rated maximum speed of 3000 revolutions per minute. Under fired engine conditions, the dynamometer maintained the speed within ±5 rpm of the set conditions. A flywheel is connected to the crankshaft in order to reduce cyclic variability and speed variations, cause by the intermittent combustion events.

3.1.4 Intake System

The intake system includes the basic air and fuel supply to the engine, along with the ability to control its parameters and to measure its behavior. The intake air is supplied by a laboratory compressed air system at a pressure of 0.56-0.69 MPa, Figure 3.3. It is filtered and the moisture content is controlled, which enhances the ability to replicate intake conditions. The use of a compressed air supply allows exploration of engine performance under supercharged conditions.

In typical operation, the main air supply pressure is reduced to 0.35 MPa using a high capacity regulator. The regulated air is routed through a Porter Instruments model 114 mass flow meter. This mass flow meter measures intake flow up to 1000 slpm with an accuracy of ±1 slpm, which is sufficient to allow a maximum engine speed of 3000 rpm.

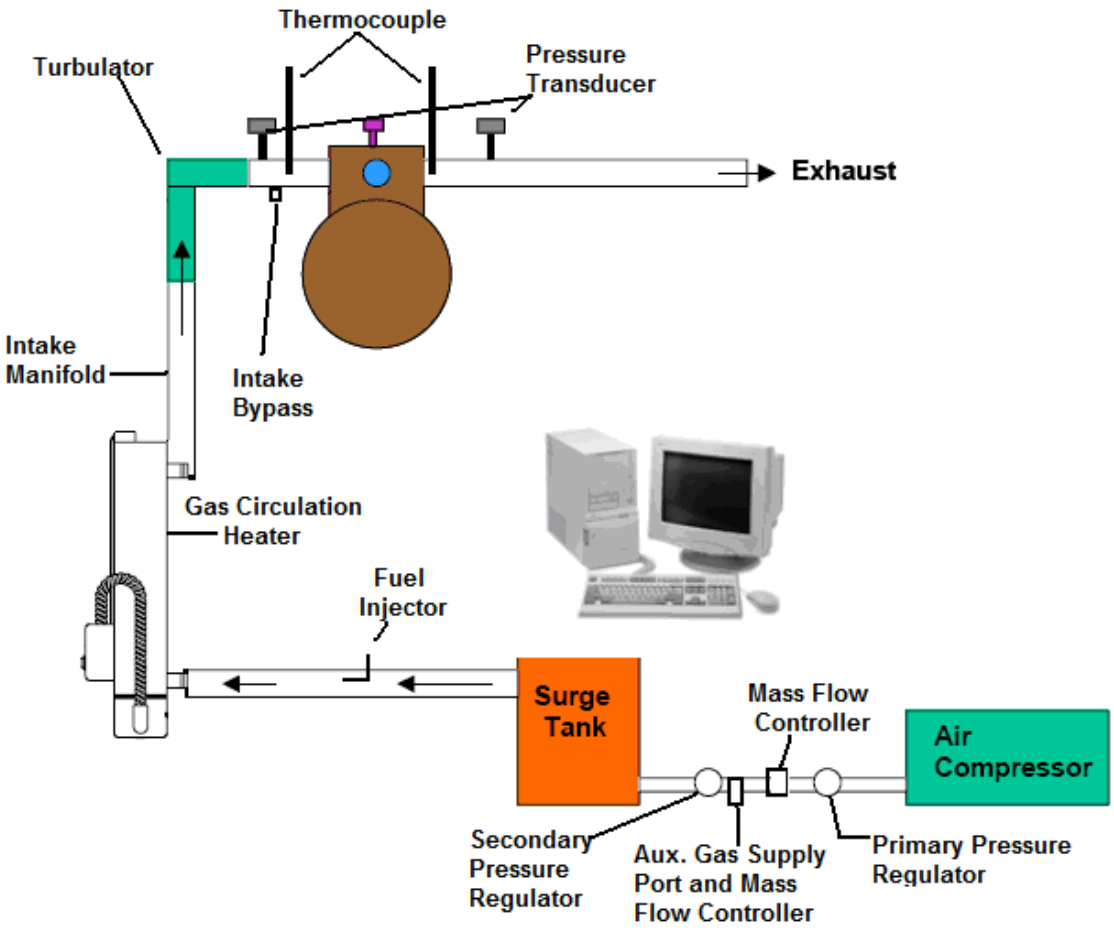

Figure 3.3: Detailed intake system schematic

An auxiliary gas supply port was incorporated into the air delivery system for the purposes of simulating the effects of external exhaust gas recirculation (EEGR). The flow to this port is controlled by a Porter Instruments model A202 mass flow controller operating at 50 psig. If EEGR is called for this controller can meter a maximum of 1000 slpm of gas with an accuracy of ±0.1 slpm. This auxiliary port joins the output flow of the mass flow meter, prior to final pressure regulation and delivery to the engine.

The final intake manifold pressure is adjusted by the secondary pressure regulator. This regulator, in conjunction with the intake pressure transducer, allows the desired intake pressure to be set and maintained. A 0.10 m^3 gallon pressure vessel was used as the surge tank to buffer intake air oscillations from the engine, and allow for accurate mass flow measurement and control.

A Chromalox 5 kW gas circulation heater (Model GCHMTI) was used to preheat the inlet air stream. This heater is a single zone immersion heater. The heating elements allow for uniform intake heating. It was monitored by a computer and was controlled by a Chromalox temperature controller (Model # 50A-25-23-29).

The engine intake temperature and pressure were monitored by a 1.5 mm type-K thermocouple and OMEGA PX656 pressure transducer, respectively, located right before the inlet valve. The intake piping is wrapped with bead heaters and then with fiberglass insulation to limit the heat loss. This is important since intake temperature is critical in maintaining the vaporization of the fuel. A large temperature drop can cause the fuel to condense in the intake system, resulting in a change in mixture composition before delivery to the engine.

Air/fuel mixing is achieved directly after the intake heating. The test fuel is injected by a standard 2.65 g/s (max) automotive fuel injector (Model 327-C). The fuel injector is operated by a 12 VDC power supply, controlled by a computer virtual interface. Post injection flow passes through a 0.40 m long turbulator. The turbulator contains six sets of oppositely mounted vanes, which the intake air and atomized fuel flow through in order to promote and achieve a homogeneous mixture for delivery to the

engine. There is an intake bypass valve, which allows complete purging of the inlet manifold when switching fuels.

3.1.5 Exhaust System

The engine exhaust system, Figure 3.4, is composed of two sub-systems, the main engine exhaust and the engine crankcase breather. The main engine exhaust is piped out of the laboratory through a roof vent. The main exhaust pipe also has outlet piping for gas analysis equipment. The crankcase breather, which operates at atmospheric pressure, was also vented to the roof through a different pipe.

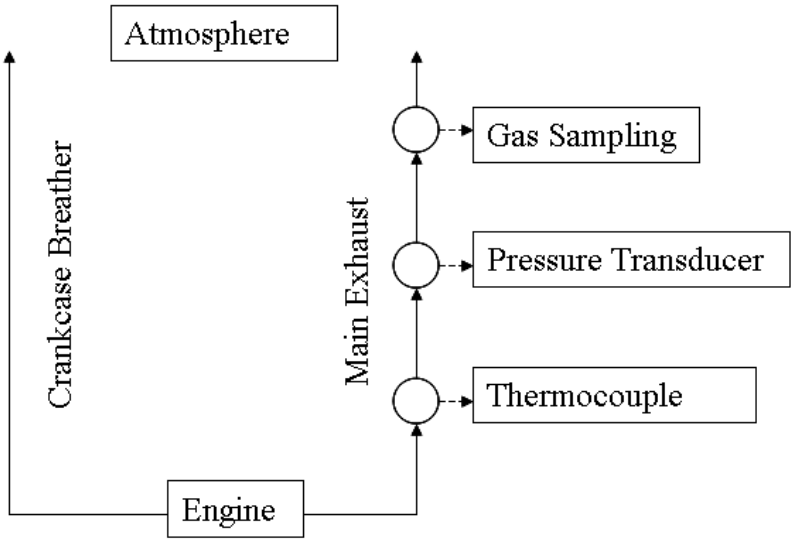

Figure 3.4: Exhaust system schematic

The main engine exhaust line has a probe that extends 0.30 m along the centerline of the exhaust pipe 1 m downstream from the exhaust valve. This port allows

the gas analysis equipment to extract a sample from the center of the exhaust flow away from the boundary layer at the wall.

The exhaust temperature is taken as the exhaust gases leave the cylinder head, via a 1.5 mm type-K thermocouple. The exhaust pressure is measured with a 0.69 MPa Omega Engineering pressure transducer. This range was selected to allow for potential future experiments with restricted exhaust flow. The pressure transducer is located two feet away from the engine to reduce temperature effects on the measurements.

Two lengths of braided flex hose are used in the exhaust piping, to account for the cylinder head movement. High temperature, vibration resistant pipe sealing compound, was used to prevent leakage from threaded connections.

3.1.6 Fuel Delivery System

A key to an engine facility is the deliver of an accurate, precise, and repeatable mass of fuel to the cylinder. As the fuels of this work were liquid hydrocarbons, the system had to accommodate liquids. The system consists of a fuel tank, fuel pumping system, and fuel flow controller. Fuel is stored in a stainless steel pressure vessel. During operation fuel is delivered by pressurizing the vessel with nitrogen. Surface reactions in the vessel are not a concern for the fuels used in this work.

Fuel composition is set by mixing the desired hydrocarbons in an external container and then pouring the mixture into the stainless steel vessel. Gaseous nitrogen is delivered to the stainless steel cylinder via a gas cylinder. The head pressure is set to

0.28 MPa and is maintained for all tests. The pressure is monitored by an external pressure gauge attached to the stainless steel vessel.

Liquid fuel at 0.28 MPa is supplied to an electromagnetic fuel injector. The fuel injector is controlled by a 12 volt square wave that is generated by a LabView Virtual Instrument (VI). When the square wave is at 12 volts, the fuel injector opens, when it is at a value less than 12 volts the fuel injector closes. The LabView VI generates a square wave with a specific frequency depending on what equivalence ratio is needed. A schematic of the fuel delivery system is presented in Figure 3.5. The fuel injection system is capable of maintaining equivalence ratio within 5 % of the setpoint.

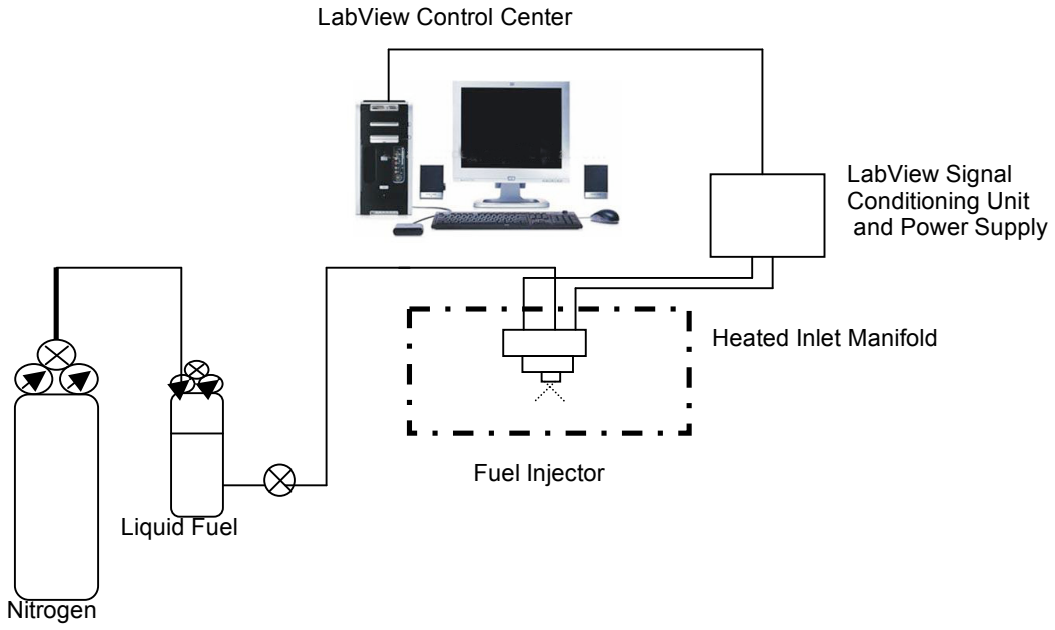

Figure 3.5: Engine fuel delivery system

3.1.7 LabView Engine Control

LabView was used to acquire all of the data in our test facility. Using LabView, we created Virtual Instruments (VI's) to measure engine parameters from various devices. The LabView program monitored outputs such as intake and exhaust temperatures and pressures. LabView also measured flow rates through the mass flow meters. The LabView program incorporates many different VI's (sub VI's), and stores them in one large VI, that serves as an interface. In order to ensure that interference from other laboratory equipment and long transmission distances are not affecting our LabView signals, a National Instruments model SC-2345 signal conditioning box, and various modules used for signal filtering were installed to serve as an interface between our measurement devices and our PC. The modules were chosen based on the output range of each device.

The base VI measures intake and exhaust temperatures and pressures, fuel flow rate, the outputs from the mass flow controller, and calculates equivalence ratio. LabView controls fuel flow rate by controlling the frequency of the electromagnetic fuel injector. Using the reading for the mass flow controller and the desired equivalence ratio the VI determines the amount of fuel to be added and selects the frequency of the injector (determined by prior calibration of the fuel injector).

Alarms were also created to monitor inlet and exhaust temperatures, and equivalence ratio. They alert the user when the facility is not operating within set allowable parameters.

3.2 Data Measurement System

The engine facility is capable of measuring in-cylinder pressure at a given crank angle degree (CAD). Combustion temperature is not measured directly. Using the in-cylinder pressure data, combustion temperature can be calculated. Using LabView a data acquisition system was developed to monitor the in-cylinder pressure. The following section describes in detail the individual components of the data measurement system.

3.2.1 In-cylinder Pressure

The analysis of the pressure and parameters derived from the pressure can tell us a great deal about the complex process of combustion. A Kistler model 7061B pressure transducer was used to monitor the in-cylinder pressure in the engine. The transducer was mounted in the port of the cylinder head used in a typical knock testing installation for the detonation pick up (knock sensor). The output of the signal is amplified by a Kistler model 5010B amplifier and converted into a voltage and conditioned before display. The pressure data are then exported and stored in a Microsoft Excel spreadsheet by another VI of the engine controller.

3.2.2 Crank Angle

To obtain crank angle resolved data, a Gurley Precision Instrument model 9125 shaft encoder was used. The encoder outputs a clock signal of 3600 pulses per revolution, and a trigger signal once per revolution. A mounting bracket was used to attach the shaft encoder to the Waukesha engine via a reduced diameter shaft. The

result of mounting the encoder to a reduced shaft is a clock signal resolution of 1/5 crank angle degree (CAD).

The bracket was designed to allow for the rotation of the encoder to adjust the timing of the tripper pulse to engine's top dead center (TDC). The TDC pulse and the 1/5 CAD resolution of the clock were used as the data acquisition clocking pulses to acquire the pressure data and identify the pressure at TDC.

3.2.3 Data Acquisition System

The requirements of a combustion data acquisition system are to record cylinder pressure data and align it with CAD. This is achieved by using a triggered acquisition, (acquisition does not begin until TDC on the exhaust stroke is reached). Data starts being recorded as fuel is being drawn into the combustion chamber. Details of data analysis can be found in the section marked, Section 3.5, Data Analysis.

3.3 Gas Analysis System

3.3.1 Fast Acting In-cylinder Sampling Valve

In-cylinder gas samples can be extracted by an electromagnetic sampling valve located in the center of the cylinder head. The sampling valve is a Tsukasa Sokken model GSD-10 type unit. The schematic of this valve is shown in Figure 3.6. A valve rod is spring fit into the seat of the valve body at one end and has an electromagnet at the other end. When the electromagnet is energized, it lifts the needle from the seat enabling cylinder gas sample flow through the valve into the outlet line. A LabView

pulse generator controls the starting CAD and the duration of the valve opening, respectively. To obtain high resolution of the species evolution measurement, short opening duration is desirable. This valve has a preset minimum opening time of 3 ms. However, by adjusting the spring force, which controls the needle lift, the sampling valve can operate at a minimum opening time of 2 ms, which is around 3 crank angle degrees at 600 RPM engine speed. The opening duration is monitored using an LED source and receiver pair. When the valve is energized the needle lifts breaking the LED beam. The voltage from the LED receiver is monitored on an oscilloscope. Although this capability is currently functional, it was not used in the present work. It will however be used in future studies

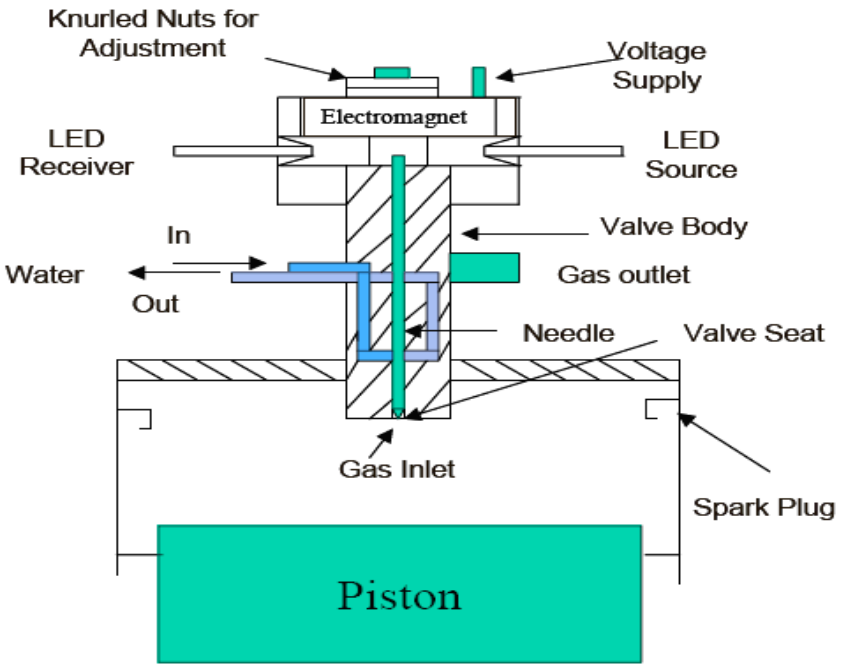

Figure 3.6: Fast acting in-cylinder sampling valve schematic

3.3.2 Sample Storage Cart

The exit of the sampling valve is connected to a three-way valve that enables a vent line to flush the system with nitrogen gas, see Figure 3.7. The flow then passes through heated 0.64 cm (0.25 in) Teflon tubing connected to a mechanical metal bellows pump that creates subatmospheric conditions. The bellows pump enables flow into a 4-port Valco Instrument valve. During the loop-fill process the 4-port "sample" position allows flow into a multi-position sample storage unit, through a backpressure valve, and out the exit port. The "GC" position on the 4-port valve enables flow from the storage unit loop into the gas chromatography system for speciation. The Multi-position

Sample Valve (MSV) unit consists of a 32-port Valco Instruments valve housed in an oven to maintain constant sample temperature. The valve is configured with 15 stainless steel sample loops with one pair of ports used as a transfer loop. Each loop has an approximate volume of 10 cm3. Between samples the system is purged with hydrogen for at least 3 minutes. At each selected CAD, samples are collected in one loop and pressurized to 170.2 kPa (10 psig) by partially closing the “back pressure” valve trapping the sample being pressurized by a bellows pump.

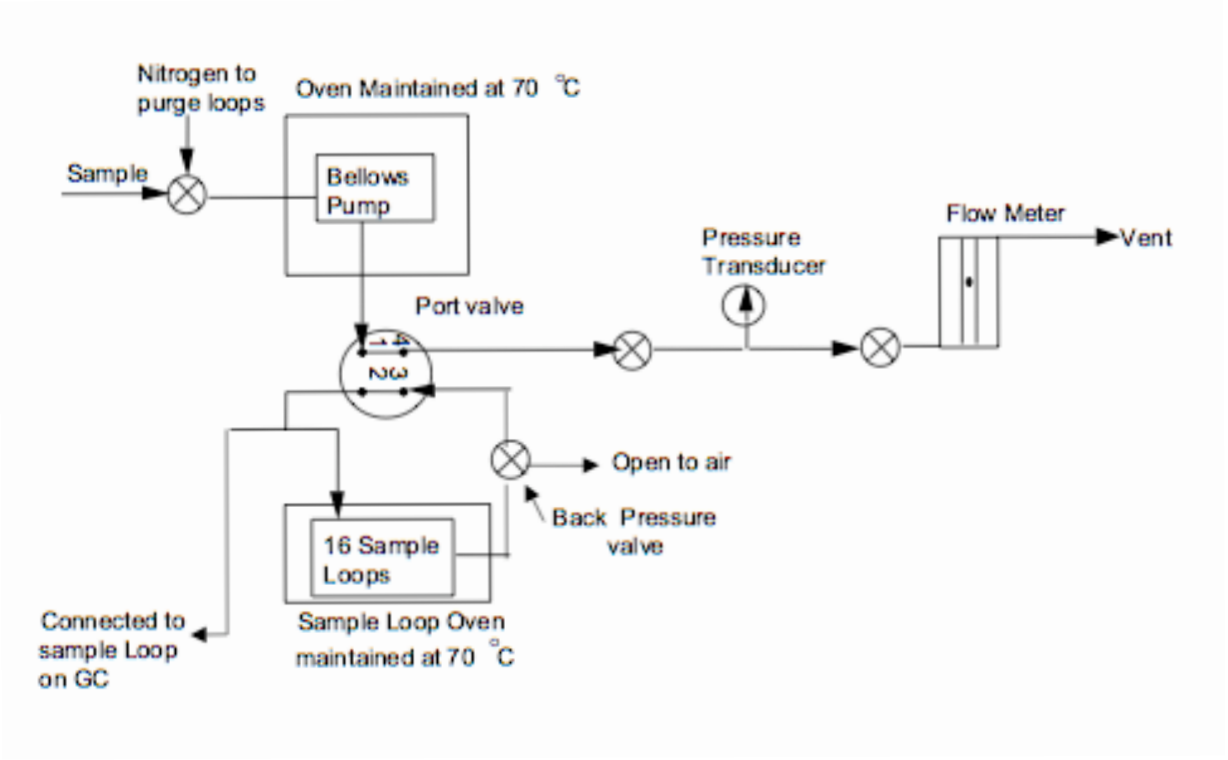

Figure 3.7:Schematic of flow path in the multi loop sampling cart in the GC inject position

The sampling time requires a period of 60 to 100 engine cycles. After filling one loop, the 32-port valve is rotated by means of an air-actuation unit that places the next sample loop in-line with the vacuum pump and sampling valve and the backpressure valve is opened to expedite purging of the system. A digital display located on top of the storage unit indicates the number of the loop being used. The storage system (Figure 3.8) was maintained at 344 K, a temperature our previous studies have shown reduces condensation and absorption of the samples (Filipe, 1992), especially for formaldehyde. The entire storage unit is located on a cart, which can be transferred to the GC system for sample speciation, once the sampling process is completed.

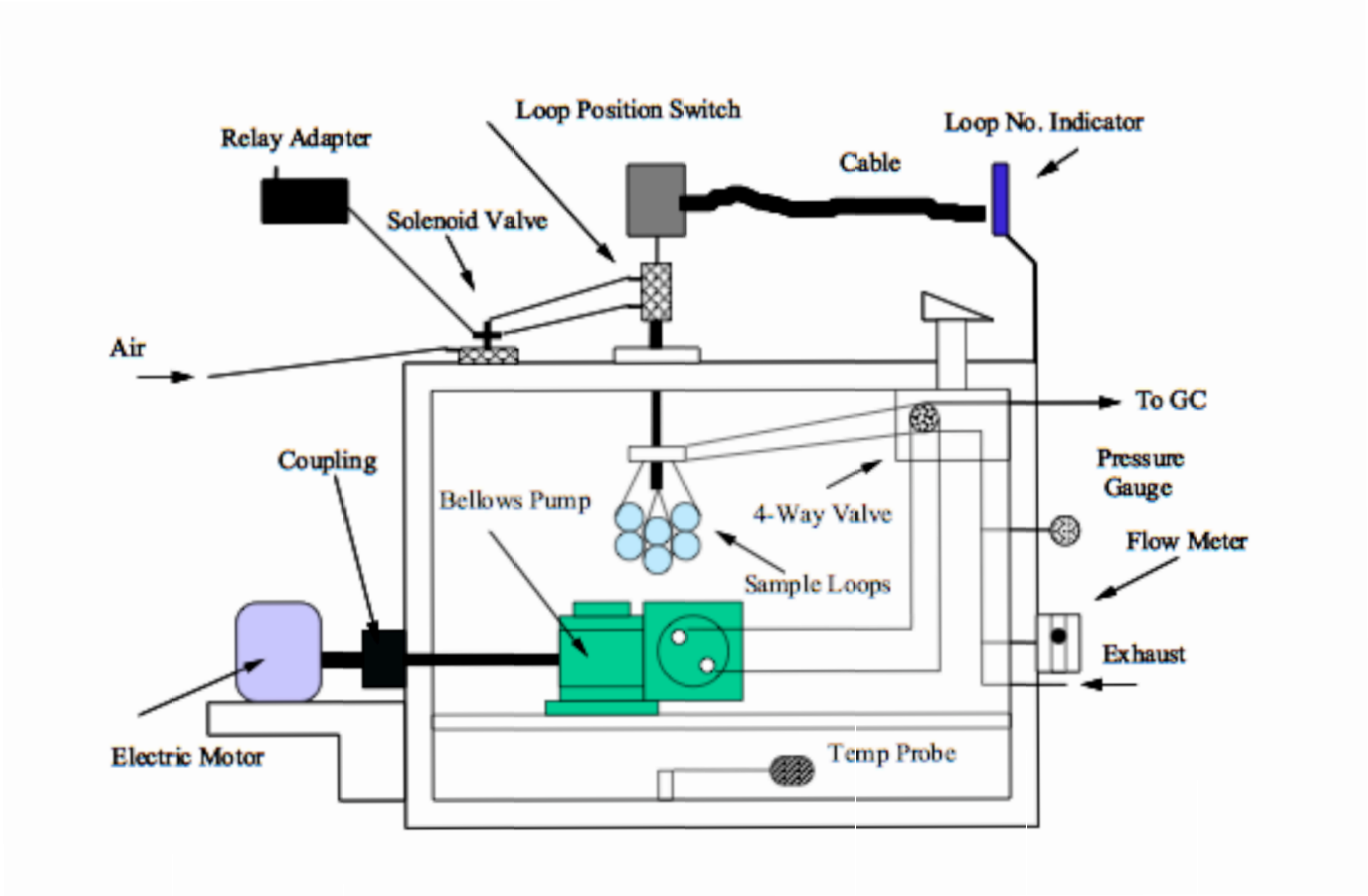

Figure 3.8: A schematic of the sample storage cart

3.3.3 GC analysis

The chemical analysis of gas samples was accomplished using a Varian 3600 gas chromatography (GC), equipped with two flame ionization detectors (FID). Figure 3.9 presents a schematic of the GC system. Sample loop(s) is (are) installed in a valve enclosure which is maintained at 125°C and located on the top of the Varian 3600 GC analyzer. The sample loop(s) can either be connected to a standard sample preparation cylinder for calibration or to the MSV system for measurement of the in-

cylinder gas samples. The amount of sample injected into the GC is controlled by a manostat, which uses a mercury column to maintain the sample loop(s) at the selected pressures. The typical manostat pressure to be used in this study was 300 torr. An important task for GC analysis was to develop appropriate GC techniques for species measurements. In this thesis, the two subjects used different fuels and the gas samples were analyzed by different GC techniques. The detailed GC techniques will be discussed later.

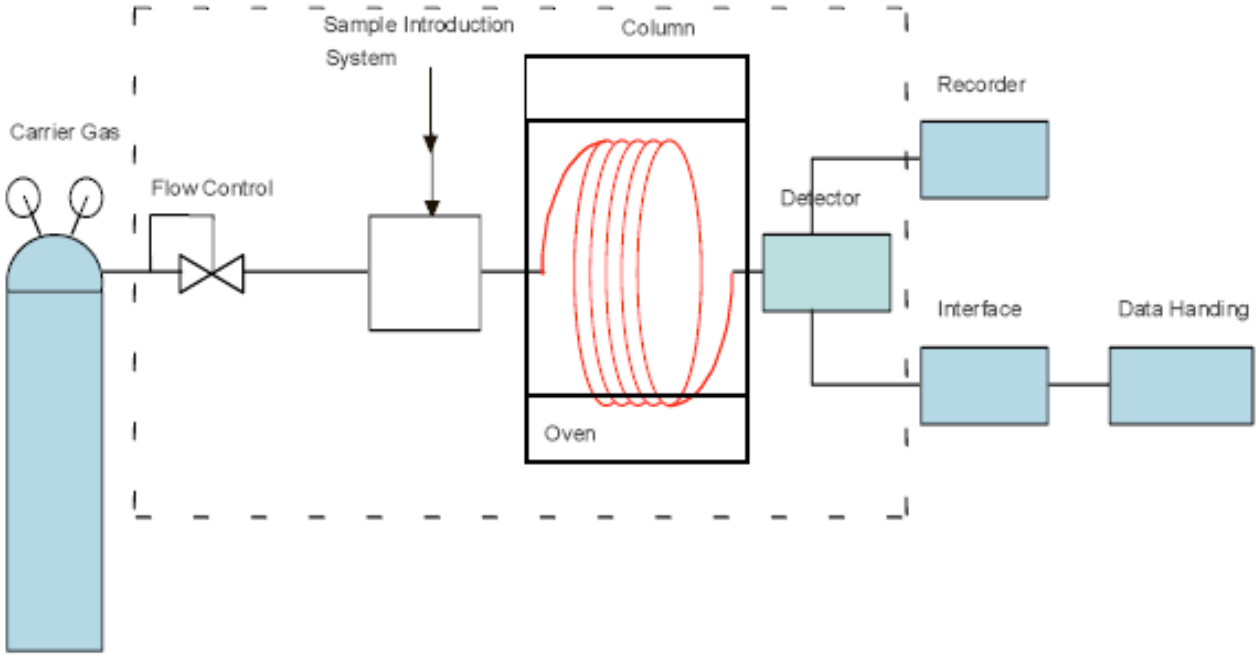

Figure 3.9: Schematic of Varian 3600 GC

3.4 Emissions Bench

In order to conduct the emissions research and monitor the engine operating conditions, an existing exhaust gas analysis bench was used. A schematic of this set up is shown in Figure 3.10. A KNF Neuberger model UN035ST.11 heated head pump is used to extract a sample from the exhaust manifold and supply it to the various gas analyzers (Table 3.2). A 40 μm particulate filter is placed before the inlet of the pump to trap particulate matter. The exhaust from the gas analyzers is vented to the roof of the laboratory. All the lines in the sampling system are heated to 70°C to minimize condensation of the sample. When samples are taken for GC analysis, the flow from the in-cylinder sampling valve is sent to a KNF Neuberger pump (model UN726.3 ATP), which is used to pressurize the loops in the multi loop sample loop cart (MSV) to about 170 kPa.

Table 3.2: Specifications of exhaust emissions meters

Species	Model	Range of Measurement	Technique
CO_2/ CO	Siemens Ultramat 22P Gas Analyser	0-20 % and 0-3 %	Non-Dispersive Infrared Absorption
NOx	Thermo Electron 12A Gas Analyzer	0-10,000 ppm	Chemiluminescent
HC	J.U.M. FID VE 7	0-10 %	Flame Ionization
O_2	Teledyne Analytical Model 326RA	0-25 %	Electrochemical

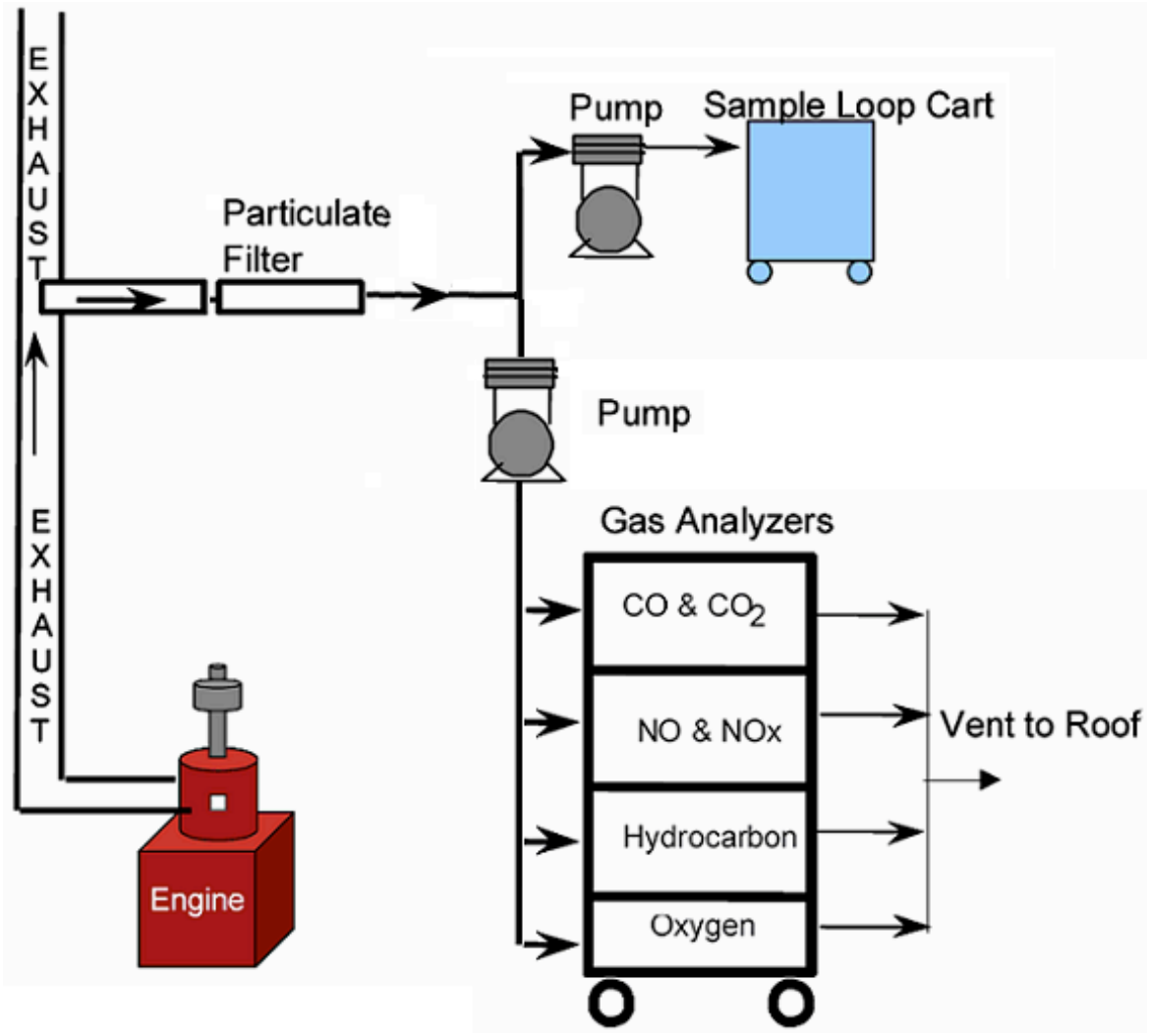

Figure 3.10: Engine emissions bench

3.5 Data Analysis

LabView was used to analyze recorded cylinder pressure data and provides processing and analysis functions that are required for combustion analysis via Excel. The following section will discuss the features of the software and the methods that have been chosen for analysis.

Start of Ignition and Ignition Delay Definition

A typical cylinder pressure trace is shown in Figure 3.11 the first stage pressure rise (P_1), and the location of the start of first stage, X_1, and second stage, X_2, ignition are easily discerned. In this work, start of ignition is considered to be where the main heat release event occurs, X_2, and ignition delay is the time in CAD it takes for the main ignition event to occur after first stage ignition, X_2- X_1. For fuels that exhibited single stage ignition, ignition delay was not defined.

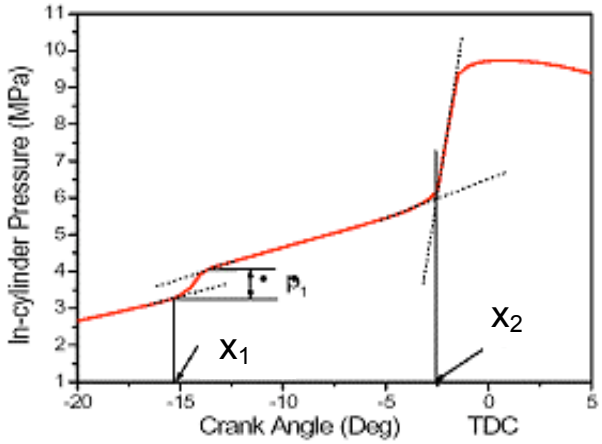

Figure 3.11: A typical pressure trace showing two-stage ignition

Start of Combustion

Under HCCI engine operation, there is no direct initiation of the start of combustion. Thus, it was crucial to determine a permanent way of extrapolating where the start of combustion was in terms of crank angle degree.

For this research the start of combustion was taken to be the start of the main combustion event. The exact position was measured by drawing a line tangent to the pressure trace before the main combustion event (hot ignition) and a line tangent to the

pressure trace as the pressure is rising due to heat release. In some cases two-stage ignitions can be observed, in this case the method of finding the start of combustion remains the same, where the second heat release event is the main combustion event.

In-cylinder Pressure Analysis

The LabView data acquisition software sees two TDC pulses per four-stroke engine cycle. Thus, it was necessary to align the correct TDC signal so that the peak pressure TDC does not start the data acquisition. The acquisition should start at the TDC signal that occurs at the beginning of the intake stroke so that the peak pressure occurs at the 360 crank angle degree mark when there is no combustion occurring. Absolute cylinder pressure is determined by setting the pressure at the inlet valve closing position to that of the inlet manifold pressure during post processing.

Rate of Pressure Rise

The rate of pressure rise is a parameter used to evaluate combustion. This parameter is calculated in Excel using a simple numerical differentiation.

$$\frac{dp}{d\theta} = \frac{p_{i+1} - p_{i-1}}{\theta_{i+1} - \theta_{i-1}} \qquad \text{Eqn. 3.1}$$

High rates of pressure rise rate may help identify the occurrence of engine knock. Engine knock occurs when the fuel-air mixture ignites before the flame front can reach it. In the case of strong knock, the uncontrolled ignition of the mixture causes it to burn in an irregular and explosive manner. A strong pressure wave results and a sizeable force is suddenly exerted on the piston and the walls on the engine. This can occur in the end

gas in the engine cylinder. As a result of engine knock, care should be taken when evaluating in-cylinder pressure data. Also, pressure traces can show some interference from other electronic devices. Therefore good quality acquisition, filtering and conditioning is required for the data to be useful.

Indicated Mean Effective Pressure (IMEP)

The area enclosed by the PV diagram of an engine is the indicated work done by the gas on the piston. The IMEP is a measure of the indicated work output per unit swept or displacement volume, a parameter independent of the size and number of cylinders in the engine and engine speed. IMEP is defined as:

$$IMEP = \frac{W_i}{V_s} \qquad \text{Eqn. 3.2}$$

where Wi is the indicated work in Newton meters and Vs is the swept volume per cylinder in cubic meters.

The formula used for calculating IMEP in this work is as followed:

$$IMEP = \frac{\Delta\theta}{V_s} \sum_{-=n_1}^{n_2} \mathrm{p(i)} \frac{dVi}{d\theta} \qquad \text{Eqn. 3.3}$$

where

p(i) is cylinder pressure at crank angle i in Pascal

V(i) is cylinder volume at crank angle i in cubic meters

V_s is cylinder swept volume in cubic meters

n_1 is BDC induction crank angle

n_2 is BDC exhaust crank angle

Mean Gas Temperature

Another parameter that is useful for combustion data analysis is the mean gas temperature. Mean gas temperature can be used to calculate start of combustion, cylinder gas temperature, and is required for the calculation of heat release. This section goes through the procedure of calculating the mean gas temperature.

Recall that for a polytropic process

$$pV^n = const \qquad \text{Eqn. 3.4}$$

So for a known reference location, such as inlet valve closure:

$$p_{ref}V_{ref} = nRT_{ref} \qquad \text{Eqn. 3.5}$$

Rearranging gives:

$$\frac{T_{ref}}{P_{ref}V_{ref}} = \frac{1}{nR} \qquad \text{Eqn. 3.6}$$

To calculate the temperature at an arbitrary position between inlet valve closure and exhaust valve opening:

$$T_{calc} = P_{calc} V_{calc} \frac{1}{nR} \qquad \text{Eqn. 3.7}$$

Assuming n and R remain constant, and no mass loss around the piston; equation 3.6 can be substituted into equation 3.7:

$$T_{calc} = P_{calc} V_{calc} \frac{T_{ref}}{P_{ref} V_{ref}} \qquad \text{Eqn. 3.8}$$

Criteria for Stable Engine Operation

Cycle to cycle variations of the combustion process in an engine can be monitored by the fluctuations in both maximum cylinder pressure and the indicated mean effective pressure (IMEP). To evaluate the operating range in this work, the fluctuation in the IMEP was used as a measure of the cycle-to-cycle variations and was expressed as the coefficient of variation of indicated mean effective pressure (COV_{IMEP}) (Amann, 1985). The COV_{IMEP}, equation 3.9, for 100 consecutive engine cycles was calculated as the standard deviation (σ_{IMEP}) divided by the mean value (IMEP) and tabulated as percent change as suggested by Koopmans and Denbratt (2002). The COV_{IMEP}) for all the data taken in this work was 5 % or less.

$$COV_{IMEP} = \frac{\sigma_{IMEP}}{IMEP} \times 100\% \qquad \text{Eqn. 3.9}$$

As the cylinder mixture get richer, the HCCI combustion rate also increases and intensifies, which causes engine knock that may potentially damage the engine. Therefore, the rich stability limit of HCCI combustion can be defined with respect to the maximum rate of pressure rise in the cylinder. The rate of pressure rise is calculated

using a simple numerical differentiation (Randolph, 1994). The maximum rate of pressure rise (MRPR) allowed in these studies was $dP/d\theta_{max}$ = 10 bar/deg.

3.6 GC Technique for Combustion Hydrocarbon Oxidation Study

An important task in this study was to develop appropriate GC techniques to measure the major stable intermediate species generated during the HCCI combustion process. Such species include CO, CO_2, alkanes, alkenes, aldehydes, acetone, oxides, etc., for a total of 30 or so individual species. These species have different molecular weight and molecular structure, which make them very difficult to identify in one sample run. Among these species, formaldehyde is the most difficult to identify, because it is difficult to sample and store reproducibly. Tremendous care has been taken to develop an appropriate sample storage and GC technique for this purpose. Since formaldehyde will condense at lower temperature, and oxidize at higher temperature, all sampling tubes and loops must be kept at 70 °C to keep formaldehyde from “disappearing”.

Based on previously used GC methods (Li 1995, Yang 2002), a basic idea for separating all desired species emerged. Specifically, we used one column for light molecular weight species, and another column for heavy molecular weight species. The first column configuration is the same as in the second technique: both consisted of Porapak Q and N packed columns in series with a post-column nickel catalyst methanizer (more information can be found in Appendix D). The methanizer is maintained at 375°C and provided with 10 ml/min H_2 to convert CO, CO_2, and formaldehyde to methane for FID identification. This column combination was used to separate and quantify carbon monoxide (CO), carbon dioxide (CO_2), formaldehyde,

propionaldehyde, acetone, and other small oxygenates. In the second column configuration, a series of DB-1 capillary columns (each 30 m and 0.53 mm I.D.) with different column film thickness (one is 0.13 um and another is 0.5 um) allowed measurement of the fuels and other carbon containing oxidation products. The flow rate of helium carrier gas was set at 21 ml/min through the packed columns and 6 ml/min through the capillary columns. The temperature program was as follows: 15 minutes at 40°C, ramp at 5°C/min to 180°C, and hold at 180°C for 15 minutes. This method was used for species measurement using n-heptane, iso-octane, and their mixtures with alkenes and aromatics components. This GC technique was successful in separating the essential species. The identified species by the two column combinations in this study are listed in Table 3-2 and Table 3-3.

In the repeatability studies conducted using standard calibration gases, the day-to-day repeatability for small alkenes and other C6 and smaller non oxygenated species was under 5 % and the run to run repeatability was within 3 %. For large liquid phase non- oxygenated species, the day-to-day repeatability was within 10 % and the run-to-run repeatability was also within 10%. For oxygenated species, the day-to-day repeatability was within 10% when using the two DB-1 columns in series and 15.0 % when using the two packed columns in series, the run-to-run repeatability was within 10% when using the two DB-1 columns in series and 20% when using the two packed columns in series. As a result most intermediate quantification and identification was taken form the DB-1 columns.

Table 3.3: Identified species from the two packed columns in series

Species	Retention Time
CO	3.89
CO_2	8.03
Ethene	9.41
Acetylene	12.9
Ethane	13.02
Formaldehyde	27.15
Propene	28.34
Propane	29.2
Propyne	30.8
Methanol	33.6
Acetaldehyde	35.3
Trimethylacetaldehyde	49.873
Isobutylene	37.66
1-butene	37.91
n-butane	38.68
1-butyne	39.05
2-butyne	41.92
Propylene oxide	41.955
Acrolein	43.18
Propionaldehyde	43.48
Acetone	43.94
1-pentene	45.48
n-pentane	46.25
Isobutylene oxide	48.5
Metharcolein	50.3
Isobutylaldehyde	51.18
Methyl vinyl ketone	51.753
Butylaldehyde	51.687

Table 3.4: Identified species from the two capillary columns in series

Species	Retention Time
Methane	6.74
Ethene	6.85
Ethane	9.2
Formaldehyde	9.25
Propene	7.317
Propane	10
Propyne	10.3
iso-butylene	10.75
Methanol	8.052
Isobutene	11.6
1-butene	8.448
n-butane	12.6
1-butyne	13
Ethanol	14.65
Acetone	10.567
Propionaldehyde	10.730 to 10.703
Proplyene oxide	10.975 to 11.008
Acrolein	16.9
2-butyne	17.05
1-pentene	11.303
3-methyl-1-butene	17.65
n-pentane	17.95
2-methyl-1-butene	18.15
isobutylene oxide	20
t-2,3-epoxy-butane	20.7
Isobutylaldehyde	20.98
Metharcolein	21.3
methyl vinyl ketone	16.008 to 16.138
Butylaldehyde	22.6
Trimethylacetaldehyde	17.397
1-hexene	17.822
n-hexane	24.7
4,4-dimethyl-2-pentene	20.13 o 20.33
1-heptene	24.103
iso-octane	24.775 to 24.282
t-3 heptene	29.95
n-heptane	24.733 to 24.702
t-2-heptene	30.25
2,4,4-trimethyl-1-pentene	25.310
2,4,4-trimethyl-2-pentene	26.2
DTBP	26.975

Experimental Procedure for gas sampling

1. Check sampling valve needle. Ensure that the needle is still acceptable for use. No chips, not badly warped. Connect sampling valve up to the sampling storage cart.
2. Actuate the sampling valve using the engine LabView controller that is used to monitor pressure used to select the starting CAD and duration of the valve opening, which is also monitored on the oscilloscope. This should be checked to ensure accuracy and proper CAD selection.
3. Ensure that all sample storage cart sample lines and connections are maintained at the correct temperature. Ensure at least 45 minutes for temperatures to stabilize.
4. Check if there is any leakage in the sampling system. With the sampling valve closed and the bellow pump running, check the flow rate through the exit port of the sampling storage system. The flow rate should read zero under normal conditions. If the flow meters gives a substantial reading then the system lines and connections should be checked, and the leak eliminated.
5. Connect pure nitrogen to the sample cart main inlet valve. Flush each sample storage loop for 30 seconds using pure nitrogen gas.
6. Actuate the sampling valve and purge the system for 45 seconds at the selected CAD's. The engine LabView controller that is used to monitor pressure used to select the starting CAD and duration of the valve opening, which is also

monitored on the oscilloscope. This should be checked before hand to ensure accuracy and proper CAD selection.

7. Collect samples for 15-30 seconds by closing the exit port. Once the loop pressure reached 10 psig, stop sampling and change the 16-port valve to a new loop position;
8. Flush the sample lines in between taking the sample and switching the sample loop for 30 seconds with pure nitrogen.
9. Once all samples are taken, transfer the sampling storage system to the GC analysis system, ensuring that correct sample temperatures are maintained.

3.7 Closure

This chapter provided a description of the single cylinder CFR octane rating engine modified to run in HCCI mode and the specific methodologies used in this work. This chapter also presented the gas analysis system and the sampling methodology and procedure.

The details of the single cylinder engine work examining the effect of select additives on the oxidation characteristics of PRFs are discussed in the preceding chapters. Chapter 4 looks at the effect of the additives on NTC behavior, while chapter 5 examines species evolution profiles for insight into the effect of the select additives on the oxidation of PRFs.

CHAPTER 4. THE EFFECT OF SELECTED ADDITIVES ON THE LOW TEMPERATURE OXIDATION OF SI PRIMARY REFERENCE FUELS

This chapter presents the results of investigating the effects of blending oxygenated additives on hydrocarbon oxidation and autoignition of primary reference fuel blends, specifically in the low temperature regime. The oxygenated hydrocarbon additives studied were propionaldehyde, and DTBP. DTBP was chosen in this study because it is used in diesel fuels as a cetane improver. Propionaldehyde was chosen because aldehydes play a large role in low temperature oxidation as well as it has been shown in several studies to have contradicting effects. While formaldehyde is the most abundant aldehyde present in the oxidation of PRF blends, it presented large challenges in injecting it into our engine facility.

4.1 Experimental Conditions

The test matrix and fuel characteristics of these oxygenated hydrocarbons and baseline fuels are presented in Table 4.1 and 4.2 respectively. The volatility and flammability properties of the fuel components are from Material Data Safety Sheets (MSDS) at 1 atmosphere.

The baseline hydrocarbon fuels selected were PRF 0 (n-heptane), 20, 50, and 87. The baseline fuels were blended with 1.5 % of either propionaldehyde or DTBP on a volumetric basis. The study was divided into two tasks: (i) examine the effects of the oxygenated hydrocarbon additives on the overall low temperature reactivity of the

baseline fuels; (ii) examine how the blending of the oxygenated hydrocarbon additives affects the autoignition behavior.

Table 4.1: Test matrix for additive studies

Fuel	CR	Engine Speed (RPM)	Phi	DTBP (%)	Propionaldehyde %
PRF 0	**13, 16**	**600**	**0.43**	**0,1.5**	**0, 1.5, 3.0**
PRF 20	**13, 16**	**600**	**0.43**	**0,1.5**	**0, 1.5, 3.0**
PRF 50	**13, 16**	**600**	**0.43**	**0,1.5**	**0, 1.5, 3.0**
PRF 87	**13, 16**	**600**	**0.43**	**0,1.5**	**0, 1.5 , 3.0**

Table 4.2: Characteristics of fuels used in this study

	n-heptane	Iso-octane	Propionaldehyde	DTBP
Flash Point (Celsius)	-4	4.5	-26	6
Vapor pressure @298 K	4.6	5.4	31.3	2.6
Boiling Point (Celsius)	98.42	99.3	46 - 50	110
Autoignition Temperature (Celsius)	285	417	175	165
Specific Gravity	0.68	0.69	0.81	0.79

The fuels in this study were run under identical motored engine conditions in a single cylinder research engine discussed in Chapter 3. An engine speed of 600 RPM, compression ratio of 13:1, inlet manifold pressure of 1 Bar and an equivalence ratio of 0.43 were used in these experiments. The inlet manifold temperature and pressure were fixed, and then the engine was motored and carbon monoxide exhaust output was collected and analyzed, the inlet manifold temperature was then increased gradually until autoignition occurred or an inlet manifold temperature of 400 K was reached. The measured carbon monoxide profiles as a function of inlet manifold temperature are shown and discussed in the following sections.

4.2 NTC behavior of PRF blends

The measured CO profiles for a range of PRF fuel blends as a function of inlet manifold temperature are presented in Figure 4.1. For each PRF represented in the figure, as the inlet manifold temperature was increased, the level of CO was initially increased indicating initiation of low temperature oxidation. For the baseline n-heptane (Figure 4.1), the reactivity initiated prior to an inlet temperature of 300 K. For the other baseline fuels tested PRF 50 and PRF 87, reactivity initiated a little after an inlet temperature of 300 K indicated by a higher molar fraction of CO. As the more reactive n-heptane is replaced with the less reactive iso-octane, a higher temperature is required for low temperature combustion to initiate.

As expected, the n-heptane showed more reactivity than blends of n-heptane and iso-octane. For all baseline fuels, as the inlet temperature is increased exhaust CO reached a maximum value, then as the temperature was further increased, stopped

increasing or gradually decreased exhibiting negative temperature coefficient behavior, or (NTC). Specifically, for n-Heptane, the CO increased to maximum at an inlet temperature of about 385 K, further increase of the inlet temperature caused a decrease of CO, which is termed NTC behavior in combustion chemistry. For PRF 50 and PRF 87, the maximum CO was observed at about 345 K, then gradually decreased, exhibiting more NTC behavior than n-heptane. For all the baseline test cases, autoignition did not occur for inlet temperatures ranging from 300 K to 400 K. This behavior is consistent with measurements made by several researchers (Leppard, 1992; Li, 1995).

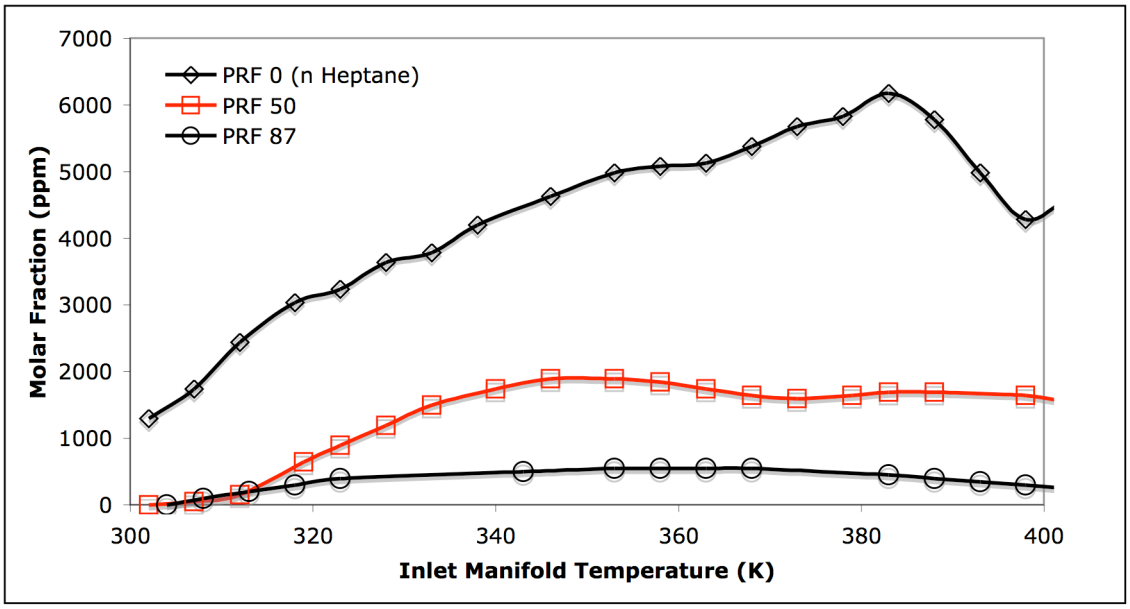

Figure 4.1:Exhaust carbon monoxide profiles for a series of primary reference fuels at a CR of 13, phi of 0.43, and an engine speed of 600 RPM

Although there is a substantial difference in the ease with which the fuels auto-ignite, as indicated by their respective octane numbers of 0 and 100, they share a set of low-temperature reactions that are unique to paraffin's and the explanation for NTC

behavior is the same. The temperature at which these reactions occur is dependent on pressure, with reactions beginning at roughly 550 K at atmospheric pressure and at 600–800 K. NTC behaviors is characterized by a decrease in the reaction rate despite an increase in temperature and pressure. For many hydrocarbons, there is a NTC temperature range, which is usually between 600 to 800 K. This is a complicated phenomenon and is described briefly in terms of the mechanism (2-1) to (2-15) in Chapter 2. As temperature increases, reaction, (2-2), $R\bullet + O_2\bullet = RO_2\bullet$ becomes effectively reversible. The alkylperoxide can further decompose, (2-3), $RO_2\bullet$ (+M) = olefin + $HO_2\bullet$ (+M) to produce alkenes, $HO_2\bullet$, and relatively stable species. Since (2-3) produces alkenes and $HO_2\bullet$, relatively stable species at these temperatures, it has an inhibiting effect on the overall reaction rate. The mechanism shift explains the decrease of overall reaction rate with the increase of temperature (due to effectively reversible reaction (2-2) and non-chain branching reaction (2-3)), known as negative temperature coefficient (NTC) behavior. As the temperature is further increased into the intermediate temperature regime, the decomposition of hydrogen peroxide becomes the dominant chain branching path, (2-12), HOOH + M = OH• + OH• and the reaction again accelerates.

4.3 The effect of oxygenates on overall reactivity

The next set of experiments examines the effect of select additives on the low temperature oxidation of PRF blends. The characteristics of these additives examined in this section are listed in Table 4.1. More detail about these additives can be found in

Chapter 2. The fuels tested were PRF 0, 50, and 87. The additives used were propionaldehyde and DTBP.

4.3.1 The effect of propionaldehyde on overall reactivity

The measured CO concentration as a function of inlet temperature for PRF 0, PRF 50, PRF 87 and its mixtures with the 1.5 % propionaldehyde by volume as an additives at a compression ratio of 13 is shown in Figures 4.2, 4.3 and 4.5, respectively.

For PRF 0, Figure 4.2, at 300 K, there is more CO produced with an addition of propionaldehyde. Although the rate of CO production decreases, there is a continuous increase in the amount of CO produced. In other words, the addition of propionaldehyde reduces the NTC behavior. With the addition of the propionaldehyde, autoignition was also observed just before 380 K.

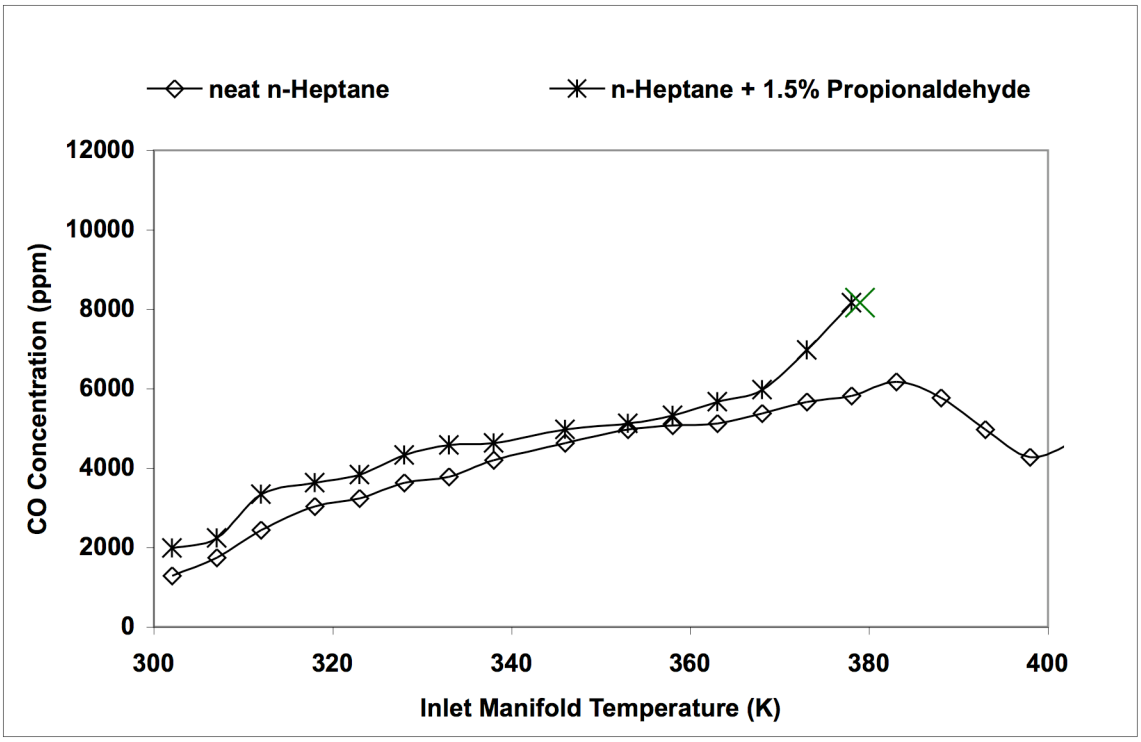

Figure 4.2 Exhaust carbon monoxide profiles for a series of PRF 0, and PRF 0 with 1.5 % propionaldehyde at a CR of 13, phi of 0.43, and an engine speed of 600 RPM

For PRF 50, Figure 4.3, at 300 K, there is no CO produced for the neat case or with an addition of propionaldehyde. Low temperature reactivity initiates at an inlet manifold temperature of about 310 K, where there is slightly more CO being produced with an addition of propionaldehyde until around 360 K. Above 360 K to 400 K there is about the same level of CO produced for the baseline PRF 50 as well as with the addition of propionaldehyde. Although there is an initial increase in the amount of CO produced with an addition of propionaldehyde, the overall effect on NTC does not change much from the baseline case.

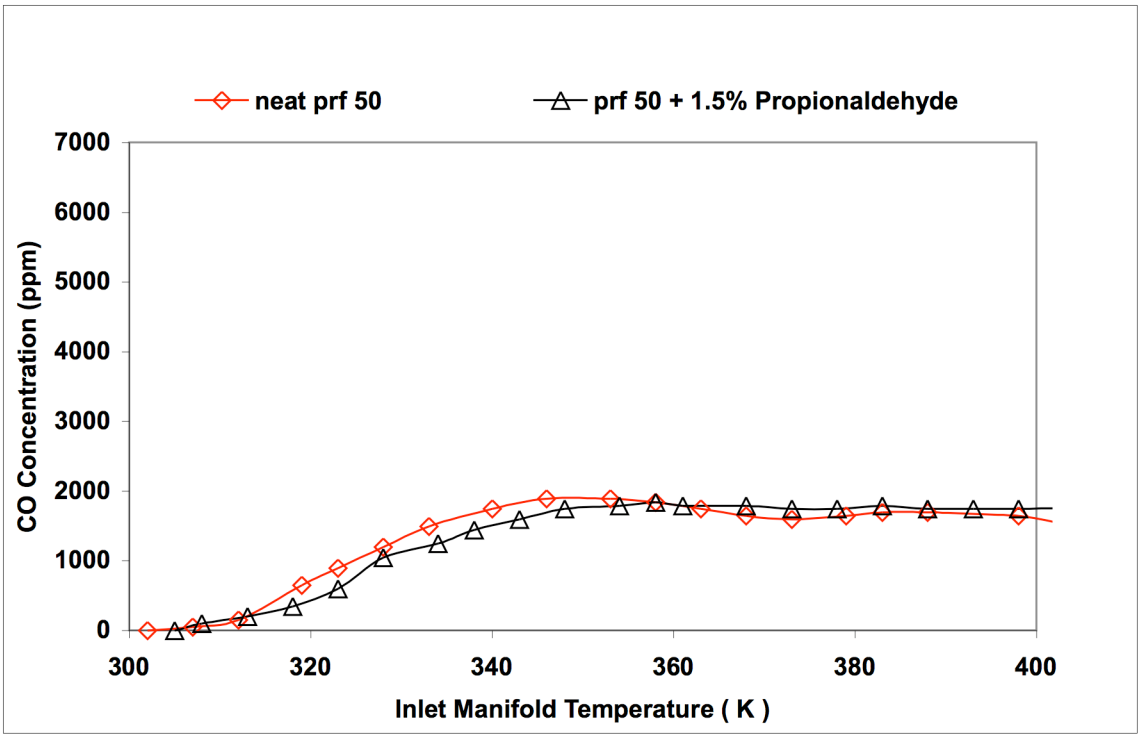

Figure 4.3: Exhaust carbon monoxide profiles for a series of PRF 50, and PRF 50 with 1.5 % propionaldehyde at a CR of 13, phi of 0.43, and an engine speed of 600 RPM

Figure 4.4 shows the effect of propionaldehyde addition on PRF 87. It was observed that PRF 87 exhibits slightly different behavior from the PRF 50, and PRF 0 cases. At 300 K, there is no CO produced for the neat case or with an addition of propionaldehyde. Low temperature reactivity initiates at an inlet manifold temperature of about 308 K, where there is slightly less CO being produced with an addition of propionaldehyde until around 340 K. From 340 K to 400 K there is a significant decrease in the level of CO produced when compared to the baseline PRF 50. NTC behavior is increased with propionaldehyde addition for PRF 87.

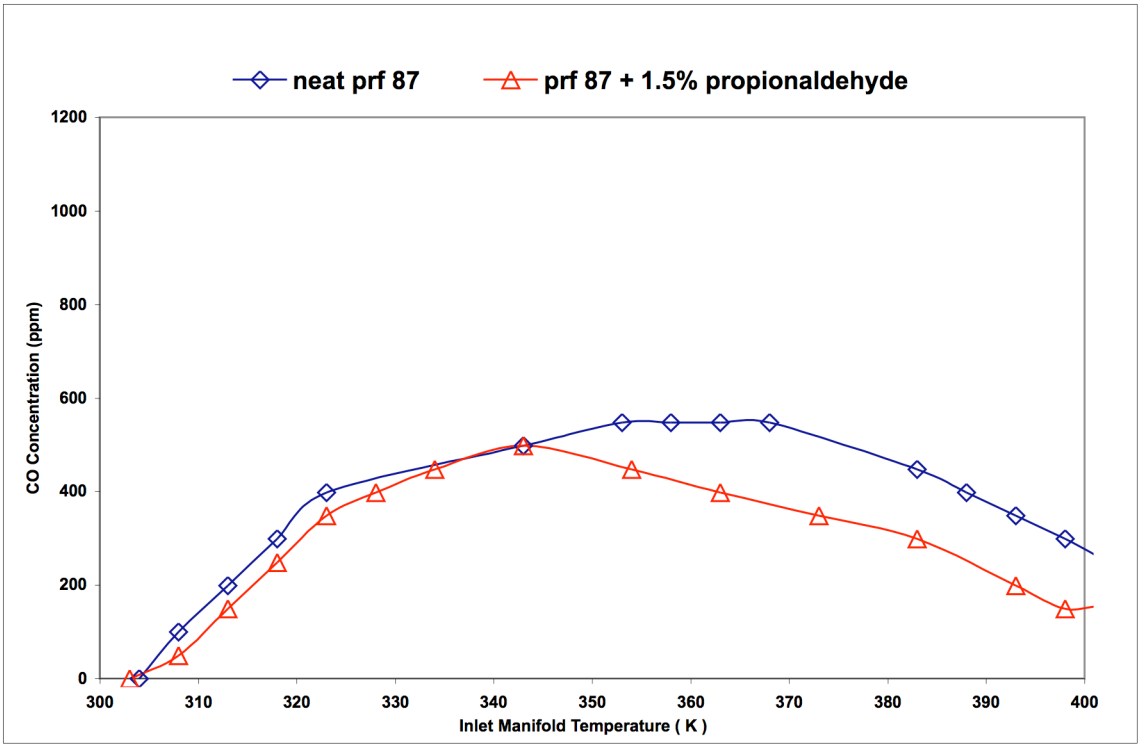

Figure 4.4: Exhaust carbon monoxide profiles for a series of PRF 87, and PRF 87 with 1.5 % propionaldehyde at a CR of 13, phi of 0.43, and an engine speed of 600 RPM

Overall the addition of propionaldehyde to PRF fuels exhibits two effects. When added to lower octane number PRFs, propionaldehyde reduces NTC behavior thus advancing ignition. As the octane number in the fuel increases, NTC behavior is increased delaying ignition. A possible explanation for the behavior is the difference in the oxidation of propionaldehyde at low and high temperatures. The data suggest that propionaldehyde acts as a hydroxyl radical scavenger at lower temperatures, where

$$C_2H_5CHO + OH\bullet = CH_3CHCHO + H_2O$$

such as with PRF 87. At higher temperatures propionaldehyde may react producing hydroxyl radicals, OH•, which aid in the destruction of the parent fuel, thus advancing

ignition. At higher temperatures the slight promotion in fuel oxidation could be caused by the increased OH production resulting from C_3H_6O oxidation (Kaiser, 1987).

$$C_2H_5CHO + O_2 = C_2H_5CO\bullet + HO_2$$

$$C_2H_5CO\bullet + HO_2 = C_2H_5CO_3\bullet$$

$$C_2H_5CO_3\bullet + RH = C_2H_5CO_3H + R\bullet$$

$$C_2H_5CO_3H = C_2H_5CO_2 + OH\bullet$$

$$C_2H_5CO_2 + RH = C_2H_5CO_2H + R\bullet$$

$$C_2H_5CO_2H = C_2H_5CO + OH\bullet$$

4.3.2 The effect of DTBP on overall reactivity

The measured CO concentration as a function of inlet temperature for PRF 0, PRF 50, PRF 87 and its mixtures with the 1.5 % DTBP as an additives at a compression ratio of 13 is shown in Figures 4.5, 4.6, and 4.7, respectively.

For PRF 0, Figure 4.5, at 300 K there is more CO produced with an addition of DTBP. The baseline case exhibited more NTC behavior than with 1.5 % DTBP addition. With the addition of the DTBP autoignition was also observed just before 370 K.

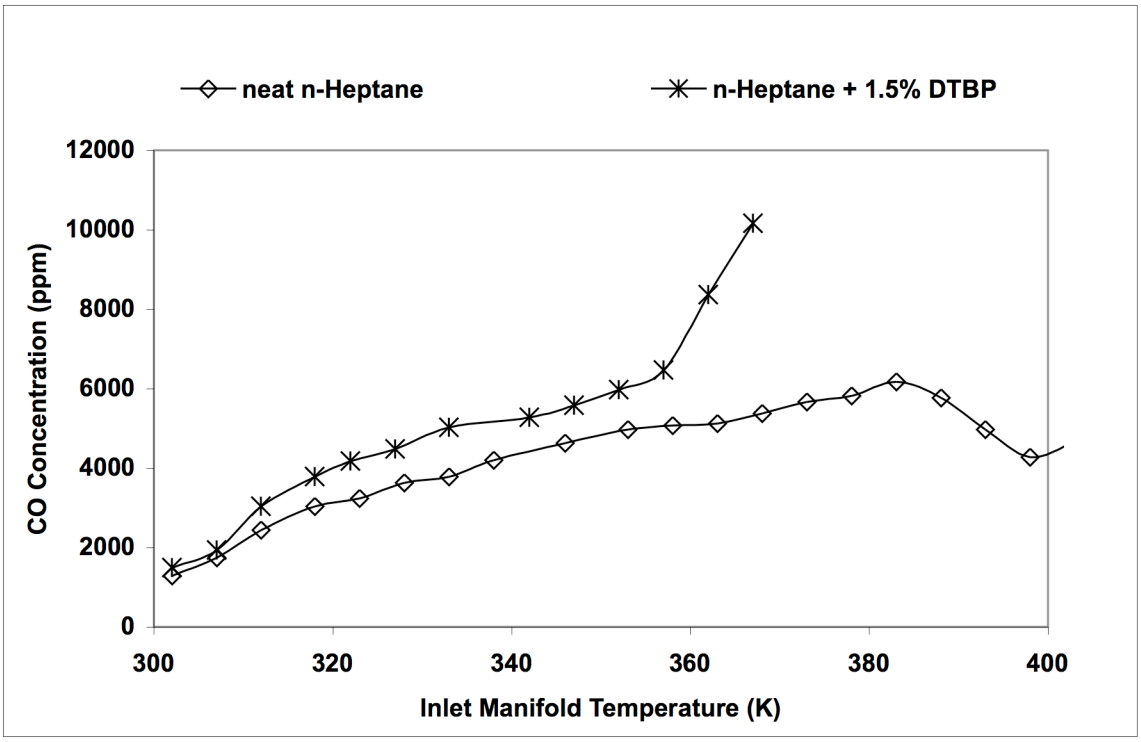

Figure 4.5: Exhaust carbon monoxide profiles for a series of PRF 0, and PRF 0 with 1.5 % DTBP at a CR of 13, phi of 0.43, and an engine speed of 600 RPM

For PRF 50, Figure 4.6, at 300 K, there is no CO produced for the neat case or with an addition of DTBP. Low temperature reactivity initiates at an inlet manifold temperature of about 310 K, where there is slightly more CO being produced with an addition of DTBP. Although autoignition is not observed for this case like the PRF 0 case, there is a continuous increase in the amount of CO produced with an addition of DTBP. There is a reduction in NTC behavior.

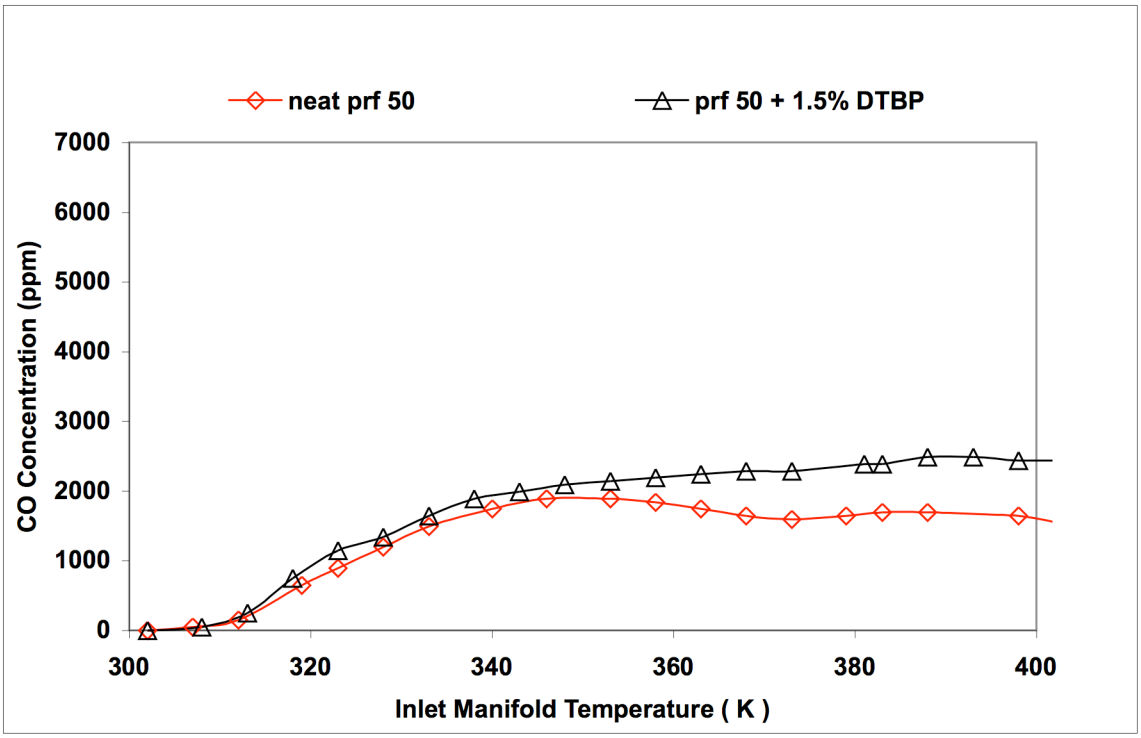

Figure 4.6: Exhaust carbon monoxide profiles for a series of PRF 50, and PRF 50 with 1.5 % DTBP at a CR of 13, phi of 0.43, and an engine speed of 600 RPM

Figure 4.7 shows the effect of DTBP addition on PRF 87. It was observed that Like the case with PRF 87 with propionaldehyde addition, PRF 87 exhibits slightly different behavior from the PRF 50, and PRF 0 cases with DTBP addition. At 300 K, there is slightly more CO produced with an addition of DTBP. At higher inlet manifold temperatures the levels of CO produced is about the same. NTC behavior for PRF 87 is shifted to a slightly lower temperature with DTBP addition.

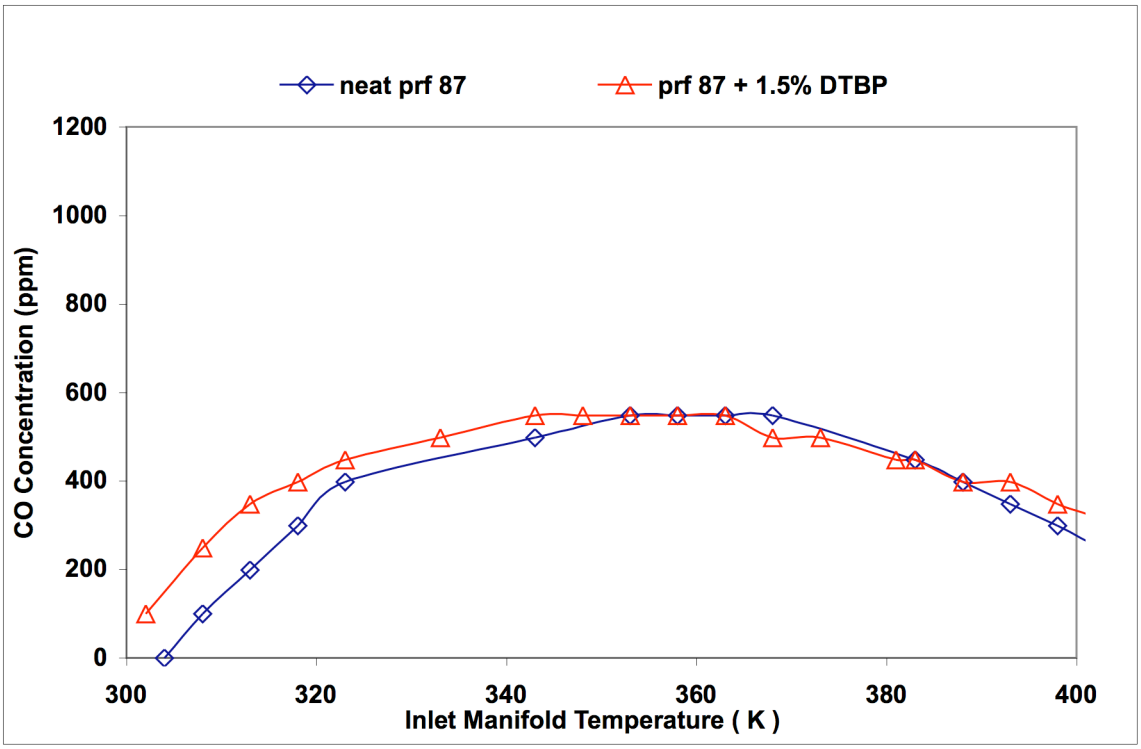

Figure 4.7: Exhaust carbon monoxide profiles for a series of PRF 87, and PRF 87 with 1.5 % DTBP at a CR of 13, phi of 0.43, and an engine speed of 600 RPM

Overall the effect of DTBP is to promote reactivity in the low temperature regime. As a result, it reduces the NTC behavior, which can lead to a reduction in ignition delay, and subsequently earlier ignition. Currently there are two views on why this may occur. In the literature, there are two modes of action DTBP addition, a chemical effect and a thermal effect (Johnson, 2007). Specifically, the decomposition of DTBP and subsequent formation of acetone is exothermic and raises the mixture temperature slightly as the decomposition occurs, this increase in temperature may advance the ignition timing. The second view states that during the decomposition of DTBP, the methyl radicals undergo oxidation on a microsecond timescale to yield molecular

products (e.g., formaldehyde, methanol and hydrogen peroxide), which can chemically alter ignition.

From this study there is not enough information present to make a determination of which effect holds. In the next chapter species evolution profiles for PRF blends with the addition of DTBP will be examined and discussed, which will attempt to answer this question.

4.4 The effect of propionaldehyde on autoignition behavior

The previous section outlines the effect of select additives, DTBP and propionaldehyde, on the NTC behavior of PRF fuel blends. NTC has a large impact on combustion characteristics. From the literature, it is observed that PRF blends often exhibit two-stage ignition behavior where there is an initial pressure rise followed by a more pronounced hot ignition. The time between the first-stage and the second- stage is referred to as ignition delay. During this period, preignition reactions continue and the chemistry moves from the low temperature region through the intermediate temperature region to ignition. NTC behavior of the PRF blends is important in controlling this transition. Therefore, it is the chemical reactions in the NTC region that determines ignition time for PRF.

The next section examines the effect of the additives, which were shown to have an effect on NTC behavior in the previous sections, on autoignition. Also previous works has shown that the addition of as little as 1.5 % DTBP by volume to PRF blends always advance ignition (Johnson, 2007; Gong et al, 2005a; Gong et al, 2005b. As a result only the effects on propionaldehyde will be discussed here.

4.4.1 The results of propionaldehyde addition on the autoignition behavior of selected PRF blends.

The representative pressure traces for n-heptane, PRF 20 and PRF 50 with an addition of 1.5 % propionaldehyde by volume at an equivalence ratio of 0.40 are shown in Figures 4.8, 4.9, and 4.10 respectively. The cases are for both neat PRF's and with 1.5 % by volume propionaldehyde. It is important to note that the addition of 1.5 % propionaldehyde did not change the equivalence ratio of the mixture significantly.

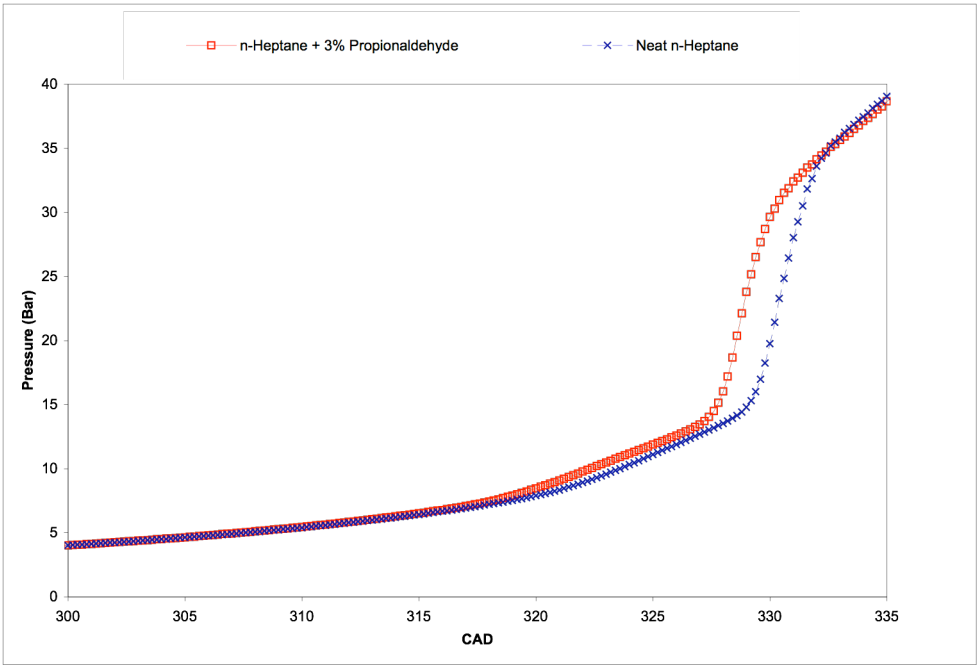

Figure 4.8: Pressure history during HCCI Operation for PRF 0 (n-heptane), and PRF 0 and propionaldehyde at 423 K Inlet T, a CR of 17, and an equivalence ratio of 0.43

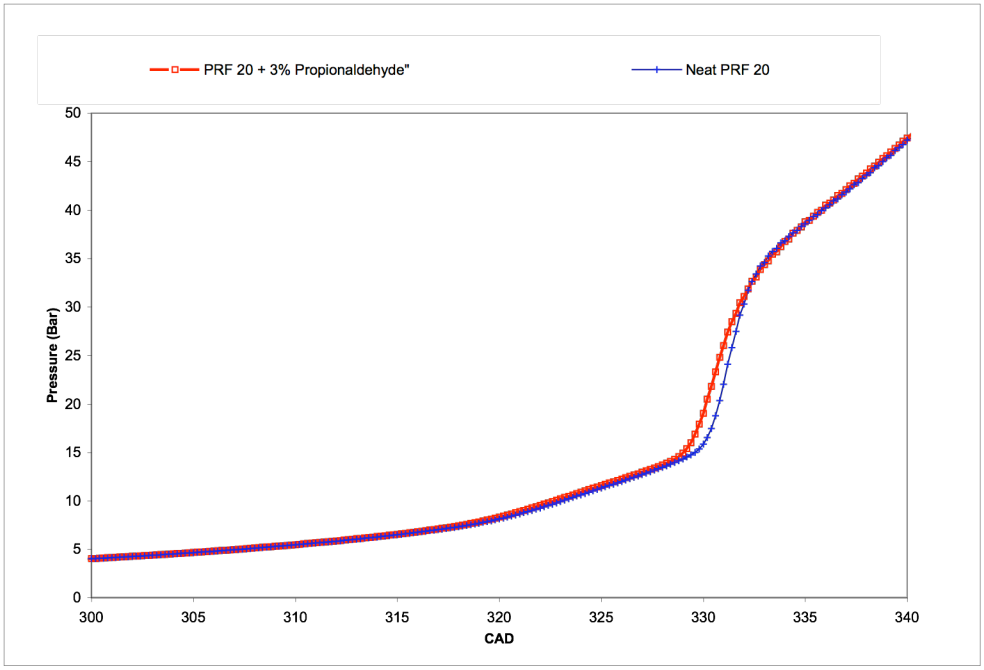

Figure 4.9: Pressure history during HCCI Operation for PRF 20, and PRF 20 and propionaldehyde at 423 K Inlet T, a CR of 17, and an equivalence ratio of 0.43

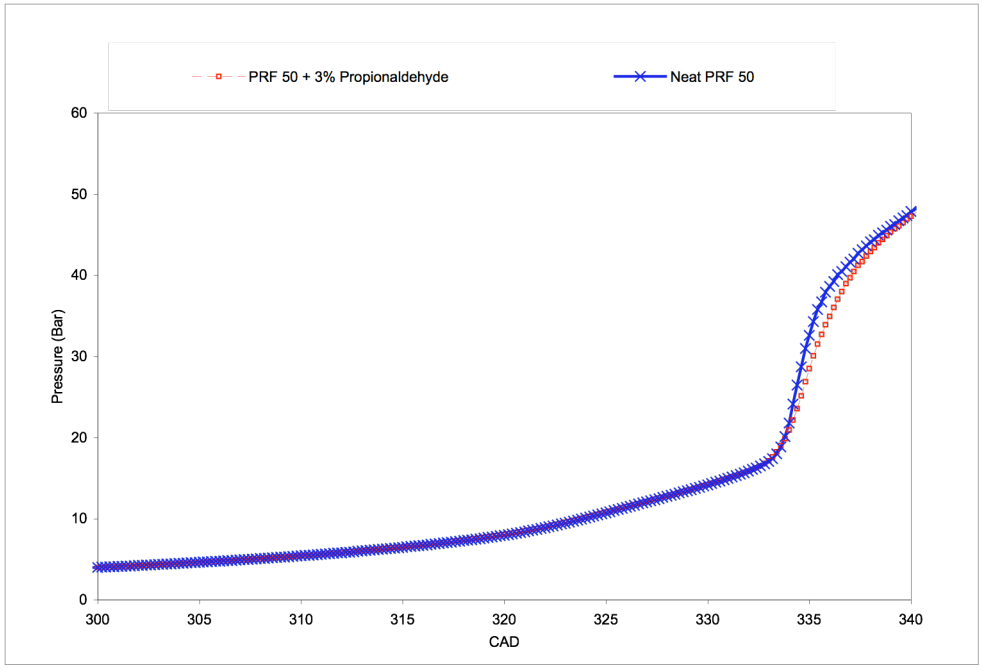

Figure 4.10: Pressure history during HCCI Operation for PRF 50 and PRF 50 and propionaldehyde at 423 K Inlet T, a CR of 17, and an equivalence ratio of 0.43

From these figures, it seems that the addition of propionaldehyde advances the ignition time of PRF 0 significantly and less so for and PRF 20. For PRF 50, the addition of propionaldehyde had a delaying effect on ignition time. This can be related to the effect of these additives on NTC behavior. From the previous section, it was observed that as the iso-octane content of the PRF blend was increased, the addition of the additive had a varying effect on NTC. For lower octane number PRF's the addition of propionaldehyde reduces the NTC behavior, which will in turn reduce the ignition delay time leading to earlier ignition. For the higher octane number PRF's, 50 and above, the addition of propionaldehyde increases NTC behavior, which will in turn increase ignition delay and retard ignition.

4.5 Closure

The results discussed in this chapter shows that the addition DTBP or propionaldehyde effects NTC behavior during HCCI combustion, and subsequently affects ignition delay. For DTBP the effect is to always reduce NTC behavior despite the octane number PRF blends examined. For propionaldehyde, the effect on NTC behavior changes with changing PRF octane number. For the same engine operating conditions, as the amount of iso-octane content in the fuel increases, the effect propionaldehyde addition goes from advancing autoignition for a mixture with 0 % iso-octane content to delaying autoignition for mixtures with over 50% iso-octane. A possible explanation for the behavior is the difference in the oxidation of propionaldehyde at low and high temperatures. The data suggest that propionaldehyde acts as a radical scavenger at lower temperatures, while at higher temperatures

propionaldehyde may react with oxygen producing hydroxyl radicals, OH•, which aid in the destruction of the parent fuel, thus advancing ignition.

The next chapter will examine the effect of these additives on the oxidation of PRF blends via species evolution profiles.

CHAPTER 5. SPECIES EVOLUTION PROFILE DEVELOPMENT FOR HCCI OPERATION WITH PRF FUELS AND SELECTED ADDITIVES

As an alternative operating mode for engines, HCCI has the potential to reduce both particulate and NOx emissions while maintaining high fuel efficiency. HCCI combustion is dominated by combustion chemistry. By modifying the temperature, pressure and composition of the fuel and air mixture, autoignition occurs in proper phasing with the piston motion. This control system is fundamentally more challenging than using a spark plug or fuel injector to determine ignition timing as in SI and CI engines, respectively.

The objective of the experiments reported in this chapter was to provide kinetic and mechanistic information of hydrocarbons oxidation under HCCI with and without additives to help develop chemical models to simulate the experimental results for predicting and controlling stable HCCI operation. This was achieved by obtaining the stable HCCI engine operation in our engine and then a fast-acting sampling valve was used to extract gas samples from the combustion chamber during combustion under selected experimental conditions. The composition of extracted gas samples was determined by gas chromatographic analysis. Finally, the species evolution profiles were used to evaluate the effect of the additives on HCCI oxidation chemistry.

DTBP was selected as an additive because of its use as a cetane improver for diesel fuels. It has also been shown to be effective in increasing the gas temperature of air (Johnson, 2007). Propionaldehyde was chosen to represent formaldehyde during the low temperature combustion.

We also wanted to provide information to clarify the mode of action of DTBP under HCCI condition. There are two modes of action DTBP addition, a chemical effect

and a thermal effect. Specifically, the decomposition of DTBP and subsequent formation of acetone is exothermic and raises the mixture temperature slightly as the decomposition occurs. During the decomposition, the methyl radicals undergo oxidation on a microsecond timescale to yield molecular products (e.g., formaldehyde, methanol and hydrogen peroxide), which can chemically alter ignition.

For the data presented the COV_{IMEP} was <5% which corresponds to stable combustion. Prior to this work, the operating range with these additive and fuel combinations was evaluated (Johnson 2007).

5.1 Experimental Conditions

Experiments were conducted using two fuels, PRF 0, and PRF 20. The latter was used to evaluate the effect of the additives in the presence of iso-octane. Gas composition was obtained via a fast sampling valve from 300 CAD to 321 CAD. The engine was operated at an engine speed of 600 RPM, which corresponds to 0.2 milliseconds per CAD. For the fuels tested, autoignition occurred around 330 CAD for heptane to 335 CAD for PRF 20. Gas sampling was stopped at 321 CAD, as a result of unstable valve operation after 321 CAD due to high pressure in the combustion chamber, which made the sampling duration unstable. The experimental parameters are presented in Table 5.1. It is also important to note that while the addition of oxygenated additives has the potential to change the engine equivalence ratio due to the change of fuel oxygen content, in the volume percents used in this study, the change was not significant.

Table 5.1: Test matrix for engine sampling experiments

Fuel	Speed	CR	Inlet Temperature (K)	% of Propionaldehyde addition	% of DTBP addition
PRF 0	600	16	400	0	0
	600	16	400	3	0
	600	16	400	0	3
PRF 20	600	16	400	0	0
	600	16	400	3	0
	600	16	400	0	3

5.2.1 N-heptane with and without additives

The species evolution profiles and carbon balance for PRF 0 (n-heptane) at equivalence ratio of 0.43 (no additive) are presented in Figure 5.1 and Table 5.2, respectively. In order to simplify the explanation, the measured 25 species are divided into five groups by chemical "family": 1) fuels and CO and CO_2 and DTBP; 2) small alkenes and alkanes, including methane, ethane, propene, 1-butene, 1-pentene, and 1-hexene; 3) C_7 alkenes, including 1 & 2-heptene; 4) aldehydes, including formaldehyde, acetaldehyde, propionaldehyde, butylraldehyde, and trimethylacetaldehyde; and 5) small non aldehyde oxygenated species, including methanol, acetone, propylene oxide, and methyl vinyl ketone.

Low temperature reactivity in this case started prior to 300 CAD. Sampling of n-Heptane begins at 300 CAD where we see the fuel molar fraction start to decrease, and the consumption of the fuel continues until 321 CAD. At 318 CAD, nearly 70 % n-heptane is consumed. After 318 CAD, the molar fractions of these two fuels remain

stable, with less than a 5.0 % decrease in molar fractions from 318 to 321 CAD. The dominant product is CO_2. The molar fraction of CO_2 starts to increase between 300 to 306 CAD, and reaches its maximum point at 321 CAD. From 300 to 306 CAD, the molar fraction of CO rises at a rate of about 550 ppm per CAD. After 306 CAD, CO_2 increases 2.5X as fast up to 321 CAD at a rate of 1756 ppm per CAD. The molar fraction of CO has a more steady increase over this CAD range and the amount of CO generated is very small compared to CO_2 with CO increasing only 2994 while CO_2 increases by 29600 ppm.

The intermediate hydrocarbon species of PRF 0 start to form at 300 CAD, however the production of most species doesn't become significant until 306 CAD. The molar fractions continue to increase until about 315 CAD where they plateau and then start to decrease until 321 CAD.

Among the small alkenes and alkanes, ethene has the highest molar fraction, followed by propene and 1-butene, then methane. The molar fraction of ethene is around 12 ppm at 300 CAD, 78 ppm at 309 CAD, 127 ppm at 315 CAD, and 124 ppm at 321 CAD. The molar fraction of ethene peaks at 315 CAD and then decreases. The molar fraction of propene increases from 3 ppm at 300 CAD to 53 ppm at 315 CAD and then decreases to 36 ppm at 321 CAD. 1-butene and methane increase to around 31 and 25 ppm, respectively, at 315 CAD, and then decrease from this level until 321 CAD. The molar fractions of 1-pentene and 1-hexene are relatively small, with a maximum level of less than 8 ppm and follow a trend similar to ethene, propene, 1-butene, and methane.

Table 5.2: Carbon balance for PRF 0 experiment

CAD	300	303	306	309	312	315	318	321
CARBON BALANCE (%)	100	69	102	101	94	98	85	102

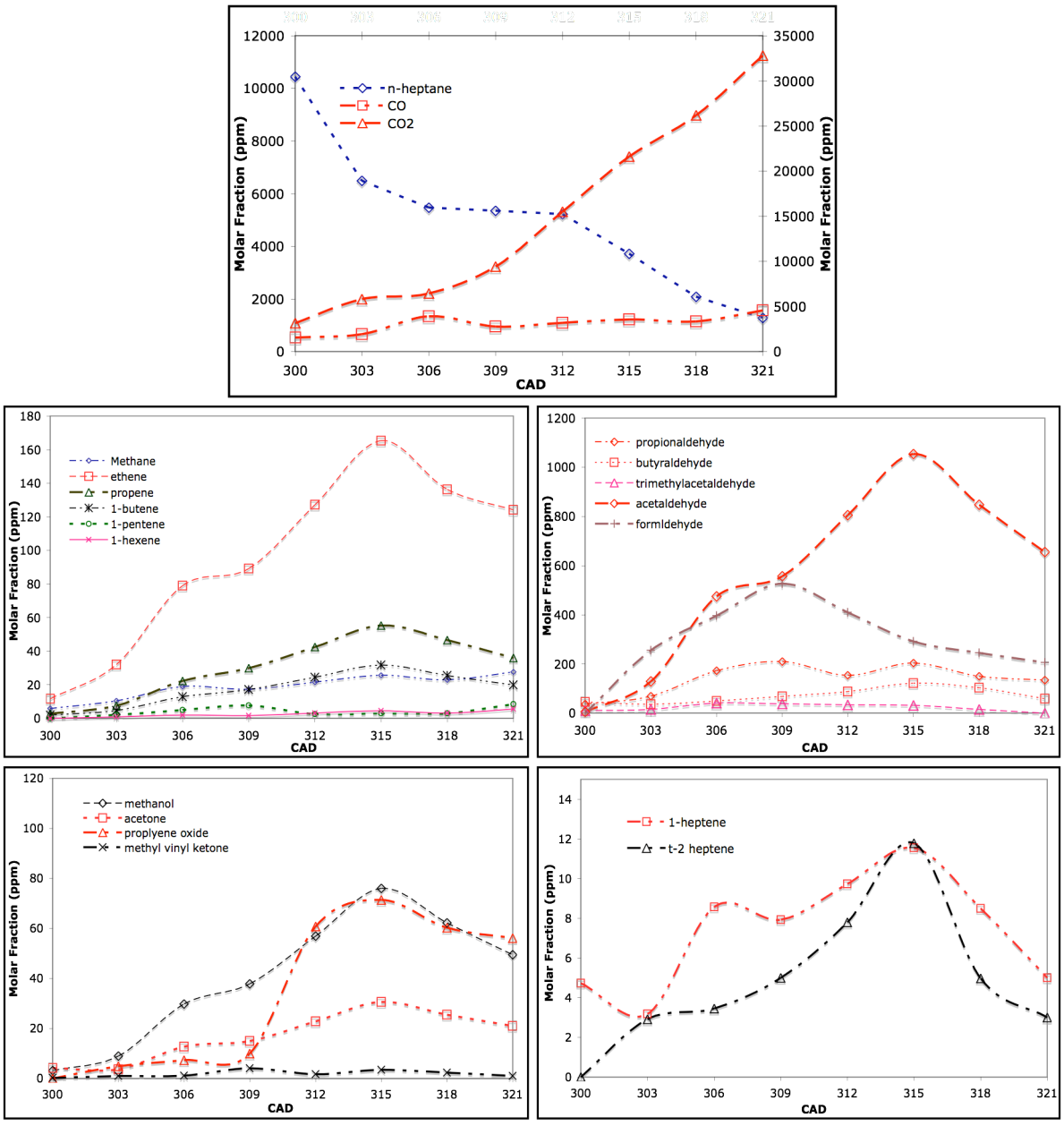

Figure 5.1: Species evolution profiles using PRF 0 (n-heptane) at an equivalence ratio of 0.43, 423 K inlet Temperature, a CR of 16:1, 600 RPM

1 and 2-heptene starts to appear at 300 CAD, increase rapidly between 303 and 315 CAD, and then decrease rapidly from this level until 321 CAD. Among the C_7 alkenes, 1-heptene has the highest molar fraction over most of the CAD sampled. The C_7 alkenes both peak to approximately the same value, which is around 12 ppm.

Acetaldehyde and formaldehyde are the principal oxygenated intermediates of PRF 0. A rapid increase in the molar fractions of acetaldehyde occurs from 303 to 315 CAD. At 315 CAD acetaldehyde production reaches a maximum molar fraction of 1054 ppm. After 315 CAD the molar fraction of acetaldehyde decreases to 655 ppm at 321 CAD. Formaldehyde peaks at 309 CAD at a molar fraction of 526 ppm. Both acetaldehyde and formaldehyde have a molar fraction that is much higher than that of propionaldehyde (210 ppm max), butylraldehyde (121 ppm max), and trimethylacetaldehyde (38 ppm max).

For the small oxygenated species, the molar fractions show trends similar to the other HC groups: production becomes evident from 300 to 306 CAD followed by an increase from 306 to 315 CAD then a slow decrease until 321 CAD. Among the four measurable small-oxygenated species, methanol has the highest molar fraction, around 78 ppm max, followed by propylene oxide (around 68 ppm max) and acetone (30 ppm max), and methyl vinyl ketone (4 ppm).

The next experimental data presented examines the effect of propionaldehyde addition on the oxidation of our baseline PRF 0. As mentioned previously, an equivalence ratio of 0.43 was selected for this experiment. The percentage of propionaldehyde addition was set at 3.0 % by volume. The species observed with of

PRF 0 plus 3.0 % propionaldehyde are the same as those generated from neat PRF 0. The species evolution profiles and carbon balance of PRF 0 with 3.0 % propionaldehyde addition are presented in Figure 5.2 and Table 5.3, respectively.

Table 5.3: Carbon balance for PRF 0 experiments with propionaldehyde addition

CAD	300	303	306	309	312	315	318	321
CARBON BALANCE (%)	100	84	96	96	92	96	101	99

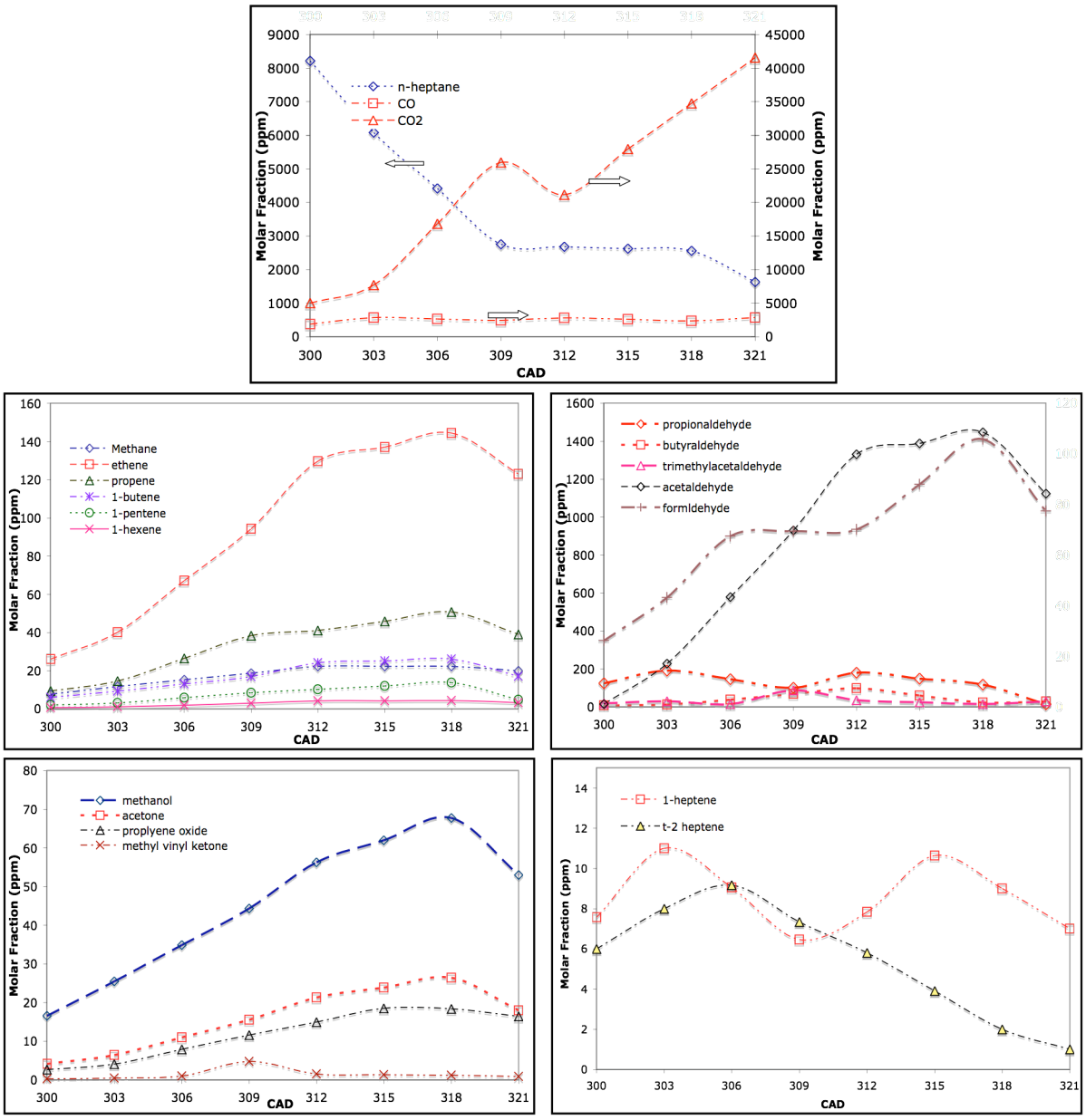

Figure 5.2: Species evolution profiles using PRF 0 (n-heptane) and 3 % propionaldehyde at an equivalence ratio of 0.43, 423 K inlet Temperature, a CR of 16:1 and 600 RPM

Similar to PRF 0 results at this experimental condition, CO_2 is the dominant product. The CO_2 molar fraction increases slowly from 300 to 303 CAD, and starts to increase rapidly after 303 CAD up to 321 CAD. At the beginning of sampling, at 300 CAD, the molar fraction of CO_2 is higher than that of the baseline case. The molar fraction of CO starts to increase at 300 CAD gradually until 321 CAD. The change in the amount of CO measured is only 984 ppm, much less than the neat PRF 0 case which showed a change in the amount of CO of 3000 ppm. The next dominant species is the parent fuel, which starts out at around 8000 ppm. Approximately a 28 % had reacted prior to 300 CAD, whereas in the baseline case it started out at around 10000 ppm, only 10 % had reacted prior to 300 CAD.

The molar fractions of intermediate hydrocarbon species of PRF 0 plus 3.0 % propionaldehyde show slightly higher oxygenate production as might be expected. The molar fraction of large and small oxygenates, small alkenes and alkanes start to appear at 300 CAD and increases rapidly up to 312 CAD and then increases at a slower rate up to 318 CAD. It then starts to decrease until 321 CAD.

Among all small alkenes and alkanes, ethene has the highest molar fraction, followed by 1-butene, propene, and methane. This is similar with PRF 0. The molar fraction of ethene start to increase rapidly from 300 to 312 CAD and slowly increases to about 150 ppm at 318 CAD. The molar fractions of propene, 1-butene, and methane also increase rapidly from 300 to 312 CAD, and reach their highest level of near 42, 23, and 20 ppm, respectively, at 318 ppm. During the entire sampling period, the molar fraction of 1-hexene is very low, and remains steady from 309 to 321 CAD. In this group, the overall molar fractions of all species are lower than measured for PRF 0 by

approximately 10 % with the exception of the aldehydes.

Like the baseline PRF 0, acetaldehyde and formaldehyde are the dominant aldehyde products of PRF 0 with 3.0 % propionaldehyde addition. Like the other intermediates discussed in this study, there is a rapid increase in the molar fractions of all aldehydes from 300 to 312 CAD and then slowly increases to their respective maximum values at 318 CAD. At 318 CAD the maximum acetaldehyde and formaldehyde are observed in a concentration of about 1400 ppm as opposed 1054 ppm for the baseline case. After 318 CAD the molar fraction of acetaldehyde and formaldehyde decreases to about 1150 ppm at 321 CAD. The molar fraction of propionaldehyde gradually decreases from 300 CAD (150 ppm) to 309 CAD (101 ppm), and then increases again to 312 CAD (180 ppm) and then begins a gradual decrease until 321 CAD (13 ppm). Both acetaldehyde and formaldehyde have a molar fraction that is much higher than that of propionaldehyde (190 ppm max), butylraldehyde (98 ppm max), and trimethylacetaldehyde (87 ppm max). Approximately 40 % of propionaldehyde had reacted prior to 300 CAD.

For the small oxygenated species, the molar fractions of all four species increase rapidly from 300 CAD to 318 CAD and then decrease until 321 CAD during the entire sampling period. Among the four measurable small oxygenated species, methanol has the highest molar fraction of around 62 ppm, followed by acetone (23 ppm), propylene oxide (18 ppm), and methyl vinyl ketone (3 ppm).

In summary, the addition of propionaldehyde into PRF 0 changes the species evolution profiles for small carbon number species, such as small alkenes, aldehydes, and oxygenated species. The molar fraction of these small species increase rapidly

from 300 to 312 CAD, and continue to increase slowly to their maximum at 318 CAD. The addition of propionaldehyde does not produce different intermediates, however, it increases the molar fractions of the aldehydes by approximately 10 %, but reduces the molar fractions of small alkenes, and other oxygenated species by the same 10 % prior to hot ignition. Unlike the other species presented, the molar fraction of propionaldehyde has a slight decrease, then increases again. The overall change in propionaldehyde molar fraction does not change more than 30 %. This is as a result of propionaldehyde both consumption and production occurring simultaneously.

The third set of experimental data presented examines the effect of di-tertiary-butyl-peroxide (DTBP) on the oxidation of our baseline PRF 0. As with neat PRF 0 and PRF 0 with propionaldehyde addition, an equivalence ratio of 0.43 was selected for this experiment. The percentage of DTBP addition was set at 3.0 % by volume. The species observed with of PRF 0 plus 3.0 % DTBP are the same as those generated from neat PRF 0. The species evolution profiles of PRF 0 plus 3.0 % DTBP are presented in Figure 5.3. Table 5.4 shows the carbon balance.

Table 5.4: Carbon balance for PRF 0 experiments with DTBP addition

CAD	300	303	306	309	312	315	318	321
CARBON BALANCE (%)	100	88	87	85	102	98	79	94

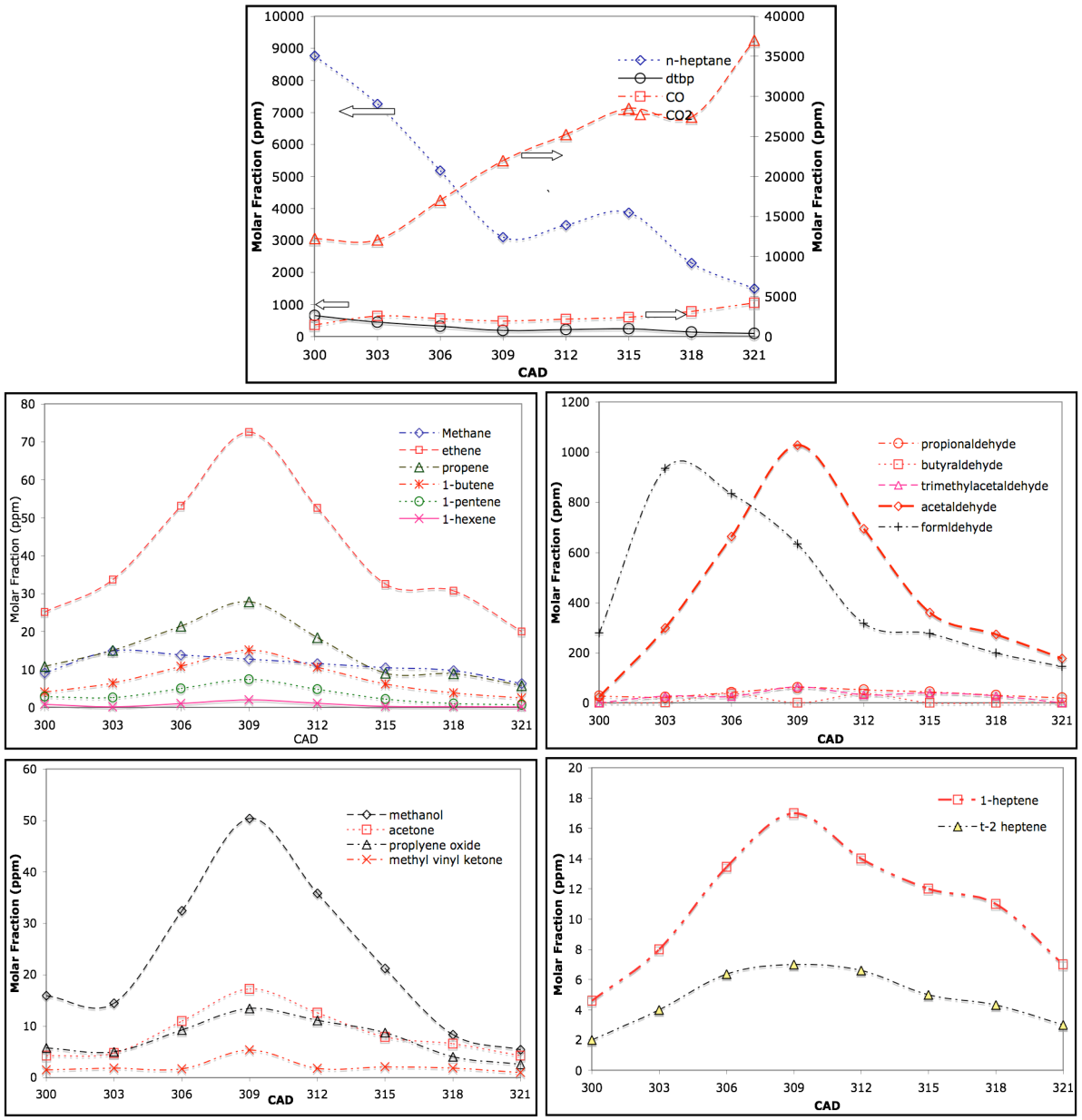

Figure 5.3: Species evolution profiles using PRF 0 (n-heptane) and 3 % DTBP at an equivalence ratio of 0.43, 423 K inlet Temperature, a CR of 16:1 and 600 RPM

Similar to two previous results at the same experimental condition, CO_2 is the dominant product. Unlike the baseline PRF 0, but like PRF 0 with propionaldehyde addition, the CO_2 molar fraction increases rapidly over the entire range of 300 to 321 CAD. At the beginning of sampling, at 300 CAD, the molar fraction of CO_2 is higher than that of the baseline case as well as the case with propionaldehyde addition. In this case CO_2 started with a molar fraction of about 10,000 ppm. The molar fraction of CO starts to increase at 300 CAD gradually until 321 CAD. The rise in the CO measured is 2774 ppm, which is much greater than the PRF 0 with propionaldehyde addition, more in the range of the baseline case. The next dominant species is the parent fuel, which starts out at around 9000 ppm, which is 19 % reacted before 300 CAD, whereas in the baseline case only 10 % reacted prior to 300 CAD.

The molar fractions of intermediate hydrocarbon species of PRF 0 plus 3.0 % DTBP shows slightly different trends from both the baseline as well as the second experimental condition, PRF 0 with propionaldehyde addition. The molar fraction of large and small oxygenates, small alkenes and alkanes start to appear at 300 CAD and increases rapidly up to 309 CAD and then decrease until 321 CAD.

Consistent with the other experimental conditions, among all small alkenes and alkanes, ethene has the highest molar fraction, followed by 1-butene, propene, and methane. The molar fraction of ethene starts to increase rapidly from 300 to 309 CAD to about 75 ppm. The molar fractions of propene, 1-butene, and methane also increase rapidly from 300 to 309 CAD, and reach their highest level of near 30, 15, and 13 ppm respectively at 309 CAD. Over the entire sampling period, the molar fraction of 1-

hexene is very low from 306 to 321 CAD. This behavior is consistent with the observations at the previous conditions. In this group, the overall molar fractions of all species are lower than measured for PRF 0 and PRF 0 with propionaldehyde addition with the exception of the aldehydes.

Like the two other experimental conditions, in this case, acetaldehyde and formaldehyde are the dominant aldehyde intermediates in this case. There is a rapid increase in the molar fractions of all aldehydes from 300 to 309 CAD and then decreases. At 309 CAD a maximum acetaldehyde, about 1000 ppm is observed compared to 1054 ppm for the baseline case. Unlike the other experimental conditions, formaldehyde peaks earlier than the other aldehyde products at a level of 980 ppm. Both acetaldehyde and formaldehyde have a molar fraction that is much higher than that of propionaldehyde (80 ppm max), butylraldehyde (63 ppm max), and trimethylacetaldehyde (76 ppm max).

For the small oxygenated species, the molar fractions of all four species increase rapidly from 300 CAD to 309 CAD and then decrease until 321 CAD during the entire sampling period. Among the four measurable small oxygenated species, methanol has the highest molar fraction of around 53 ppm, followed by acetone (20 ppm), propylene oxide (12 ppm), and methyl vinyl ketone (5 ppm). The molar fractions of the small oxygenated species of PRF 0 with DTBP addition are reduced by 30% compared to the baseline case.

In summary, the addition of DTBP into PRF 0 changes the species evolution profiles for small carbon number species, like small alkenes, aldehydes, and oxygenated species. The molar fraction of these small species increase rapidly from

300 to 309 CAD, and continue to increase and then quickly decrease up to 321 CAD. The addition of DTBP does not produce different intermediates, however, it reduces the molar fractions of small alkenes, and other oxygenated species by approximately 30 %, however, and the molar fractions of the aldehyde species remain almost the same prior to hot ignition.

5.2.2 PRF 20 with and without additives

The species evolution profile and carbon balance for PRF 20 at equivalence ratio of 0.43 (no additive) are presented in Figure 5.4 and Table 5.5, respectively. As with the PRF 0 data, the measured species are divided into five groups: 1) fuels, CO and CO_2 and DTBP; 2) small alkenes and alkanes, including methane, ethane, propene, 1-butene, 1- pentene, and 1-hexene; 3) C_7 and C_8 alkenes, including 1 & 2-heptene, 2,4,4- trimethyl-1& 2-pentene, and 4,4-dimethyl-2-pentene; 4) aldehydes, including formaldehyde, acetaldehyde, propionaldehyde, butylraldehyde, and trimethylacetaldehyde; and 5) small oxygenated species, including methanol, acetone, propylene oxide, and methyl vinyl ketone.

PRF 20 oxidation begins around 300 CAD, and sampling is conducted up to 321 CAD. At 309 CAD, nearly 50 % n-heptane is consumed and nearly 50 % iso-octane is consumed. After 312 CAD, the molar fractions of these two fuels plateau, with less than a 5.0 % decrease in molar fractions from 318 to 321 CAD with the exception at 321 CAD. Much like the other experiments discussed earlier, for this condition, CO_2 is the dominant product, however the trend is a little different. The molar fraction of CO_2 starts increases slowly between 300 to 306 CAD, where after it increases quickly from 306 to 312 CAD, and then continues to increase slowly to a maximum at 321 CAD.

From 300 to 321 CAD, the molar fraction of CO rises at a gradual rate.

The intermediate hydrocarbon species and products of PRF 20 start to form at 300 CAD, however, the concentration is very small. The big molar fraction jump for most species occurs at 306 CAD. For most species, the molar fractions increase dramatically between 303 to 318 CAD. After 318 CAD, most species molar fractions start to decrease until 321 CAD. The exception to this case occurs with the C_7 and C_8 alkenes, which start out with a higher molar fraction, peak at 303 CAD and then decreases dramatically from 303 to 312 CAD.

Among the small alkenes and alkanes, ethene has the highest molar fraction, followed by propene and 1-butene, then methane. The molar fraction of ethene is around 6 ppm at 300 CAD, as opposed to 12 ppm for the PRF 0 baseline case, and peaks at 318 CAD with a molar fraction of 136 ppm. The molar fraction of ethene peaks at 318 CAD and then decreases. The other small alkenes follow the same trend. The molar fraction of propene increases from 2 ppm at 300 CAD, reaches a peak molar fraction of 46 ppm at 318 CAD and then begins to decrease. Both 1-butene and methane increase to around 31 and 22 ppm respectively at 318 CAD, and then begin to decrease. Like the other experimental data of PRF 0, the molar fractions of 1-pentene and 1-hexene are relatively small, with a maximum level of less than 10 ppm and follow a trend similar to ethene, propene, 1-butene, and methane.

Table 5.5: Carbon balance for PRF 20 experiments

CAD	300	303	306	309	312	315	318	321
CARBON BALANCE (%)	100	97	92	82	78	102	97	88

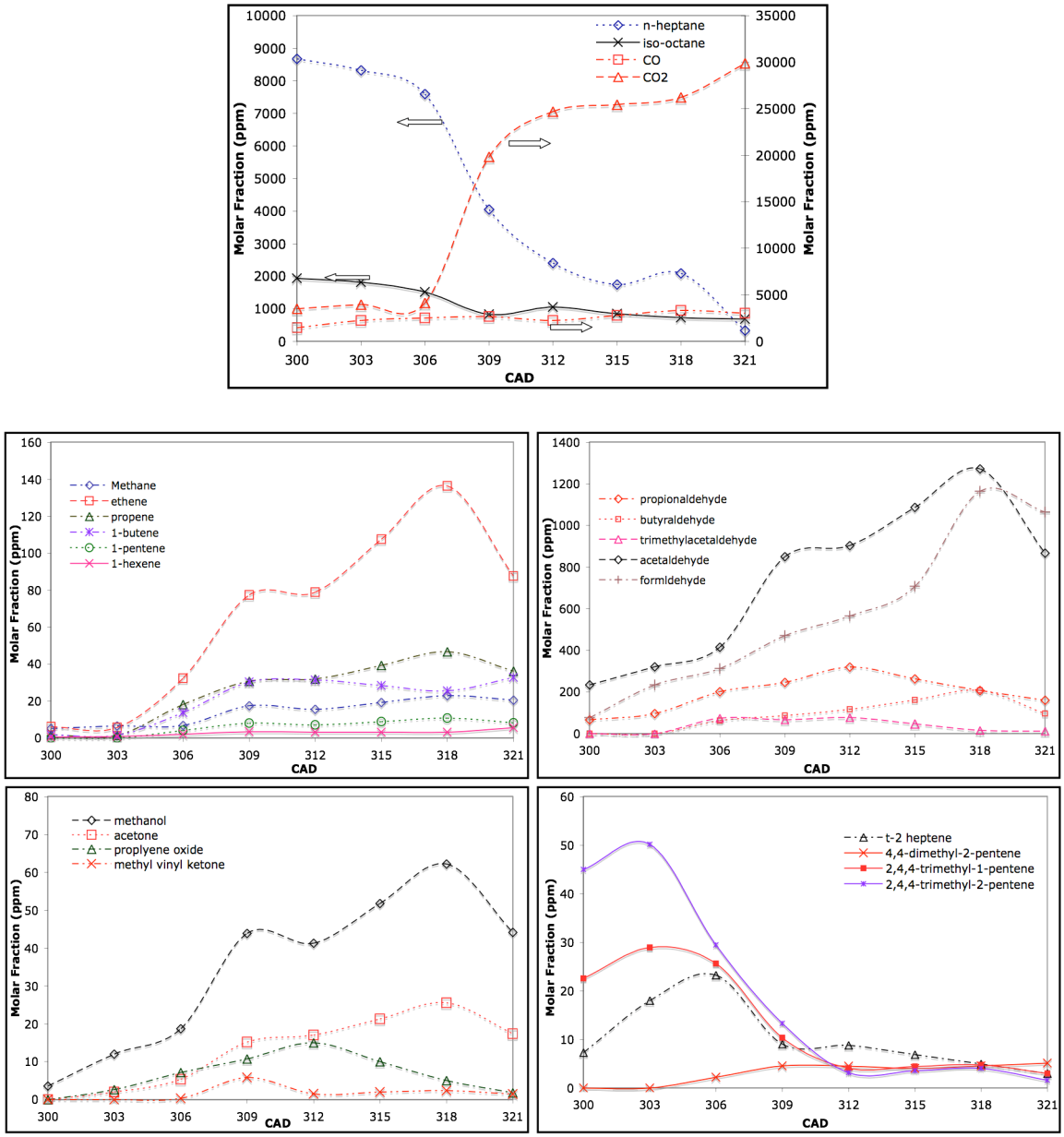

Figure 5.4: Species evolution profiles using PRF 20 at an equivalence ratio of 0.43, 423 K inlet Temperature, a CR of 16:1 and 600 RPM

For the C_7 alkenes, 1-heptene was not presented in this data because its retention time, and therefore its peak is overlapped by iso-octane peak. In the PRF 20 oxidation, 2,4,4-trimethyl-2 pentene and 2,4,4-trimethyl 1-pentene starts to appear at 300 CAD in large amounts. In this case more 2,4,4-trimethly-2-pentene was observed than 2,4,4 –trimethly-1-pentene, however they followed each other closely. 2-heptene was the next highest molar fraction C_7 alkenes observed. 4,4-dimethyl-2-pentene was also observed in a very small amount (less than 5 ppm). For the C_7 and C_8 alkenes, 2,4,4-trimethly-2-pentene and more 2,4,4-trimethly-1-pentene peak at 303 CAD and molar fractions of 50 and 28 ppm, respectively, and then begin to decrease quickly until 312 CAD then plateaus. 2-heptene peaks later at 306 CAD at a molar fraction of about 22 ppm until 309 CAD then decreases to 309 CAD and then remains stable up to 321 CAD. 4,4-dimethyl-2 pentene doesn't peak until 312 CAD at a molar fraction of about 5ppm and then remains stable until 321 CAD.

The aldehyde intermediates are present at 200 ppm higher molar fraction than in the baseline PRF 0, similar to the other experimental conditions, acetaldehyde and formaldehyde are the dominant aldehyde products of PRF 20. A gradual increase in the molar fractions of all acetaldehyde and formaldehyde occurs from 303 to 306 CAD. After 306 CAD there is a rapid increase in the molar fractions of acetaldehyde and formaldehyde up to 318 CAD. At 318 CAD, the molar fractions of acetaldehyde and formaldehyde are 1300 and 1260 ppm, respectively, and then begin to decrease quickly. Both acetaldehyde and formaldehyde have a molar fraction that is much higher than that of propionaldehyde (320 ppm max), butylraldehyde (207 ppm max), and

trimethylacetaldehyde (77 ppm max).

For the small oxygenated species, the molar fractions show trends similar to the other HC groups in this experiment. From 300 to 306 CAD there is a gradual increase in the molar fraction of the small oxygenated species. After 306 CAD there is a rapid increase in the molar fraction up to 318 CAD, then there is a rapid decrease. Among the four measurable small oxygenated species methanol has the highest molar fraction, around 62 ppm, followed by acetone (27 ppm) then propylene oxide (17 ppm) and finally methyl vinyl ketone (4 ppm).

The next experimental data presented examines the effect of propionaldehyde addition on the oxidation of PRF 20. As mentioned previously, an equivalence ratio of 0.43 was selected for this experiment. The percentage of propionaldehyde addition was set at 3.0 % by volume. The species observed are the same as those generated from neat PRF 20. The species evolution profiles and carbon balance are presented in Figure 5.5 and Table 5.6, respectively.

For this case, CO_2 remains the dominant product. The intermediate species development is different from the baseline PRF 20. Unlike the baseline PRF 20, with propionaldehyde addition the CO_2 molar fraction increases slowly from 300 to 312 CAD then quickly increases. At the beginning of sampling, at 300 CAD, the molar fraction of CO_2 is higher than the baseline case. In this case CO_2 started with a molar fraction of about 11000 ppm. The molar fraction of CO increases gradually from 300 CAD until 321 CAD. The change in the amount of CO measured is 1360 ppm, less than the PRF 20 baseline case, which was 1890 ppm. The next dominant species is the parent fuel, which in this case is a mixture of iso-octane and n-heptane. At 300 CAD the molar

fraction of n-heptane is about 3600 ppm and the molar fraction of iso-octane is about 600 ppm. These values are significantly lower than for the baseline case. The baseline PRF 20 started out with an n-heptane molar fraction of about 8700 ppm and iso-octane started out with 2000 ppm molar concentration. For PRF 20 with propionaldehyde, the molar concentration of the remaining parent fuel at 300 CAD decreases slowly until about 312 CAD, followed by a more rapid decrease.

Following the pattern, CO_2 and parent fuel, the molar fractions of the intermediate hydrocarbon species show different trends from the baseline fuel condition. The molar fractions of small oxygenates, small alkenes and alkanes start to appear at 300 CAD and increases slowly up to 306 CAD, it then increases at a more rapid rate up to 315 CAD, after that they decrease quickly.

Similar to the other experimental conditions discussed, among all small alkenes and alkanes, ethene has the highest molar fraction, followed by 1-butene, and propene. The molar fraction of ethene starts to increase slowly from 300 to 306 CAD, then increase rapidly to about 130 ppm at 315 CAD, and then decreases quickly. The molar fractions of propene and 1-butene, also increase rapidly from 300 to 306 CAD, and reach their highest level of near 52 and 48 ppm respectively at 315 CAD. Like the other experimental conditions, over the entire sampling period, the molar fraction of 1-hexene is very low, and remains steady from 300 to 321 CAD. In this group, the overall molar fractions of all species are lower than measured for PRF 20 with propionaldehyde addition with the exception of the aldehydes.

Acetaldehyde and formaldehyde are the dominant aldehyde products for this condition. Unlike the other intermediates discussed for PRF 20 with PRF 20 with 3.0 %

propionaldehyde in this study, there is a rapid increase in the molar fractions of both acetaldehyde and formaldehyde from 300 to 315 CAD followed by an equally rapid decreases. At 315 CAD the most acetaldehyde and formaldehyde is observed in molar fractions of about 1400 ppm as opposed 1300 ppm for the baseline case. Like the other cases examined, both acetaldehyde and formaldehyde have a molar fraction that is much higher than that of propionaldehyde (140 ppm max), butylraldehyde (157 ppm max), and trimethylacetaldehyde (45 ppm max). The molar fraction of propionaldehyde remains stable until about 315 CAD and then begins to decrease slowly. Similar to PRF 0 with propionaldehyde addition, about 40 % propionaldehyde had reacted prior to 300 CAD.

For the small oxygenated species, the molar fractions of all four species increase slowly from 300 to 309 CAD, and then increases rapidly to 315 CAD, at which point they decrease. Among the four measurable small oxygenated species, methanol has the highest molar fraction of around 70 ppm. Acetone and propylene oxide has approximately the same molar fraction from 300 to 312 CAD, at which point acetone increases rapidly to a molar fraction of about 24 ppm at 318 CAD. Propylene oxide has its highest molar fraction of about 18 ppm at 318 CAD. The molar fraction of methanol is increased slightly over the baseline case while the other small oxygenated species remains about the same.

The C_7 and C_8 alkenes are present in much smaller molar fractions. 2,4,4-trimethly-2-pentene and 2,4,4-trimethyl-1-pentene starts to appear at 300 CAD in a larger amount than the other C_7 and C_8 alkenes and are relatively stable. 2-heptene was the next highest molar fraction C_7 alkenes observed and was not as stable as the C_8 alkenes.

4,4-dimethyl-2-pentene was also observed in the lowest amount small amount. It peaked at 315 CAD and then remained relatively stable.

In summary, the addition of propionaldehyde into PRF 20 changes the species evolution profiles for small carbon number species, such as small alkenes, aldehydes, and oxygenated species. The molar fraction of these small species increase slowly from 300 to 309 CAD then quickly increases up to 315 CAD, then decreases. The addition of propionaldehyde does not produce additional intermediates in measurable amounts.

Table 5.6: Carbon balance for PRF 20 experiments with propionaldehyde addition

CAD	300	303	306	309	312	315	318	321
CARBON BALANCE (%)	100	98	96	87	100	90	94	88

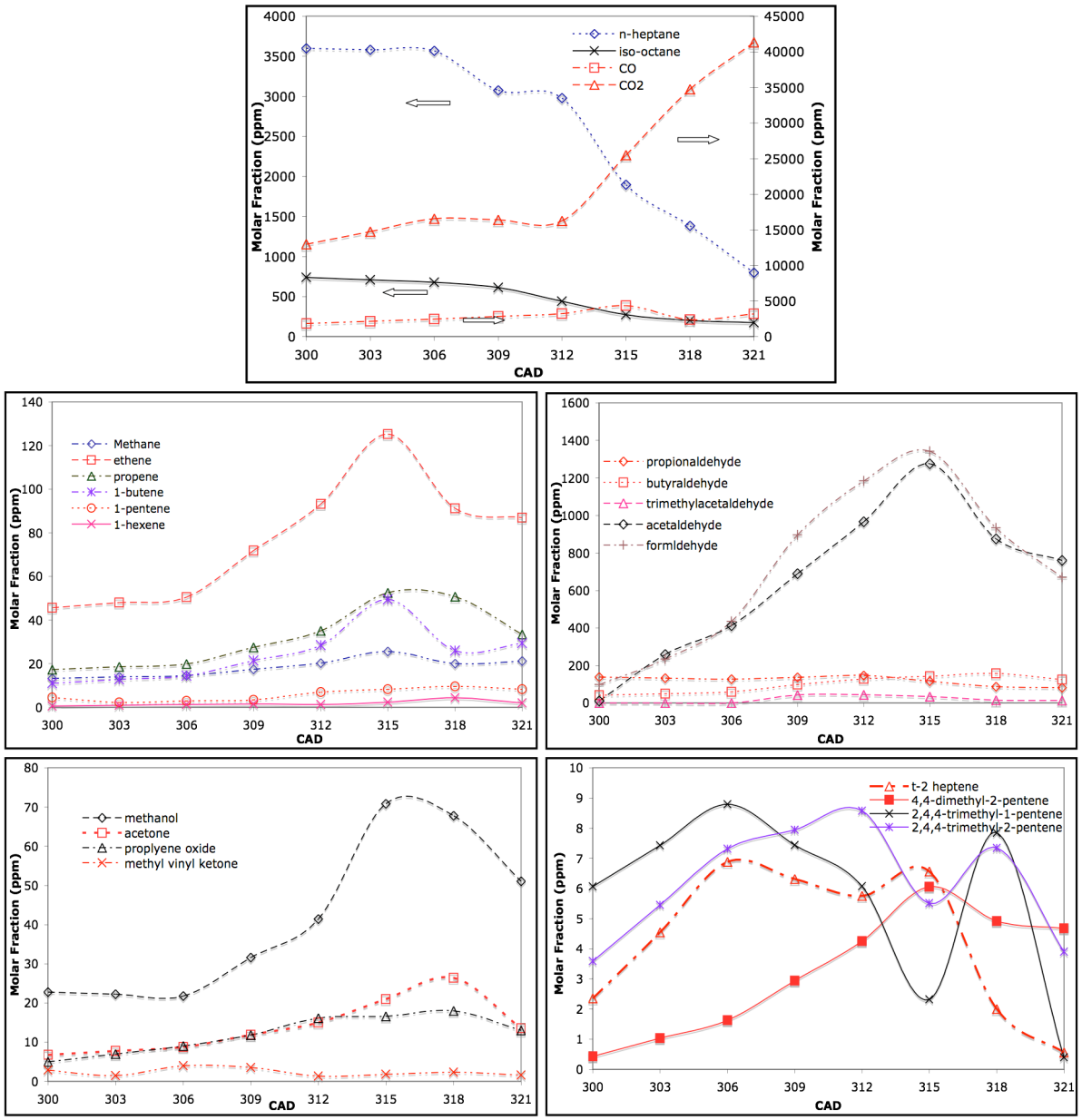

Figure 5.5:Species evolution profiles using PRF 20 and 3 % propionaldehyde at an equivalence ratio of 0.43, 423 K inlet Temperature, a CR of 16:1 and 600 RPM

The last set of experimental data presented examines the effect of DTBP on the oxidation of baseline PRF 20. As mentioned previously, an equivalence ratio of 0.43 was selected and DTBP addition was set at 3.0 % by volume. The species observed with of PRF 20 plus 3.0 % DTBP are the same as those generated from neat PRF 20. The species evolution profiles of PRF 20 plus 3.0 % DTBP are presented in Figure 5.6. The carbon balance for this condition is also presented in Table 5.7.

For PRF 20 with DTBP addition CO_2 is still the dominant product. The trend of intermediate species development is different from the other PRF 20 studies. Unlike the baseline PRF 20, with propionaldehyde addition the CO_2 molar fraction increases slowly from 300 to 303 CAD then quickly increases until 309 CAD. At this point, CO_2 production remains stable until 318 CAD where it increases again. At the beginning of sampling, at 300 CAD, the molar fraction of CO_2 is higher than that of the baseline case, but less than the propionaldehyde case. In this case CO_2 started with a molar fraction of about 7000 ppm, as opposed to 4000 ppm for the baseline case. The molar fraction of CO increases gradually starting at 300 CAD to 312 CAD and then increases at a faster thereafter.

The next most abundant species is the parent fuel, which in this case is a mixture of iso-octane and n-heptane. At 300 CAD the molar fraction of n-heptane is about 3300 ppm and the molar fraction of iso-octane is about 700 ppm. These values are dramatically less than with the baseline case which is around 8900 ppm for n-heptane and 2000 ppm for iso-octane. For PRF 20 with DTBP, the molar concentration of the parent fuel over the entire sampling period is similar to the baseline PRF except the parent fuel is present in a lower molar fraction. CO_2 production is also similar with the

exception that it starts to increase more rapidly earlier.

Much like the CO_2 and parent fuel, the molar fractions of the intermediate hydrocarbon species of PRF 20 plus 3.0 % DTBP also shows different trends from the baseline fuel condition. The molar fractions of small oxygenates, small alkenes and alkanes start to appear at 300 CAD, increases rapidly up to 309 CAD, then decreases slowly.

Among all small alkenes and alkanes, ethene has the highest molar fraction, followed by 1-butene, and propene. The molar fraction of ethene starts to increase slowly from 300 to 309 CAD, where it reaches a molar fraction of 83 ppm, then decreases slowly. The molar fractions of propene and 1-butene, also increase rapidly from 300 to 309 CAD, and reach their highest level of near 37 and 33 ppm respectively at 315 CAD. The molar fractions of 1-pentene and methane are very low, under 15 ppm. The molar fraction of 1-hexene is very low compared to the other small alkenes, and remains steady from 300 to 321 CAD. In this group, the overall molar fractions of all species are lower than measured for PRF 20 with DTBP addition with the exception of the aldehydes, which stays about the same.

For PRF 20 with DTBP, acetaldehyde and formaldehyde are the primary aldehyde products. There is a rapid increase in the molar fractions of all acetaldehyde and formaldehyde from 300 to 309 CAD and then decreases gradually. At 309 CAD the most acetaldehyde and formaldehyde is observed in molar fractions of about 1100 ppm and 1000 ppm about the same as for the baseline case. Both acetaldehyde and formaldehyde have a molar fraction that is much higher than that of propionaldehyde, butylraldehyde, and trimethylacetaldehyde, which are all, present in much lower

concentrations than the baseline case.

For the small oxygenated species, the molar fractions of all four species also increase rapidly from 300 to 309 CAD, and then gradually decrease. Of the oxygenated species, methanol has the highest molar fraction of around 60 ppm. Acetone and propylene oxide has approximately the same molar fraction (about 17 ppm max) from 300 to 321 CAD. Methyl vinyl ketone follows the same trend but is present in molar fraction of less than 8 ppm.

For PRF 20 oxidation with propionaldehyde addition the C_7 and C_8 alkenes are present in much smaller molar fractions than the baseline PRF 20. Of the C_7 and C_8 alkenes, 2-heptene is present in the highest amount. 2,4,4-trimethly-2-pentene and 2,4,4-trimethyl-1-pentene are present in the second largest amount. 4,4-dimethyl-2-pentene was also observed in the lowest amount. It peaked at 309 CAD and then remained relatively stable.

In summary, the addition of DTBP into PRF 20 changes the species evolution profiles for small carbon number species, like small alkenes, aldehydes, and oxygenated species. The molar fraction of these small species increase rapidly from 300 to 309 CAD then gradually decreases. The addition of DTBP did not produce additional intermediates in measurable amount.

Table 5.7: Carbon balance for PRF 20 experiments with DTBP addition

CAD	300	303	306	309	312	315	318	321
CARBON BALANCE (%)	100	99	96	101	89	100	96	93

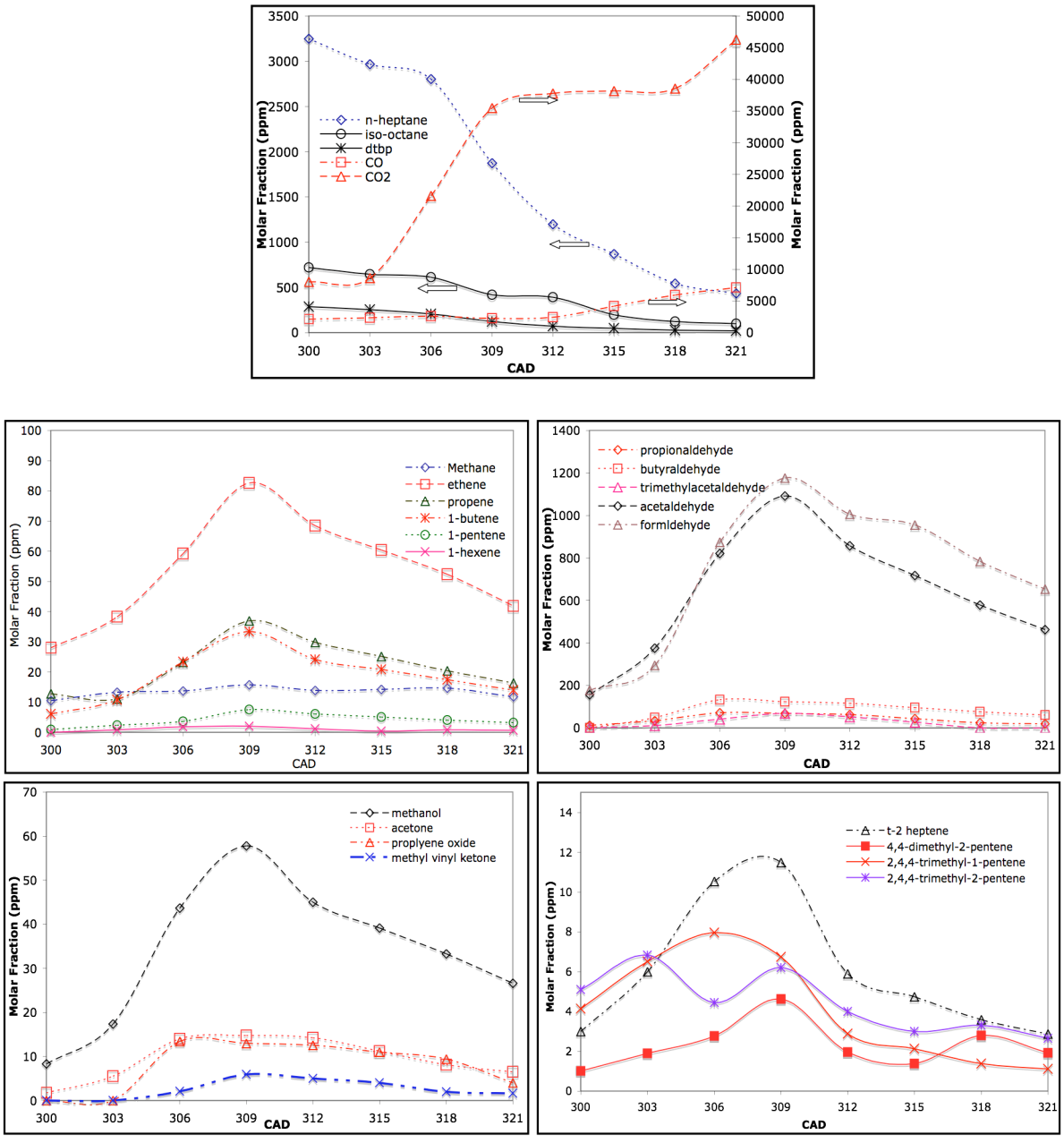

Figure 5.6: Species evolution profiles using PRF 20 and 3 % DTBP at an equivalence ratio of 0.43, 423 K inlet Temperature, a CR of 16:1 and 600 RPM

5.2.3 Discussion

For PRF 0 and PRF 20, the addition of DTBP, or propionaldehyde promotes ignition. In chapter 4, it was shown that addition of either of these additives reduces the NTC behavior. This effect on NTC behavior will be the basis of the explanations presented.

For n-heptane oxidation, the addition of propionaldehyde and DTBP changes the trends of intermediate products produced. The addition of DTBP produces a higher concentration of CO and CO_2, than either the neat case or with propionaldehyde addition. Compared to DTBP, propionaldehyde consumes slightly more fuel initially. With DTBP there are much lower levels of C_6 and lower alkenes, than neat n-heptane case and with propionaldehyde addition. There are also lower levels of small oxygenates produced with DTBP. DTBP also produced more formaldehyde than the neat heptane case, as well as neat PRF 20. With DTBP there are much lower levels of C_6 and lower alkenes, than neat n-heptane case and with propionaldehyde addition. There are also lower levels of small oxygenates as well as propionaldehyde, butylraldehyde, and trimethylacetaldehyde produced with DTBP addition for the PRF 0 case. However with the PRF 20 case, the addition of DTBP produces similar levels of small oxygenates, but the levels of propionaldehyde, butylraldehyde, and trimethylacetaldehyde are still reduced.

For PRF 20 oxidation, the addition of propionaldehyde and DTBP also changes the trends of intermediate products produced. With the addition of propionaldehyde a higher concentration of CO and CO_2 was produced than the neat case or with DTBP addition. This is different from PRF 0 with DTBP, where as DTBP produced the most

CO and CO_2. Compared to propionaldehyde, DTBP consumes slightly more fuel initially. PRF 20 oxidation with DTBP exhibits similar trends to PRF 0, where there are lower levels of C_6 and lower alkenes, as well as small oxygenates.

DTBP seems to react more with PRF 20 as opposed to PRF 0. For PRF 20, at 300 CAD 287 ppm DTBP is observed, For PRF 0, there is much more DTBP present at 300 CAD, 654 ppm. This suggests that DTBP reacts more favorable with the iso-octane present in the mixture.

For both PRF 0 and PRF 20, an addition of propionaldehyde increases the molar fractions of the acetaldehyde. There is no noticeable change in the production of the other aldehydes observed in the samples.

From the oxidation mechanism for n-heptane and iso-octane (Li, 1995) observed separately, most of the alkenes in the system are generated from heptane oxidation. As a result it is not unexpected that the species evolution profiles for heptane generate more alkenes observed than does the PRF 20 mixture, which contains 20 % iso-octane. Subsequently, we will focus the discussion on heptane oxidation where relevant. Heptane oxidation is initiated when H atoms are abstracted either by an active species either oxygen or some other active molecules.

$$RH + X = R\bullet + XH$$

Where RH and R• represent the fuel and its alkyl radical (n-heptyl) respectively, and X represents oxygen or an active radical such as hydroxyl, OH•, hydroperoxyl, HO_2•, and alkylperoxyl, RO_2•. Once the n-heptyl radical is formed, it can react with molecular oxygen or it can decompose to form a lower molecular weight alkene and an alkyl radical. With DTBP addition, the production of alkenes is significantly inhibited while the

production of small oxygenates is slightly inhibited. The mechanism by which this occurs is proposed below. This suggests that the n heptyl radical is reacting with molecular oxygen, however alkenes are not being produced in large amounts like the neat heptane case.

$$R\bullet + O_2 = RO_2\bullet \qquad (R1)$$

RO_2 can decompose to form alkenes and a hydroperoxyl radical.

$$RO_2\bullet = \text{alkenes} + HO_2\bullet \qquad (R2)$$

The shift of the $RO_2\bullet$ reaction mechanism to the alkene formation path can explain behavior such as NTC. Results from Chapter 4 showed that the addition of DTBP reduces NTC behavior. From the species evolution profiles presented, there is no evidence of a significant change in chemical pathways that would suggest a chemical effect of DTBP. In combination with the species evolution profiles shown here with DTBP addition to n-heptane, and the results shown in chapter 4, we can conclude that the addition of DTBP has a thermal effect which is similar to raising inlet manifold temperature, which subsequently reduces NTC behavior inhibiting the formation of the alkenes, and small oxygenates observed.

Another pathway for alkene formation is through an alternative pathway for RO_2 decomposing is to form QOOH• where QOOH• is formed when an H atom is transferred to the O-O site of $RO_2\bullet$. QOOH• represents the hydroperoxyalkyl This reaction is important for larger molecular weight fuels (> C_4). Further decomposition of QOOH can yield aldehydic products and other alkenes.

$$RO_2\bullet = QOOH\bullet \qquad (R3)$$

$$QOOH\bullet = RHCO + \text{alkene} + OH\bullet \qquad (R4)$$

Following the same explanation, the yield of aldehydes as well as alkene products is also reduced due to the effects on NTC from DTBP addition as a result of a rise in the local gas temperature due to the exothermic decomposition of DTBP.

DTBP addition did show an increase in measured formaldehyde. This could be the result of the decomposition of DTBP (Griffiths et al., 1990). DTBP is seen to thermally decompose into two t-butoxy radicals, in the 600-650K temperature range, ($C_3H_{18}O_2 \rightarrow CH_9CO\bullet + CH_9CO\bullet$). These radicals internally rearrange very quickly, primarily forming acetone (C_3H_6CO) and a methyl radical ($CH_3\bullet$). The acetone is stable and lingers in the cycle until the main ignition promoting reactions commencing at temperatures of approximately 1100 K. Unlike acetone, the methyl radicals undergo oxidation on a microsecond timescale to yield molecular products, formaldehyde being one of them.

For PRF 20, the addition of DTBP exhibits similar behavior to PRF 0, however the magnitude of the reduction of alkenes produced is slightly lower, 53 % to 39 %, for PRF 0, and PRF 20 respectively. This can be attributed to the presence of iso-octane reducing the reactivity of n-heptane. The presence of DTBP does reduce the NTC behavior, however the effect is not as great as with n-heptane. While DTBP increases the local gas temperature promoting oxidation, iso-octane acts as a radical scavenger. Also there is more DTBP that has reacted initially with PRF 20 than with PRF 0, 71 % and 34% respectively. A possible explanation is that, the presence of iso-octane slows down the chemistry occurring at low temperatures, as a result of the radical scavenging. This allows more time for the breakdown of DTBP. The explanation for the slight reduction in small oxygenates described by R4 also holds for the PRF 20 case.

The addition of propionaldehyde to PRF 0 and PRF 20 has slightly different behavior than that of DTBP addition. Much like DTBP, the addition of propionaldehyde promotes oxidation or the fuels tested, PRF 0 and PRF 20, but while the C_8 and lower alkenes are reduced, the reduction is not significant as compared with that of DTBP. Also, what is very different from DTBP addition is that, with the addition of propionaldehyde, there are higher levels of acetaldehyde observed. The molar fractions of the other aldehydes remain almost the same. An explanation could be that there is a promotion is oxidation as a result of propionaldehyde reacting by itself producing OH•. The mechanism for this is described in chapter 4.

5.2 Closure

In summary it was shown that For PRF 0 and PRF 20, the addition of DTBP, or propionaldehyde has a promoting effect ignition under HCCI conditions. Species evolution profiles were obtained at identical engine operating conditions to analyze the combustion chemistry. It has been suggested that the mechanism behind the ignition promoting effect is due to a reduction in NTC behavior for DTBP, and propionaldehyde reacting with itself producing OH•. Specifically it is the shift of the RO_2• reaction mechanism to the alkene formation path can explain NTC behavior. With a reduction in NTC with DTBP addition, it is expected that there is a reduction in the molar fractions of alkenes formed. Also, from the species evolution profiles presented, there is no evidence of a significant change in chemical pathways that would suggest a chemical effect of DTBP. As a result it is concluded that the mode of action of DTBP to promote oxidation is thermal for the fuels tested.

While the addition of propionaldehyde to PRF 0 and PRF 20 promotes oxidation the reason is different from that of DTBP. An explanation could be that there is a promotion in oxidation as a result of propionaldehyde reacting by itself producing OH radicals as described in Chapter 4.

CHAPTER 6. SUMMARY, CONCLUSIONS AND RECOMMENDATIONS

The work carried out consisted of two major parts, (1) the effect of selected oxygenated hydrocarbon additives on the low temperature oxidation of PRF blends and (2) investigating of the effects on oxidation when blending SI PRFs and their blends with selected oxygenates specifically, di-tertiary-butyl-peroxide (DTBP) and propionaldehyde, under homogeneous charge compression ignition engine operation. The results and conclusions are summarized in this chapter, followed by recommendations for additional work.

6.1 Summary

This thesis reports studies on the effects of selected oxygenates on the oxidation of SI Primary Reference Fuels under HCCI conditions. The effect on NTC behavior, and overall oxidation was reported. The key finding of this work were that the addition of propionaldehyde and DTBP alters the autoignition for PRFs by having a direct impact on NTC behavior. Specifically, DTBP advances ignition timing over a range of engine operating conditions as a result of the reduction of NTC behavior, which decreases ignition delay, while propionaldehyde can both promote and suppress ignition depending low and high temperature chemistry. The combustion temperature is the mechanism responsible for the reversal in propionaldehyde addition, where at low temperatures autoignition is suppressed as a result of propionaldehyde acting as a radical scavenger, while at higher temperatures it is promoted as a result of propionaldehyde reacting with itself producing radicals. Further recommendations on oxygenates/PRF behavior under HCCI conditions are also provided.

6.2 Results and Conclusions

This work was conducted in a single cylinder Cooperative Fuels Research (CFR) octane rating engine modified to run in HCCI mode. The effect of select additives on PRF blends were tested and evaluated.

In chapter 4, a single cylinder engine was motored with PRF blends neat, as well as with an addition of propionaldehyde or DTBP. The exhaust CO concentration was selected and monitored as it is a good indication of reactivity. The CO concentration was measured and reported. The results showed that, propionaldehyde promotes preignition reactivity of both n-heptane and PRF 50 slightly. It was shown that as the Octane number of the fuel was increased, the effect of propionaldehyde goes from promoting reactivity to inhibiting reactivity. The addition of propionaldehyde to PRF fuels is seen to have a direct impact on NTC behavior. A possible explanation for the behavior is the difference in the oxidation of propionaldehyde at low and high temperatures. The data suggest that propionaldehyde acts as a hydroxyl radical scavenger at lower temperatures. At higher temperatures propionaldehyde may react producing hydroxyl radicals, OH•, which aid in the destruction of the parent fuel, thus advancing ignition. Similar conclusions were reached by other researchers (Kaiser, 1987, Zheng et al, 2005). Kuwahara et al., (2004) showed that aldehyde addition, specifically formaldehyde, may have either a suppressing or promoting effect on autoignition.

Chapter 4 also presented the effect of DTBP on low temperature reactivity. It was observed that DTBP promotes reactivity in the low temperature regime. As a result, it

reduces the NTC behavior, which can lead to a reduction in ignition delay, and subsequently earlier ignition.

In chapter 5, species evolution profiles were measured for select fuels and additives under select engine operating conditions. This was to investigate the effects of the oxygenated hydrocarbon additives on PRF oxidation under HCCI conditions. It was shown that For PRF 0 and PRF 20, the addition of DTBP, or propionaldehyde has a promoting effect on ignition under HCCI conditions. The species evolution profiles showed an increase in the destruction of fuel leading to autoignition for both additives. There was also a slight decrease in the production of alkenes for both fuels, with propionaldehyde addition, while for DTBP there was a great decrease in the production of alkenes. It was suggested that the mechanism behind the changes in ignition was a direct effect on NTC behavior from additives. DTBP causes a reduction in NTC behavior while propionaldehyde can both decrease and increase NTC behavior by acting as a radical scavenger at low temperatures and reacting with itself producing OH•. With a reduction in NTC with DTBP addition, it is expected that there is a reduction in the molar fractions of alkenes formed. Also, from the species evolution profiles presented, there is no evidence of a significant change in chemical pathways that would suggest a chemical effect of DTBP. As a result it is concluded that the mode of action of DTBP to promote oxidation is thermal for the fuels tested.

6.3 Recommendations for Future Work

While substantial work has been completed and reported in the HCCI area, additional work is necessary in both the experimental and modeling areas to further

improve the understanding of effects of selected oxygenates on HCCI operation. Specifically, the following extensions to the present work are recommended.

Measure Critical Radical Species under HCCI Conditions

In this work, significant information on the oxidation behavior of various fuels with selected oxygenates were presented. However there is lack of evidence to suggest what is going on in terms of the radical activity in the combustion chemistry. Specifically, there is a paucity of detailed information on some critical radicals such as OH, HO_2, RO_2, etc. Measurement of these radicals would be extremely useful for providing insight into the reaction pathways leading to hot ignition and for developing and validating chemical kinetic models. Compared with molecular species, the radicals generated during preignition reactions are more difficult to measure.

Develop Chemical Kinetic Models

Obtaining species evolution profiles from in-cylinder sampling yield information on the stable intermediates formed during the oxidation of the PRF blends and the additives used in this study. This allows for the opportunity to develop chemical kinetic models that could model autoignition under HCCI conditions with various fuels and selected oxygenates. Using the measurement of critical radical species in conjunction with the species evolution profiles, a clear picture of the combustion chemistry can be obtained. The model will need to be able to model autoignition under a broad range of engine conditions. Second, the model needs to be able to model a broad range of fuels.

LIST OF REFERENCES

Aceves, S. M., Flowers, D., Martinez-Frias, J., Espinosa-Lopez, F., Pitz, W. J. and R. Dibble (2003) "Fuel and Additive Characterization for HCCI Combustion," Paper Number 2003-0130, JSAEEAE International Spring Fuels & Lubricants Meeting, Yokohama, Japan, May 19-22.

Aceves, S.M., Smith, J. R., Westbrook, C. K. and Pitz, W. (1999) "Compression Ratio Effect on Methane HCCI Combustion," ASME Journal of Gas Turbines and Power, 121, 569-574.

Amann, C. A. (1985), "Cylinder-Pressure Measurement and Its Use in Engine Research," SAE Paper 852067.

Amneus, P., Mauss, F., Kraft, M., Vressner, A., and Johansson, B. (2005) ''NO_x and N_2O Formation in the HCCI Engine,'' SAE Paper No. 2005-01-0126.

Benson, S.W. (1981), "The Kinetics and Thermochemistry of Chemical Oxidation with Application to Combustion and Flames," Prog. Energy Combust. Sci., 7, 125-134.

Bhave, A., Kraft, M., Mauss, F., Oakley, A. and Zhao, H. (2005), "Evaluating the EGR-AFR Operating Range of a HCCI Engine," SAE paper No. 2005-01-0161.

Christensen, M. and Johansson, B. (1998), ''Influence of Mixture Quality on Homogeneous Charge Compression Ignition,'' SAE Paper No. 982454.

Christensen, M. and Johansson, B. (2000), ''Supercharged Homogeneous Charge Compression Ignition with Exhaust Gas Recirculation and Pilot Fuel,'' SAE Paper No. 2000-01-1835.

Christensen, M., Hultquist, A. and Johansson, B. (1999), ''Demonstrating the Multi Fuel Capability of a Homogeneous Charge Compression Ignition Engine with Variable Compression Ratio,'' SAE Paper No. 1999-01-3679.

Christensen, M., Johansson, B. and Einewall, P. (1997), ''Homogeneous Charge Compression Ignition (HCCI) Using Iso-octane, Ethanol and Natural Gas – A Comparison with Spark Ignition Operation,'' SAE Paper No. 972874.

Christensen, M., Johansson, B., Amneus, P. and Mauss, F. (1998), ''Supercharged Homogeneous Charge Compression Ignition,'' SAE Paper No. 980787.

Dechaux, J.C. (1973), "The Negative Temperature Coefficient in the Oxidation of Hydrocarbons," Oxidation and Combustion Reviews, 6, 75.

Dryer, F.L. (1991), "The Phenomenology of Modeling Combustion Chemistry," Fossil Fuel Combustion-A Source Book, 121-213, W. Bartok and A.F. Sarofim, eds., Wiley Interscience, New York.

Dryer, F.L. and Glassman, I. (1978), "Combustion Chemistry of Chain Hydrocarbons," Progress in Astronautics and Aeronautics, 62, 255 - 273.

Eng, J.A., Leppard, W.R. and Sloane, T. (2003), "Effect of Di-Tertiary Butyl Peroxide (DTBP) Addition to Gasoline on HCCI Combustion," SAE Paper No. 2003-01-3170, 2003.

Filipe, D.J. (1992): "Reactivity studies of primary reference fuel blends in a motored engine", M.S. Thesis, Drexel University, Philadelphia, PA.

Flowers, D. L., Aceves, S.M., Smith, J.R., Torres, J., Girard, J. and Dibble, R. (2000), "HCCI in A CFR Engine: Experiments and Detailed Kinetic Modeling," SAE Paper No. 2000-01-0328.

Flynn P.F., Hunter, G.L., Zur Loye, A.C., Akinyemi, W.C., Durrett, R.P., Moore, G.A., Muntean, G.G., Peters, L.L., Pierz, P.M., Wagner, J.A., Wright, J.F. and Yeager, J.M. (1999a), "Premixed Charge Compression Ignition Engine with Optimal Combustion Control," International Patent WO9942718, World Intellectual Property Organization.

Flynn, P.F., Russell, P.D., Hunter, G.L., Axel, O.L. and Akinyemi, O.C. (1999b), "Diesel Combustion: An Integrated View Combining Laser Diagnostics, Chemical Kinetics, and Empirical Validation," SAE Paper No. 1999-01-0509.

Gluckstein, M.E. and Walcutt, C (1964), "End-Gas Temperature Pressure Histories and Their Relation to Knock," SAE Transactions, 69. 529-531.

Gong, X., Zheng, J., Lenhert, D., Miller, D.L. and Cernansky, N.P. (2005a), "The Effect of DTBP Additive on the Oxidation of Gasoline Primary Reference Fuels in a Pressurized Flow Reactor," Paper No. C03, The 4th U.S. Sections of the Combustion Meeting, Philadelphia, PA, March 2005.

Gong, X., Johnson, R.O., Miller, D.L. and Cernansky, N.P. (2005b), "Effects of DTBP on the HCCI Combustion Characteristics of SI Primary Reference Fuels," SAE Paper Offer No. 05FFL-121, Powertrain & Fluid Systems Conference & Exhibition, San Antonio, Texas, October 24-27, 2005.

Gong, X., Zheng, J., Miller, D.L. and Cernansky, N.P. (2005c), "Experimental and Computational Study on Preignition Chemistry of SI Primary Reference Fuels in a Pressurized Flow Reactor," Paper No.18587, 37th ACS Middle Atlantic Regional Meeting (MARM), Rutgers University, NJ, May 22-25, 2005.

Gray III, A. W. and Ryan III, T. W. (1997), "Homogeneous Charge Compression Ignition (HCCI) of Diesel Fuel," SAE Paper No.971676.

Green, J. B., Domingo, N. Storey, J. M. E., Wagner, R. M. and Armfield, J. S. (2000), "Experimental Evaluation of SI Engine Operation Supplemented by Hydrogen Rich Gas from a Compact Plasma Boosted Reformer," SAE paper No. 2000-01-2206

Griffiths, J. F., Halford-Maw, P.A. and Mohamed, C. (1997), "Spontaneous Ignition Delays as a Diagnostic of the Propensity of Alkanes to Cause Engine Knock," Combustion and Flame, 111(4), 327-337.

Griffiths, J.F., Inomata, T. and A.J. Pappin (1990), "The Role of Additives as Sensitizers for the Spontaneous Ignition of Hydrocarbons," Twenty-Third International Symposium on Combustion, The Combustion Institute, 1990, 1759-1766.

Gupta, A., Miller, D. L and Cernansky, N. P. (2006), "Effect of DTBP on PRF Combustion in HCCI Engines," Paper No. C5, Technical Meeting of the Central States Section of the Combustion Institute, Cleveland, OH, May 21-23.

Heywood, J.B. (1988), "Internal Combustion Engine Fundamentals," McGraw-Hill, Inc., ISBN 0-07-028637-X, 1988

Hurn, R.W. and Hughes, K.J. (1956), "Autoignition Accelerator and Auto-Autoignition Environment," Industrial and Engineering Chemistry, 48 (10), 1904-1908.

Ishibashi, Y. and Asai, M. (1996), "Improving the Exhaust Emissions of Two-Stroke Engines by Applying the Activated Radical Concept," SAE Paper No. 960742.

Johnson, R.O., (2007), A Fundamental Study of the Autoignition Behavior of SI Primary Reference Fuels with Propionaldehyde and DTBP as an Additive, M.S Thesis, Drexel University, Philadelphia, PA.

Kaahaaina, N.B., Simon, A.J., Caton, P.A. and Edwards, C.F. (2001), "Use of Dynamic Valving to Achieve Residual-Affected Combustion," SAE paper 2001-01-0549.

Kaiser, E.W. (1987), "A Modeling Study of the Oxidation of Propionaldehyde in the Negative Temperature Coefficient Regime," International Journal of Chemical Kinetics, 19, 457-486.

Koert, D.N. (1990), Effects of Pressure on Hydrocarbon Oxidation Chemistry, Ph.D. Thesis, Drexel University, Philadelphia, PA.

Koopmans, L. and Denbratt, I. (2002), "Cycle to Cycle Variations and Their Influence on Cycle Resolved Unburned Hydrocarbons and Gas Temperature from a Camless Gasoline Compression Ignition Engine," SAE paper No. 2002-01-0110.

Kuwahara, K., Ando, H., Furutani, M. and Ohta, Y. (2004), "Impact of Formaldehyde Addition on Auto-Ignition in Engines," The Sixth International Symposium on Diagnostics and Modeling of Combustion in Internal Combustion Engines, Yokohama, Japan, 2-5 August.

Law, D., Allen, J. and Chen, R. (2001), "On the Mechanism of Controlled Auto Ignition" SAE Paper No. 2001-01-0421.

Leppard, W.R. (1992), "The Autoignition Chemistry of Primary Reference Fuels, Olefin/Paraffin Binary Mixtures, and Non-Linear Octane Blending," SAE Paper No. 922325, SAE Trans., 101(4), 1683-1705.

Li, H., (1995), Autoignition Chemistry Studies of Primary Reference Fuels and Their Mixtures Oxygenates in a Research Engine, PhD Thesis, Drexel University, Philadelphia, PA.

Litzinger, T.A. (1990), "A Review of Experimental Studies of Knock Chemistry in Engines," Prog. Energy Combust. Sci., 16, 155-167.

Lovell, W.G. (1948), "Knocking Characteristics of Hydrocarbons," Ind. and Eng. Chem., 40 (12), 2388-2438.

Lü, X.C. and Qian, Z.Q. (2006), "Characteristics of HCCI Engine Operation for Additives, EGR, and Intake Charge Temperature While Using Iso-octane as a Fuel," Journal of Zhejiang University, 7 (2). 252-258.

Lü, X.C., Chen, W. and Huang, Z. (2005), "A Fundamental study on the Control of the HCCI Combustion and Emissions by Fuel Design Concept Combined with Controllable EGR. Part 2. Effect of Operating Conditions and EGR on HCCI Combustion,' Fuel, 84, 1084–1092.

Mack, J.H., Flowers, D.L., Dibble, R.B. and Buchholz, B.A. (2005), "The Effect of Di-Tertiary Butyl Peroxide (DTBP) Additive on HCCI Combustion of Fuel Blends of Ethanol and Diethly Ether," SAE Paper No. 2005-01-2135.

Milovanovic, N. and Chen, R. (2001), "A Review of Experimental and Simulation Studies on Controlled Auto-ignition Combustion," SAE Paper No. 2001-01-1890.

Najt, P. and Foster, D. E. (1983), ''Compression-Ignited Homogeneous Charge Combustion,'' SAE Paper No. 830264.

Noguchi, M., Tanaka, Y., Tanaka, T. and Takeuchi, Y. (1979), ''A Study on Gasoline Engine Combustion by Observation of Intermediate Reaction Products during Combustion,'' SAE Paper No. 790840.

Oakley, A., Zhao, H., Ladommatos, N. and Ma, T. (2001), ''Experimental Studies on Controlled Auto-ignition (CAI) Combustion of Gasoline in a 4 Stroke Engine,'' SAE Paper No. 2001-01-1030.

Olsson, J.O., Tunestal, P. and Johansson, B. (2001), "Closed-Loop Control of an HCCI Engine," SAE Paper No. 2001-01-1031.

Onishi, S., Jo, S. H., Shoda, K., Jo, P. D. and Kato, S. (1979), ''Active Thermo-Atmosphere Combustion—A New Combustion Process for Internal Combustion Engines,'' SAE Paper No. 790501.

Pease, R. N. and Munro, W. R. (1929), "Characteristics of the Non-explosive Oxidation of Propane and the Butanes" Am. Chem. Soc., 51, 1839-1846.

Pilling, M.J. (1997), Comprehensive Chemical Kinetics, Elsevier, Leeds, UK

Randolph, A. L. (1994), "Cylinder-Pressure-Based Combustion Analysis in Race Engines," SAE Paper 942487.

Rassweiler, G.R. and Withrow, L. (1933), "Spectrographic Detection of Formaldehyde in an Engine Prior to Knock" Ind. Eng. Chem., 25(12), 1359 – 1366.

Ryan III, T.W. and Callahan, T.J. (1996), "Homogeneous Charge Compression Ignition of Diesel Fuel," SAE Paper No. 961160.

Ryan III, T.W. and Matheaus, A. (2003), "Fuel Requirements for HCCI Engine Operation," SAE Paper No. 2003-01-1813.

Salooja, K.C. (1962), "The Role of Combustion Promoters," J. Inst. Petroleum, 48 (460), 119-129.

Sellnau, M. (2006), "2-Step Variable Valve Actuation: System Optimization and Integration on an SI Engine," SAE Paper 2006-01-0040.

Semenov, N.N. (1958), Some Problems in Chemical Kinetics and Reactivity, Vol. 2, Chapter XII, Princeton University Press.

Sharke, P. (2000), "Otto or Not, Here it Comes," Mechanical Engineering, 122 (6), 62-66.

Sjöberg, M., Dec, J.E. and Cernansky, N.P. (2005), "Potential of Thermal Stratification and Combustion Retard for Reducing Pressure-Rise Rates in HCCI Engines, Based on Multi-Zone Modeling and Experiments," SAE Paper No. 2005-01-0113.

Smith, J. R., Green, R. M., Westbrook, C. K. and Pitz, W. J. (1985), "Experimental and Modeling Studies of Engine Knock," Proc. Combust. Inst., 20, 91-100.

Soylu, S., (2005), "Examination of Combustion Characteristics and Phasing Strategies of a Natural Gas HCCI Engine," Energy Conversion and Management, 46, 101–119.

Stanglmaier, R. and Roberts, C.E. (1999), "Homogeneous Charge Compression Ignition (HCCI): Benefits, Compromises, and Future Engine Applications," SAE Paper No 1999-01-3682

Tanaka, S., Ayala, F., Keck, J.C. and Heywood, J.B. (2003), "Two-stage Ignition in HCCI Combustion and HCCI Control by Fuels and Additives," Combustion and Flame, 132, 219–239.

Thring, R.H. (1989), "Homogeneous Charge Compression Ignition (HCCI) Engines," SAE Paper No. 892068.

Walsh, A.D. (1963), "The Knock Ratings of Fuels," Proc. Combust. Inst., 9, 1046-1055.

Wang, S. (1999), Experimental and Modeling Study of Preignition Chemistry of Hydrocarbons, Ph.D. Thesis, Drexel University, Philadelphia, PA.

Westbrook, C.K., Pitz, W.J. and Leppard, W.R. (1991), "The Autoignition Chemistry of Paraffinic Fuels and Pro-Knock and Anti-Knock Additives: A Detailed Chemical Kinetic Study," SAE Paper No. 912314, SAE Trans., 100(4), 605-622.

Wilk, R.D. (1986), Pre-ignition Oxidation Characteristics of Hydrocarbon Fuels, Ph.D. Thesis, Drexel University, Philadelphia, PA.

Yang, W. (2002), The Chemistry Controlling Post Combustion Hydrocarbon Oxidation and Homogeneous Charge Compression Ignition, Ph.D. Thesis, Drexel University, Philadelphia, PA.

Zheng, J., Gong, X., Lenhert, D.B., Miller, D.L. and Cernansky, N.P. (2005), "Preignition Behavior of n-Heptane, iso-Octane, and Propionaldehyde Blends in a Pressurized Flow Reactor," P 05, 4th United States Combustion Meeting, Drexel University , 20-23 March.

Zheng, J., Miller, D.L., Cernansky, N.P., Liu, D. and Zhang, M. (2003), "The Effect of Active Species in Internal EGR on Preignition Reactivity and on Reducing UHC and CO Emissions in Homogeneous Charge Engines," SAE Paper No. 2003-01-1831, SAE Trans. 112, Section 4, 1246-1254.

APPENDIX A: ENGINE PROCEDURE

- Turn on main power on back wall circuit breaker
- Toggle switch on wall to engine #2 (CFR)
- Turn on Autotherm, set coolant temp
- Turn on GE controller power
- On GE controller computer, open GE control toolbar
    - Press the online key? (This connects GE control toolbar to GE controller) for Dyno
- Turn on air supply
- Deal in needed RF flow fate with flow control valves
- Turn on Heater for inlet piping on Chromalox and the bead? Heaters (Chromalox heater contol is located on wall above the GE control computer)
- In input variables on GE control toolbox, set engine speed
- Enable engine by depressing icon? In GE control toolbox, then click Run
- Engine should start to Run at this point
- Now set Equivalence ratio In Tool? Control VI on LabVIEW on the GC control computer
- Verify Equivalence ratio manually by measuring the fuel flow from the fuel injector vs. flow rate of air
- To take pressure data open controller VI on the LabVIEW engine control computer
- Set the # of cycles you want to record (100)
- Run controller VI and save file to desire location

Appendix B: Engine sampling procedure

Note: Refer to Appendix A for engine start-up procedure

- Heat up sample storage cart for 1 hour
- Flush sample storage cart lines and loops with Nitrogen
- Select opening duration and CAD location on control VI on engine control computer
- Connect LabVIEW signal output to sampling valve power supply
- Connect power to sample valve
- Check opening duration
- Start auto-ignition via fuel flow VI on the GE controller computer
- Perform leak check on valve by leaving sample valve closed and running vacuum pump and checking pressure
- Fill desired loop to 5 psia (this should take approximately 3 min)
- Flush lines and next loop with Nitrogen
- Continue filling loops and flushing in between until all desired loops are filled

Appendix C Sample Valve circuits

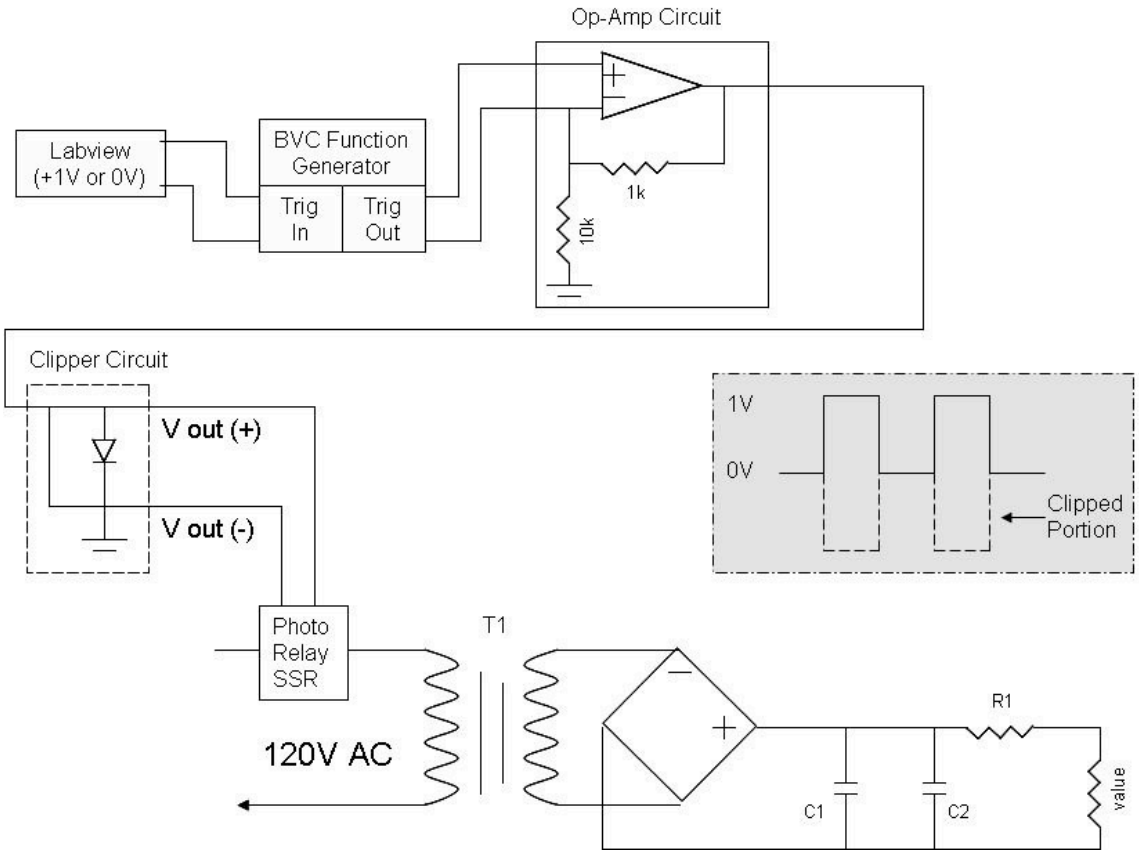

Appendix D: Methanizer

The methanizer consists of a 6" x 1/8" stainless steel tube which is mounted alongside the two multi-position valve of the Varian 3600 gas chromatography (GC), and is heated by heating bar/heating tapes coupled with a thermostat to 380°C. The stainless steel tube is packed with a special nickel catalyst powder(Varian, Product No.: 03 911600 02) with a mesh of 80/120, the same mesh as the packed column. The tube is sealed with GC class glass wool at each end. Column effluent is mixed with 10 ml/min of hydrogen just prior to the methanizer entrance. Under these conditions, CO, CO_2, and formaldehyde are converted to methane while passing through the methanizer. Hydrocarbons such as ethane, propane, etc. pass through the methanizer unaffected. Because the CO, CO2, and formaldehyde are converted to methane, they can be detected by the FID down to 1 ppm.

It is important to remember that the methanizer is located after the column, so the CO and CO_2 and peaks pass through the column as CO or CO_2. They are not converted to methane until they exit the column and methanizer, so the retention times are not affected.

VITA

Rodney O. Johnson was born on April 10, 1981 in Lowmans Windward, St. Vincent. He attended Lowmans Windward Anglican School until age 7. At the age of 7, he moved to East Orange, New Jersey, where he attended Columbian Elementary School for 2nd Grade. The following year, he moved to Woodbury, NJ where he attended West End Elementary School. He continued his education in the Woodbury School District and graduated from Woodbury Jr Sr High School in 1999.

Rodney attended Rowan University as an undergraduate and majored in Mechanical Engineering. He graduated from Rowan in 2003 and decided to pursue a graduate degree at Drexel University in Philadelphia, PA. During his graduate program, he studied the autoignition and oxidation of hydrocarbon mixtures under HCCI conditions, where he has co- authored 2 technical papers and made several technical presentations. He is a member of the Combustion Institute, SAE International (Society of Automotive Engineers), American Society of Mechanical Engineers, and the American Chemical Society.

Upon completion of his Ph.D., Rodney will start a career as an emissions catalyst engineer at BASF in Union, NJ.